RESOURCE OPTIMIZATION FOR MULTI-ANTENNA COGNITIVE RADIO NETWORKS

ZHANG LAN

NATIONAL UNIVERSITY OF SINGAPORE

2009

RESOURCE OPTIMIZATION FOR MULTI-ANTENNA COGNITIVE RADIO NETWORKS

ZHANG LAN

(*M. Eng., University of Electronic Science and Technology of China*)

A THESIS SUBMITTED

FOR THE DEGREE OF DOCTOR OF PHILOSOPHY

DEPARTMENT OF ELECTRICAL AND COMPUTER ENGINEERING

NATIONAL UNIVERSITY OF SINGAPORE

2009

Acknowledgement

First of all, I would like to express my sincere gratitude and appreciation to my advisors Dr. Yan Xin and Dr. Ying-Chang Liang for their valuable guidance and helpful technical support throughout my Ph.D course. Had it not been for their advices, direction, patience and encouragement, this thesis would certainly not be possible.

I would like to thank Dr. Rui Zhang in Institute for Infocomm Research A-STAR, Prof. H. Vincent Poor in Princeton University, Prof. Xiaodong Wang in Columbia University, and Prof. Shuguang Cui in Texas A&M University, with whom I have had the good fortune to collaborate.

I would like to thank Dr. Xudong Chen for his help and support. My thanks also go to my colleagues in the ECE-I^{2}R Wireless Communications Laboratory at the Department of Electrical and Computer Engineering and research group in Institute for Infocomm Research A-STAR for their friendship and help.

Finally, I would like to thank my family for their understanding and support. I would like to thank my wife for her support and encouragement.

Contents

Summary

One of the fundamental challenges faced by the wireless communication industry is how to meet rapidly growing demands for wireless services and applications with limited radio spectrum. Cognitive radio (CR) is a promising solution to tackle this challenge by introducing the secondary (unlicensed) users to opportunistically or concurrently access the spectrum allocated to primary (licensed) users. However, such spectrum access by secondary users (SUs) needs to avoid causing detrimental interference to the primary users (PUs). There are two popular CR models: the opportunistic spectrum access (OSA) model and spectrum sharing (SS) model. In an opportunistic spectrum access model, the SUs are allowed to access the spectrum only if the PUs are detected to be inactive. In a spectrum sharing model, the SUs are allowed to coexist with the PUs, subject to the constraint, namely the interference power constraint, which defines the maximum tolerable interference power from the SUs to the PUs.

This thesis studies a number of topics in multi-antenna CR networks under the spectrum sharing model. First, we study the resource optimization problems for three different multi-antenna CR channels, including the CR single-input multiple-output multiple access channels (SIMO-MAC), the CR multiple-input multiple-output broadcast channels (MIMO-BC), and the CR multiple-input single-output (MISO) channels. Then, we apply the solution of the resource allocation problem for CR MIMO channels to solve the capacity computation problem for secrecy MIMO channels.

Specifically, for the CR SIMO-MAC, we first consider the joint beamforming and

power allocation for the sum rate maximization problem subject to transmit and interference power constraints. A capped multi-level water-filling algorithm is proposed to obtain the optimal power allocation. Secondly, we consider the signal-to-interference-plus-noise ratio (SINR) balancing problem, in which the minimal ratio of the achievable SINRs relative to the target SINRs of the users is maximized. It is proved that the linear power constraints can be completely decoupled, and thus a high-efficiency algorithm is proposed to solve the corresponding problem.

For the CR MIMO-BC, we focus on determining the optimal transmit covariance matrix to achieve the entire capacity region. Conventionally, the MIMO-BC is subject to a single sum power constraint, and the corresponding capacity computation problem can be transformed into that of a dual MIMO-MAC by using the conventional BC-MAC duality. This duality, however, cannot be applied to the CR case due to the existence of the extra interference power constraints. To handle this difficulty, a generalized BC-MAC duality is proposed for the MIMO-BC with multiple linear constraints. By exploiting the new duality, a subgradient based algorithm is developed.

For the CR MISO channels, we consider a robust design problem, where the channel state information (CSI) of the channel from the SU transmitter to the PU is assumed to be partially known by the SU. Our design objective is to determine the transmit covariance matrix that maximizes the rate of the SU while the interference power constraint is satisfied for all possible channel realizations. This problem is formulated as a semi-infinite programming (SIP) problem. Two solutions, including a closed-form solution and a second order cone programming (SOCP) based solution, are proposed.

Finally, we apply the resource allocation solution for the CR MIMO channels to solve the capacity computation problem for secrecy MIMO channels. By exploiting the relationship between these two channels, the capacity computation problem for secrecy MIMO channels is transformed to a sequence of optimization problems for CR MIMO channels, through which several efficient algorithms are proposed.

List of Figures

List of Tables

List of Notations

a	lowercase letters are used to denote scalars
$\boldsymbol{a}$	boldface lowercase letters are used to denote column vectors
$\boldsymbol{A}$	boldface uppercase letters are used to denote matrices
$(\cdot)^T$	the transpose of a vector or a matrix
$(\cdot)^H$	the conjugate transpose of a vector or a matrix
$\mathbb{E}[\cdot]$	the statistical expectation operator
$\boldsymbol{I}_M$	the $M \times M$ identity matrix
$\mathbf{1}_M$	the $M \times 1$ vector with all elements being one
$\text{diag}(\mathbf{x})$	the diagonal matrix with the diagonal elements being vector $\mathbf{x}$
$\text{tr}(\cdot)$	the matrix trace operation
$\text{Rank}(\cdot)$	the matrix rank operation
$\lvert\boldsymbol{S}\rvert$	the determinant of a matrix $\boldsymbol{S}$
$\mathbb{R}$	the field of real numbers
$[x]^+$	$\max(x, 0)$
$(\cdot)^{\text{b}}/(\cdot)^{\text{m}}$	the quantities associated with a BC or a MAC,

List of Abbreviations

BS	Base Station
CR	Cognitive Radio
DMCPA	Decoupled Multiple-Constraint Power Allocation algorithm
CML	Capped Multi-Level
DFE	Decision Feedback Equalizer
MMSE	Minimum Mean-Square-Error
PU/PU$_n$	Primary User/Primary User n
QoS	Quality-of-Service
RDPA-2 (N)	Recursive Decoupled Power Allocation algorithm with Two (N) primary users
SIMO	Single-Input Multiple-Output
MISO	multiple-input single-output
MIMO	multiple-input multiple-output
SINR	Signal-to-Interference-plus-Noise Ratio
SU/SU$_i$	Secondary User/Secondary User i
ZF	Zero-Forcing
CSI	channel state information
SOCP	second order cone programming
BC	broadcast channel
MAC	multiple access channel

IC	interference channels
SU-Tx	SU transmitter
SU-Rx	SU receiver
PU-Tx	PU transmitter
PU-Rx	PU receiver
CSCG	circularly symmetric complex Gaussian
SIC	successive interference cancelation
DPC	dirty paper coding
RV	random variable

Chapter 1

Introduction

Traditional spectrum regulation is based primarily on the command-and-control strategy that assigns users to prescribed frequency bands, and restricts the potential users to dynamically access the allocated radio spectrum. In a report published by the Federal Communications Committee (FCC) [1], it has been shown that a significant amount of the licensed radio spectrum is unused for 90% of time in the United States. Similar observations have been made in other countries [2]. This static spectrum allocation policy, together with the rapid deployment of various wireless services, leads to increasing scarcity and congestion in the radio spectrum. Cognitive Radio (CR) that allows the secondary (unlicensed) users to opportunistically or concurrently access the licensed spectrum, show a great potential to improve the spectrum utilization [3, 4].

This thesis investigates the resource optimization problems for three multi-antenna based CR channels, including the CR single-input multiple-output multiple access channels (SIMO-MAC), CR multiple-input multiple-output broadcast channels (MIMO-BC), and CR multiple-input multiple-output (MISO) channels, and applies the resource allocation results of CR MIMO channels to solve the capacity computation problem for secrecy MIMO channels. In this chapter, we briefly introduce the recent development and challenges of CR research, provide overviews on resource allocation for multi-

antenna systems and secrecy communication systems, and present the contributions and organization of this thesis.

1.1 Cognitive Radio Models

According to the definition in [4], CR is an intelligent wireless communication system that is aware of its surrounding environment, adapts its transmission to the electromagnetic environment, and improves the utilization efficiency of the radio spectrum. When a CR is operating in a spectrum allocated to a primary user (PU), the CR is also called the secondary user (SU). According to the capability of the SU in obtaining its surrounding spectrum environment, the CR models can be classified into three categories: the opportunistic spectrum access model, the spectrum sharing model, and the overlay model. In the opportunistic spectrum access model, the SU has the lowest capability in understanding its radio spectrum environment, i.e., it can only detect whether the PU is on or off. If the SU finds that the spectrum is unoccupied by the PU, then the SU can access this spectrum; otherwise, it cannot. In spectrum sharing model, the SU regulates its transmission power such that the caused interference power at the PU is lower than one threshold. In this case, the SU can access the spectrum even if the PU is active. In overlay model, the SU is assumed to have *a priori* knowledge of the PU's messages. With that, the SU transmitter is able to send messages to its own receiver and, at the same time, compensate for the resultant interference to the PU by assisting the PU transmission.

1.1.1 The Opportunistic Spectrum Access Model

In opportunistic spectrum access model, the SUs are allowed to access the spectrum only if it is not being used by the PUs as shown in Fig. 1.1. The key point in this model

is to accurately detect the existence of the PUs, and the process to detect the PU's activity is termed as *spectrum sensing*. Spectrum sensing is one of the most fundamental elements in a CR due to its crucial role in discovering spectrum opportunities. There

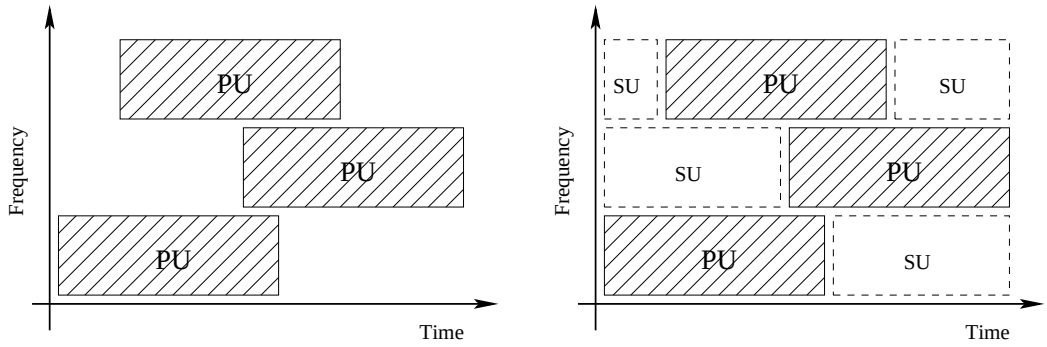

Figure 1.1: The opportunistic spectrum access model: The SU is allowed to access the spectrum only if the PU is inactive. The shadowed area denotes the spectrum occupied by the PU. The area with dash line denotes the spectrum which could be utilized by the SU.

are several well-known conventional spectrum sensing algorithms, including the energy detection [5], matched filter [6–9], and feature detection [10, 11]. Recently, there are several new algorithms proposed for CR spectrum sensing, such as the eigenvalue based algorithm [12, 13] and the covariance based algorithm [14, 15]. These spectrum sensing algorithms usually rely on the local observations of a single SU. However, using the observations from a single SU might result in a *hidden terminal problem* [16], with which the detection for PU may fail due to the shadowing. An efficient approach, which is termed as cooperative spectrum sensing [16–20], is to have several SUs to cooperate with each other for detecting the presence of the PU. If the SUs span a distance that is larger than the correlation distance of the shadowing fading, it is unlikely that all of them are under a deep shadow simultaneously. Thus, cooperative sensing has better PU detection performance with the cost of additional operations and overhead traffic.

In order to protect the PUs, from medium access perspective, each medium access control frame needs to have one sensing slot to sense the PU's activity and one data transmission slot for SU transmission in case the spectrum is found to be available. The longer duration of the sensing slot, the better performance of the PU detection, and thus the better protection to PUs. However, the longer sensing slot leads to the shorter transmission time, and thus the lower SU throughput. The tradeoff between the sensing time and the SU throughput was studied in [21].

1.1.2 The Spectrum Sharing Model

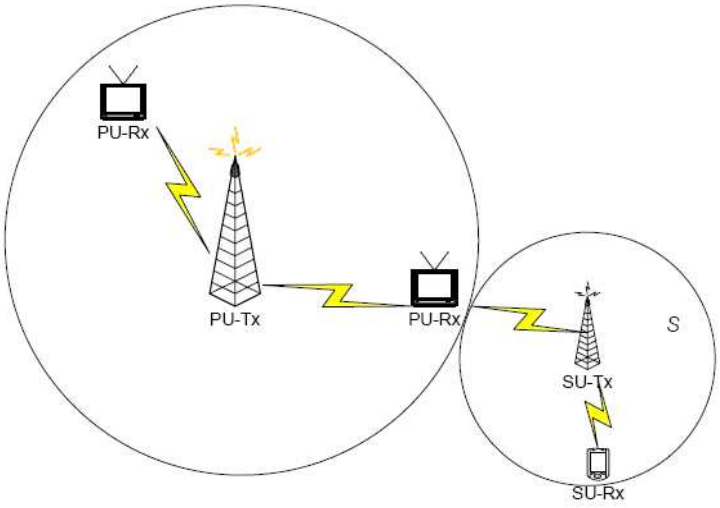

Figure 1.2: The spectrum sharing model: the SU can share the same spectrum with the PU provided that its interference power at PU is lower than a threshold. SU-Tx, SU-Rx, PU-Tx and PU-Rx denote the SU transmitter, the SU receiver, the PU transmitter and the PU receiver, respectively. Within the region $\boldsymbol{S}$, the interference power caused by the SU is larger than the interference power threshold.

In spectrum sharing model, the SU is allowed to transmit simultaneously with the PU provided that the interferences from the SU to the PU will not cause the resultant

performance loss of PU to an unacceptable level. As shown in Fig. 1.2, the SU should regulate its transmission power such that the caused interference at the PU is lower than a threshold, which is called interference power constraint [22–24]. To achieve this power constraint, the SU may also need to have the channel state information (CSI) of the channel from the SU transmitter to the PU receiver.

To enable the spectrum sharing, dynamic resource allocation becomes crucial, whereby the transmit power, bit-rate, bandwidth, and antenna beam of the CR need to be dynamically adjusted based upon the CSI available at the CR transmitter. A lot of existing studies for spectrum sharing model focus on the resource allocation to optimize the performance of the SU networks [25–28].

For the single-antenna spectrum sharing CR fading channels, the power allocation problem to achieve the ergodic/outage capacity has been studied in [29] under the average/peak interference power constraint, and in [30,31] under the combined interference power and transmit power constraints. It has been shown in [32] that the average interference power constraint is superior over the peak interference power constraint in terms of maximizing the achievable ergodic capacities of both PU and SU.

In the past decade, multi-antenna communication systems have received considerable attention due to their capability to achieve many desirable functions, including the interference suppression for multi-user transmissions [33], the capacity gain without bandwidth expansion [34], and the diversity gain via space-time coding [35]. In addition to achieve the above functions, in CR networks, multi-antennas can be utilized to suppress the interference to the PU. Transmit optimization for a single secondary MIMO/MISO link in a CR network under interference power constraint is considered in [36]. Multi-antennas were exploited at the secondary transmitter to optimally tradeoff between throughput maximization and interference avoidance. However, the role of multi-antennas in multi-user CR systems is not completely understood yet. Moreover, it is unclear how to fully exploit the spatial degrees of freedom provided by the

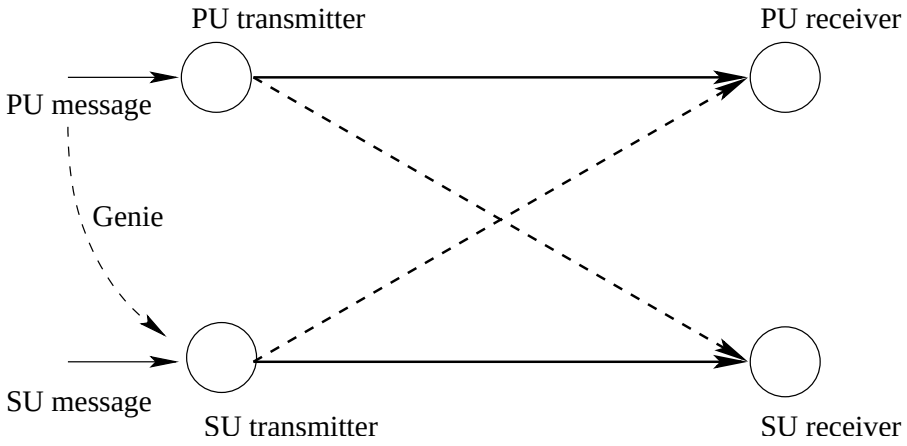

Figure 1.3: The overlay model: the SU transmitter has *a priori* knowledge of the PU's message.

multi-antenna SUs.

1.1.3 The Overlay Model

In overlay CR model, the SU is assumed to have perfect a priori knowledge on the message being transmitted by the PU, which is illustrated in Fig. 1.3. Thus, the SU can allocate part of its power for secondary transmission and the rest to assist the primary transmission. Most of the studies on the overlay CR model are based on information theory [37–43]. Complex coding schemes that including cooperative coding, collaborative coding, and dirty paper coding, have been developed to improve the achievable rate of the CR channel. Moreover, the power allocation problem to achieve the capacity of overlay CR MIMO channel has been studied in [44]. The proposed power allocation scheme therein has been proved to be optimal under certain conditions. In [45], recent results for overlay CR have been summarized from an information-theoretic perspective.

1.2 Related Work

The topics of this thesis focus on the resource optimization for multi-antenna CR systems and its application in secrecy transmission problems. For the sake of better illustration, we provide a brief overview on the resource allocation for multi-antenna systems and the secrecy communication systems.

1.2.1 Resource Allocation for Multi-Antenna Systems

Most of the existing resource allocation problems for multi-antenna systems, including MIMO-MAC, MIMO-BC, and MISO channels, are formulated as optimization problems [46]. By applying certain powerful optimization tools, such as the convex optimization techniques, high-efficiency algorithms are developed. One important class of resource allocation problems for multi-antenna systems is to design the optimal transmit strategy, e.g., determining the transmit covariance matrix, to achieve the capacity region for corresponding channels. In [47], the sum capacity computation problem for MIMO-MAC, which is also called sum rate maximization problem, was explored. The objective of the problem is to design the optimal transmit covariance matrices to achieve the sum capacity of the MIMO-MAC. By applying the Karush-Kuhn-Tucker (KKT) conditions of the problem, a high-efficiency algorithm, which is called iterative water-filling (IWF) algorithm, was developed. In [48], the sum rate maximization problem for MIMO-BC with a single transmit power constraint was studied. By exploiting the relationship between BC and MAC, the problem can be transformed into an equivalent MIMO-MAC sum rate maximization problem, which can be solved by IWF. In [49], the transmit optimization problem for a MISO channel was studied, where the transmitter is assumed to have imperfect CSI. The objective of this problem is to determine the optimal transmit covariance matrix such that the average transmission rate of the MISO channel is maximized. Moreover, another class of resource allocation

problems is studies from an signal processing perspective [50–52]. The objective is to find the transmit/receive vectors and the transmit power for MISO-BC/SIMO-MAC with Signal-to-Interference-plus-Noise Ratio (SINR) constraint or transmit power constraint. These problems, which are called BC/MAC beamforming problem, can be transformed into the second order cone programming (SOCP) problems [50], and solved by efficient interior point algorithm [53].

1.2.2 Secrecy Communication Systems

Due to the broadcast nature of the wireless communication systems, the wireless transmission is particularly susceptible to eavesdropping. Hence, security and privacy have now become a critical factor in designing a wireless communication system. In 1975, Wyner introduced a secrecy transmission model in his seminal work [54] on information-theoretic secrecy. In this model, the secrecy transmitter sends confidential messages to a legitimate receiver subject to the requirement that the messages cannot be decoded by an eavesdropper. The information-theoretic study of the secrecy transmission problem has been continued and extended to many other channel models, including BC [55–58], MAC [59–61], and interference channels (IC) [62, 63]. Very recently, the secrecy capacity of the MIMO channel has been characterized by Khisti and Wornell [64], and Oggier and Hassibi [65]. In their studies, the secrecy MIMO channel with a single eavesdropper having multiple antennas was transformed into a degraded MIMO-BC, whose capacity is an upper bound on the secrecy capacity. It was shown in [64, 65] that this capacity upper bound is indeed tight for the Gaussian noise case, i.e., the exact secrecy capacity. However, this computable secrecy capacity cannot be extended to the general case of multiple eavesdroppers. In [66], Liu and Shammai also derived the MIMO secrecy capacity by using the channel enhancement technique [67]. However, no computable characterization of the secrecy capacity was

provided in [66]. It is still unclear how to compute the secrecy capacity of the channels with multiple eavesdroppers.

1.3 Motivations and Challenges

Many of the resource allocation problems for the conventional communication systems can be formulated as convex optimization problems [46, 47, 50]. Compared to those conventional systems, the spectrum sharing based CR networks experience extra interference power constraints. Although the interference power constraint is a linear constraint, and does not change the convexity of the related problems, many existing high-efficiency algorithms cannot be applied to CR cases due to the presence of the extra constraint. For example, in the CR SIMO-MAC, although the corresponding power allocation problem is a convex optimization problem, the conventional water-filling algorithm is not applicable. Moreover, for MIMO-BC, the conventional transmit optimization depends on the conventional BC-MAC duality. However, this duality is not applicable to the CR MIMO-BC, where the transmitter is subject to both the transmit power constraint and the interference power constraint. Efficient algorithms need to be designed to handle the difficulties caused by the extra interference power constraint.

In the exiting literature [36, 68], it is usually assumed that the CSI of all the channels in CR networks are perfectly known by the SU transmitter. However, unlike the conventional wireless communication systems, it is difficult for the SU to obtain the accurate CSI of the channel from the SU transmitter to the PU due to the loose cooperation between them. A more practical scenario needs to be considered for the spectrum sharing based CR networks. A straightforward problem is how to design the optimal transmission strategies for the SU transmitter when only partial CSI is available.

Finally, in a secrecy transmission system, the transmitter is required to send its confidential messages to legitimate destinations while keeping other eavesdroppers as

ignorant of this information as possible. One possible strategy for the secrecy transmitter is to regulate its transmission power such that the received power at eavesdroppers is low enough. While it is easy to observe that there is a similarity between the secrecy transmission and spectrum sharing based CR transmission, i.e., both of them need to regulate their transmission power, explicit description for the relationship of these two transmissions is needed. Moreover, it would be interesting to investigate how we can utilize the results of the resource allocation problem for spectrum sharing CR networks to solve the related problems for the secrecy transmissions.

1.4 Contributions and Organization of the Thesis

The main contributions of this thesis are to develop new optimization algorithms for spectrum sharing based CR networks and apply the relationship between secrecy transmission and CR transmission to solve the capacity computation problem for secrecy channels.

In Chapter 2, we consider two joint beamforming and power allocation problems for the CR SIMO-MAC. The first problem focuses on determining the optimal power allocation and the receive beamforming vectors to maximize the sum rate of the channel. A capped multi-level water-filling algorithm is proposed by exploiting the special structure of the CR SIMO-MAC channel. The second problem is to determine the optimal power allocation and the receive beamforming vectors such that the target SINR of different users is met in a fair manner, which is termed as the SINR balancing problem. We prove that the linear power constraints in the SINR balancing problem can be completely decoupled, and thus the problem can be handled through solving multiple single-constraint sub-problems. Therefore, the computational complexity is reduced significantly.

In Chapter 3, we consider the transmit optimization problem to achieve the ca-

pacity region of the CR MIMO-BC, which is called the capacity computation problem. Traditional MIMO-BC capacity computation problem can be solved by solving a dual MIMO-MAC problem via a BC-MAC duality. However, the conventional BC-MAC duality can only be applied to the case where the transmitter is subject to a single sum power constraint. In CR MIMO-BC, the transmitter is not only subject to the sum power constraint, but also to the interference power constraint. Thus, the conventional BC-MAC duality cannot be applied. To handle this difficulty, we propose a new generalized BC-MAC duality, and apply it to solve the capacity computation problem for the CR MIMO-BC with multiple linear constraints. This result generalizes all the existing BC-MAC duality results as its special cases. Moreover, we propose a subgradient based algorithm, which is shown to be able to converge to the globally optimal solution.

In Chapter 4, we consider a robust design problem for a CR MISO channel. We assume that the CSI of the channel from the SU transmitter to the PU is partially known at the SU, due to the loose cooperation between the SU and the PU. With the uncertainty of the channel, our design objective is to determine the transmit covariance matrix that maximizes the rate of the SU while guaranteeing that the interference power constraint is satisfied for all the possible channel realizations. This problem is formulated as a semi-infinite programming (SIP) problem. By exploiting its properties, this problem is first transformed into the SOCP problem, and is solved via a standard interior point algorithm. Then, an analytical solution with much reduced complexity is developed from a geometric perspective.

In Chapter 5, we study the achievable rates for the MIMO secrecy channel with multiple single-/multi-antenna eavesdroppers. According to [64–66], by assuming Gaussian input, the achievable secrecy rate can be maximized via optimizing over the transmit covariance matrix of the secrecy user to maximize the minimum difference between the mutual information of the secrecy channel and those of the channels

from the secrecy transmitter to different eavesdroppers. It can thus be shown that the resulting secrecy rate maximization problem is a non-convex max-min optimization problem, which is difficult to solve via existing methods. To address this problem, we consider an auxiliary CR channel with multiple PUs bearing the same channel responses as those eavesdroppers in the secrecy channel in Chapter 5. We then establish a relationship between this auxiliary CR channel and the secrecy channel by proving that the optimal transmit covariance matrix for the secrecy channel is the same as that for the CR channel with properly selected IT constraints for the PUs. Thereby, finding the optimal complex transmit covariance matrix for the secrecy channel becomes equivalent to searching over a set of real IT constraints in the auxiliary CR channel, thus substantially reducing the computational complexity. Based on this relationship, we transform the non-convex secrecy rate maximization problem into a sequence of convex CR spectrum sharing capacity computation problems, under various setups of the secrecy channel. For the case of multiple-input single-output (MISO) or MIMO secrecy channel with single-antenna eavesdroppers, we propose efficient algorithms to compute the maximum achievable secrecy rate, while for the case with multi-antenna eavesdropper receivers, we obtain various new bounds on the achievable secrecy rate.

Finally, we summarize and conclude our work in Chapter 6, and discuss a few interesting questions and directions for further research.

Chapter 2

Joint Beamforming and Power Allocation for CR SIMO-MAC

In this chapter, we consider a spectrum sharing based CR SIMO-MAC network. Subject to interference power constraints for the PUs as well as transmit power constraints for the SUs, two optimization problems involving a joint beamforming and power allocation for the CR SIMO-MAC are considered: the sum-rate maximization problem and the SINR balancing problem. For the sum-rate maximization problem, zero-forcing based decision feedback equalizers (ZF-DFE) are used to decouple the SIMO-MAC, and a capped multi-level (CML) water-filling algorithm is proposed to maximize the achievable sum-rate of the SUs for the single PU case. For the SINR balancing problem, it is shown that, using linear minimum mean-square-error (MMSE) receivers, each of the interference constraints and transmit power constraints can be completely decoupled, and thus the multi-constraint optimization problem can be solved through multiple single-constraint sub-problems.

2.1 Introduction

Conventionally, to improve the spectral efficiency and reliability of MAC, multi-antennas are often deployed at the base station (BS) [69], [51]. On the other hand, single-antenna mobile users are quite common due to the size and cost limitations of mobile terminals. We simply term this setting as SIMO-MAC. It is well known that the minimum mean-square-error based decision feedback equalizer (MMSE-DFE) is a sum-rate capacity achieving scheme for the SIMO-MAC [70]. Additionally, it was shown in [71] that the ZF-DFE is asymptotically optimal in both low and high signal-to-noise ratio (SNR) regimes.

For SIMO-MAC systems, given the SINR targets for each user, a sum-power minimization problem has been studied in [52] using linear MMSE receivers. Joint beamforming and power allocation algorithms have been proposed under the assumption that there exists a feasible solution for the prescribed SINRs. A related problem of [33] has been studied, i.e., the SINR balancing problem, in which the minimal ratio of the achievable SINRs relative to the target SINRs of the users in the system is maximized under a sum-power constraint. When the ratio is greater than or equal to one, the power minimization problem has been considered for the given SINR targets. Through introducing SINR balancing, the work in [72] is able to justify the feasibility to achieve the SINR targets. In [72] and [73], the power allocation vector for a given beamforming matrix was derived using a single-step solution instead of iterative schemes as in [52] and [33]. Moreover, the SINR balancing problem has been studied using MMSE-DFE receivers in [74].

In this chapter, we consider a spectrum sharing based CR SIMO-MAC network. Two sets of constraints are considered: interference power constraints, and transmit power constraints. Based on these constraints, we study two optimization problems for the SUs: the sum-rate maximization problem and the SINR balancing problem.

For the sum-rate maximization problem, a ZF-DFE is used to decouple the subchannels associated with each SU. We propose a CML water filling algorithm to maximize the sum-rate under the individual transmit power constraint and the interference constraint for a single PU. We also propose a power allocation scheme, called recursive decoupled power allocation algorithm, for the case where multiple PUs exist. For the SINR balancing problem, linear MMSE receivers are considered. It is proven that the multi-constraint optimization problem can be completely decomposed into multiple single-constraint optimization problems. Therefore, the globally optimal solution to the multi-constraint problem can be obtained through computing the solutions to the decomposed sub-problems.

The rest of the chapter is organized as follows. In Section 2.2, we present the signal model for CR SIMO-MAC and formulate two optimization problems. In Section 2.3, the sum-rate maximization problem is studied, for which a recursive decoupled power allocation algorithm is proposed. In Section 2.4, we consider the SINR balancing problem, and propose a decoupled multi-constraint power allocation algorithm. Numerical examples are given in Section 2.5. Finally, Section 2.6 concludes this chapter.

2.2 System Model and Problem Formulation

Consider a CR SIMO-MAC with K SUs operating in a spectrum allocated to N PUs each with a single transmit antenna and a single receive antenna. The SUs, as shown in Fig. 2.1, communicate with the same BS equipped with N_r receive antennas. The transmit-receive signal model from the SUs to the BS can be represented as:

$$\boldsymbol{y} = \boldsymbol{H}\boldsymbol{x} + \check{\boldsymbol{H}}\check{\boldsymbol{x}} + \boldsymbol{z},$$

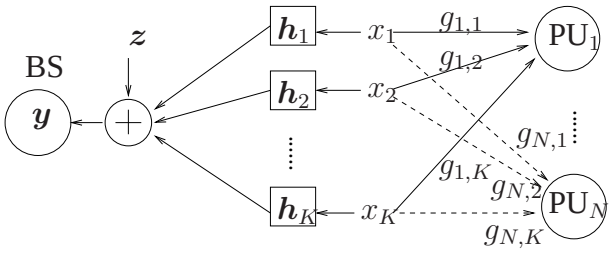

Figure 2.1: The system model for CR SIMO-MAC. There are K SUs and N PUs. The BS has N_r receive antennas. Each SU is equipped with a single transmit antenna.

where $\boldsymbol{y}$ denotes the $N_r \times 1$ received signal vector, $\boldsymbol{H} = [\boldsymbol{h}_1, \cdots, \boldsymbol{h}_K]$ denotes the $N_r \times K$ channel matrix with $\boldsymbol{h}_i$ being the channel responses from the ith SU (SU$_i$) to the BS, $\boldsymbol{x}$ is the $K \times 1$ transmit signal vector whose ith entry, x_i, denotes the signal transmitted from SU$_i$, $\check{\boldsymbol{H}} = [\check{\boldsymbol{h}}_1, \cdots, \check{\boldsymbol{h}}_N]$ denotes the $N_r \times N$ channel matrix where $\check{\boldsymbol{h}}_n$ is the channel response from the nth PU (PU$_n$)'s transmitter to the BS, $\check{\boldsymbol{x}}$ is the $N \times 1$ transmit signal vector from the PUs[1], and $\boldsymbol{z}$ is the Gaussian noise vector whose entries are assumed to be independent Gaussian random variables (RVs) with mean zero and variance σ^2.

Furthermore, we assume that the transmit power, p_i, of SU$_i$, is subject to a transmit power $\bar{P}_i$, i.e., $p_i \leq \bar{P}_i$, $i = 1, \cdots, K$. Let $g_{n,i}$ be the power gain between SU$_i$ to PU$_n$. The interference power received by PU$_n$ from all SUs is characterized by $\boldsymbol{g}_n^T \boldsymbol{p}$, where $\boldsymbol{g}_n = [g_{n,1}, \cdots, g_{n,K}]^T$ and $\boldsymbol{p} := [p_1, \cdots, p_K]^T$. Defining $\boldsymbol{G} = [\boldsymbol{g}_1, \ldots, \boldsymbol{g}_N]^T$[2]. In this chapter, the proposed algorithms are performed at the BS of the CR SIMO MAC, and it is assumed that the BS has perfect CSI. To do so, the SUs need to be "cognitive users"

[1]It will be clear in the following that the influence of the PU transmission can be viewed as noise for SU.

[2]Throughout this thesis, we assume a *block fading* channel model, i.e., the channel matrices $\boldsymbol{H}$, $\check{\boldsymbol{H}}$, and $\boldsymbol{G}$ are fixed during each transmission block and change independently from one block to another according to the ergodic random processes.

which are aware of the environment [3]. In practice, certain cooperation in terms of parameter feedback between the PUs and the SUs may be required. To achieve that, the protocol for SUs can be designed as follows: every frame contains sensing sub-frame and data transmission sub-frame. During the sensing sub-frame, all SUs remain quiet, and thus the BS can measure the effect from the PU and background noise. During the first portion of the data transmission sub-frame, the SUs can transmit training sequences to the BS as well as to the PUs so that the BS can estimate the channel matrix $\boldsymbol{H}$, and the PUs can measure the matrix $\boldsymbol{G}$. After that, the PUs will feedback the matrix $\boldsymbol{G}$ to the BS so that further processing can be carried out.

As discussed in Chapter 1, in spectrum sharing based CR networks, to guarantee the quality of service (QoS) of the PU, the SU transmitter should regulate its transmission power such that the caused interference at the PU is lower than certain threshold. On the other hand, with ensured QoS of the PUs, power allocation in a CR network should be appropriately determined to optimize the performance metrics of the SUs, which can be reflected through the parameters such as the sum-rate or SINR.

Motivated by the considerations described above, we formulate the designs of CR SIMO-MAC into two optimization problems. The first problem of our interest is to maximize the sum-rate of the SUs subject to individual transmit power constraints, as well as the interference power constraints. This problem is termed as the *sum-rate maximization* problem, which, mathematically, can be formulated as

$$\max_{\boldsymbol{U},\boldsymbol{p}} \sum_i r_i \tag{2.1}$$

$$\text{subject to: } p_i \leq \bar{P}_i, \;\; i = 1, 2, ..., K,$$

$$\boldsymbol{g}_n^T \boldsymbol{p} \leq \Gamma_n, \;\; n = 1, \cdots, N, \tag{2.2}$$

where $\boldsymbol{U}$ is defined as $[\boldsymbol{u}_1, \ldots, \boldsymbol{u}_K]$ with $\boldsymbol{u}_i$ denoting the receive beamforming vector for SU_i, and r_i is the information rate of SU_i, and Γ_n represents the interference power threshold for PU_n. The expression of information rate r_i depends on the receiver

employed by the BS, and it will be discussed in Section 2.3.

In the preceding formulation, the fairness in QoS for SUs in the CR SIMO-MAC is not taken into account. Since each user's QoS is related to its SINR, ensuring the QoS of each SU can be realized through pre-setting the SINR targets. The output SINR of SU_i after applying beamforming to the received signal vector is given by [52], [72]

$$\text{SINR}_i(\boldsymbol{u}_i, \boldsymbol{p}) = \frac{p_i \boldsymbol{u}_i^H \boldsymbol{R}_i \boldsymbol{u}_i}{\boldsymbol{u}_i^H (\sum_{k \neq i} p_k \boldsymbol{R}_k + \sigma^2 \boldsymbol{I}_{N_r} + \sum_{n=1}^{N} \check{p}_n \check{\boldsymbol{R}}_n) \boldsymbol{u}_i}, \tag{2.3}$$

where $\check{p}_n$ is the transmit power of PU_n, $\boldsymbol{R}_i = \boldsymbol{h}_i \boldsymbol{h}_i^H$ for $i = 1, \cdots, K$, and $\check{\boldsymbol{R}}_n = \check{\boldsymbol{h}}_n \check{\boldsymbol{h}}_n^H$ for $n = 1, \cdots, N$.

Mathematically, the SINR balancing problem for a CR SIMO-MAC can be formulated as

$$\max_{\boldsymbol{U}, \boldsymbol{p}} \min_{1 \leq i \leq K} \frac{\text{SINR}_i(\boldsymbol{u}_i, \boldsymbol{p})}{\gamma_i}, \tag{2.4}$$

$$\text{subject to: } p_i \leq \bar{P}_i, \;\; i = 1, 2, ..., K,$$

$$\boldsymbol{g}_n^T \boldsymbol{p} \leq \Gamma_n, \;\; n = 1, \cdots, N, \tag{2.5}$$

where γ_i is the preset SINR target for SU_i. Similar to [72], the objective function (2.4) is to find a power allocation such that all SUs can achieve their target SINRs in a fair manner.

2.3 Sum-Rate Maximization Problem

In this section, we study the sum-rate maximization problem using a ZF-DFE at the BS. We further assume $N_r \geq K$. Applying the QR decomposition to the channel matrix $\boldsymbol{H}$ of SUs, and defining M as the rank of $\boldsymbol{H}$, we can write $\boldsymbol{H} = \boldsymbol{Q}\boldsymbol{R}$, where $\boldsymbol{Q} = [\boldsymbol{q}_1, \cdots, \boldsymbol{q}_M] \in \mathbb{C}^{N_r \times M}$ has orthogonal columns and $\boldsymbol{R} \in \mathbb{C}^{M \times K}$ is an upper triangular matrix with $r_{m,k}$ denoting its (m,k)th entry. Using equalizer $\boldsymbol{Q}^H$ to the

received signal and using successive interference cancellation, the channel is decomposed as M independent sub-channels, each associated with one SU. This receiver can also be viewed as receive beamforming in the sense that the beamforming vectors are determined by the QR decomposition of the channel matrix $\boldsymbol{H}$. Thus, we only need to determine the power allocation vector that maximizes the sum-rate. In this case, assuming Gaussian signal inputs, we rewrite (2.1) and (2.2) as

$$\max_{\boldsymbol{p}} \sum_{i=1}^{K} \log\left(1+\frac{p_i d_i}{\sigma_i^2}\right) \tag{2.6}$$

$$\text{subject to: } p_i \le \bar{P}_i, \;\; i=1,2,...,K,$$

$$\boldsymbol{g}_n^T \boldsymbol{p} \le \Gamma_n, \;\; n=1,2,\ldots,N, \tag{2.7}$$

where $d_i = |r_{i,i}|^2$, and $\sigma_i^2 = \sigma^2 + \sum_{n=1}^{N} \check{p}_n \boldsymbol{q}_i^H \check{\boldsymbol{R}}_n \boldsymbol{q}_i$ is the interference-plus-noise power after receive beamforming $\boldsymbol{q}_i$ is applied. Eq. (2.6) defines the sum rate achieved through the ZF-DFE based receiver. In the above, we formulate the problem for the general case of K sub-channels. However, if $M < K$, we can choose $d_i = 0$ and $p_i = 0$ for $i = M+1, \cdots, K$.

If the power constraints in (2.7) are replaced by a single total power constraint, $\sum_{i=1}^{K} p_i \le P_{\max}$, then the optimal power allocation achieving the maximum sum-rate is described by *the conventional water-filling principle* [75]:

$$p_i = \left[\mu - \frac{\sigma_i^2}{d_i}\right]^+, \;\; i=1,\cdots,K, \tag{2.8}$$

where $[x]^+ := \max(x,0)$, and μ is the water level for which the power constraint is satisfied with equality. In the following, we will derive the power allocation policies for CR SIMO-MAC.

2.3.1 A Single PU Constraint

Instead of tackling problem (2.6) under multiple interference constraints described by (2.7), we first consider a relatively simple scenario where only one PU is present. In

this case, as described in (2.7), there are one interference constraint and K transmit power constraints. The solution to the general problem with multiple PUs will be discussed in Section 2.3.2. For notional simplicity, we write the interference power threshold for the PU as Γ, and the power gain from SU$_i$ to this PU as g_i for $i = 1, \cdots, K$.

The Lagrange function of (2.6) and (2.7) with $N = 1$ is given by

$$L(\boldsymbol{p}, \lambda, \nu_1, \cdots, \nu_K) = \sum_{i=1}^{K} \log\left(1 + \frac{p_i d_i}{\sigma_i^2}\right) + \lambda\Big(\Gamma - \sum_{i=1}^{K} g_i p_i\Big) + \sum_{i=1}^{K} \nu_i(\bar{P}_i - p_i),$$

where λ and ν_i, $i = 1, ..., K$, are Lagrange multipliers. The Karush-Kuhn-Tucker (KKT) conditions are listed as:

$$\left(\sigma_i^2 d_i^{-1} + p_i\right)^{-1} - \lambda g_i - \nu_i = 0, \tag{2.9}$$

$$\lambda\left(\Gamma - \sum_{i=1}^{K} g_i p_i\right) = 0, \tag{2.10}$$

$$\nu_i(\bar{P}_i - p_i) = 0, \tag{2.11}$$

where $\lambda \geq 0$ and $\nu_i \geq 0$ for $i = 1, \cdots, K$. According to (2.9), the power allocation for SU$_i$ is given by

$$p_i = \left[\frac{1}{\lambda g_i + \nu_i} - \frac{\sigma_i^2}{d_i}\right]^+, \; i = 1, \cdots, K. \tag{2.12}$$

The parameters λ and ν_is can be obtained through substituting (2.12) into (2.10) and (2.11). Eq. (2.12) resembles the conventional water-filling solution shown in (2.8). However, the key difference is that the conventional water-filling principle indicates that all users use the same water level, μ, while the solution in (2.12) suggests that the water level can be different for different SUs. Specifically, for SU$_i$, its water level is determined by $w_i = 1/(\lambda g_i)$. Define T as $1/\lambda$. Because the parameter T is the same for all SUs, and g_i quantifies the power gain from SU$_i$ to the PU, the SU causing stronger interference to the PU has a lower water level, and vice versa.

Eq. (2.12) involves $(K+1)$ Lagrange multipliers, and thus computing (2.12) becomes more complex as compared to the conventional water filling which only has a single Lagrange multiplier. Fortunately, since $p_i \leq \bar{P}_i$, the powers allocated to each SU are upper-bounded by their transmit power constraints. Therefore, the power allocation scheme is called capped multi-level (CML) water-filling.

In the following theorem, we show that it is unnecessary to calculate the Lagrange multipliers ν_is.

Theorem 2.1 *For the sum-rate maximization problem* (2.6) *with K transmit power constraints and a single interference constraint, the optimal power allocation for SU$_i$ can be computed as*

$$p_i = \begin{cases} \bar{P}_i, & \text{if } (\lambda g_i)^{-1} - \sigma_i^2 d_i^{-1} \geq \bar{P}_i, \\ 0, & \text{if } (\lambda g_i)^{-1} - \sigma_i^2 d_i^{-1} \leq 0, \\ (\lambda g_i)^{-1} - \sigma_i^2 d_i^{-1}, & \text{otherwise}. \end{cases}$$

$Proof:$ First, we will show that under condition $(\lambda g_i)^{-1} - \sigma_i^2 d_i^{-1} \geq \bar{P}_i$, the power allocation for SU i is $p_i = \bar{P}_i$. We will prove it by contradiction. Suppose that $p_i \neq \bar{P}_i$, i.e., $0 \leq p_i < \bar{P}_i$ since $p_i \leq \bar{P}_i$. The complementary slackness condition (2.11) implies that $\nu_i = 0$. Substituting $\nu_i = 0$ into (2.12), we can obtain $p_i = (\lambda g_i)^{-1} - \sigma_i^2 d_i^{-1} \geq \bar{P}_i$, which contradicts the assumption that $0 \leq p_i < \bar{P}_i$. Hence, $p_i = \bar{P}_i$, if $(\lambda g_i)^{-1} - (\sigma_i^2) d_i^{-1} \geq \bar{P}_i$. For the other two cases, $(\lambda g_i)^{-1} - \sigma_i^2 d_i^{-1} < \bar{P}_i$. From (2.11), $\nu_i = 0$. Therefore, (2.12) becomes conventional water-filling, and the results follow immediately. ■

Example 2.1 *In Fig. 2.2 we provide an example of power allocation results using the CML water-filling algorithm. All SUs have the same transmit power, and the same power gain to the PU, except that the power gain of SU$_4$ is 1.5 times those of the other SUs. It is seen that the allocated powers for SU$_5$ & SU$_6$ are limited by their transmit*

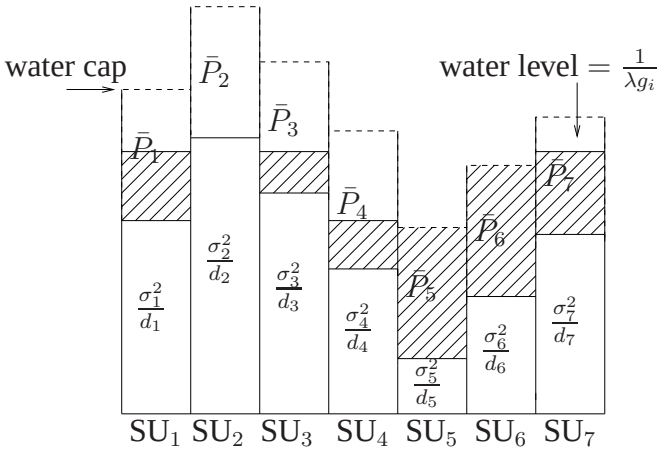

Figure 2.2: An example of power allocation results using CML water filling algorithm. All seven SUs have the same transmit power and same power gain, except that SU$_4$'s power gain is 1.5 times the power gain for others. The shadowed area for each sub-channel denotes the power allocated to the corresponding SU.

powers, while the sub-channel for SU$_2$ is too weak such that no power is allocated to this user. The other sub-channels share the same water level, except that SU$_4$ has a slightly lower level, due to its stronger interference to the PU.

In the CML water-filling algorithm, it is crucial to determine the T-parameter $1/\lambda$ in order to determine water-level for each SU. Let us denote $t_i = g_i(\sigma_i^2/d_i + \bar{P}_i),\ i = 1, 2, \cdots, K$. It is clear that t_i in fact defines the maximum T-parameter which SU$_i$ can support due to its transmit power constraint. We then order all SUs as $t_1 \leq t_2 \leq \cdots \leq t_K$. Next, we define the variable f_j as the interference power introduced by the SUs to the PU when the SUs with index $i \leq j$ use their transmit powers, while the T-parameter for the other SUs is set to be t_j, i.e.,

$$f_j = \sum_{i=1}^{j} g_i \bar{P}_i + \sum_{i=j+1}^{K} g_i \left[\frac{t_j}{g_i} - \frac{\sigma_i^2}{d_i} \right]^+ .$$

Based on these definitions, one can conclude that $f_1 \leq f_2 \leq \cdots \leq f_K$, and f_K corresponds to the case when all SUs use their transmit powers. Thus, for a given Γ, if

$\Gamma > f_K$, all SUs can be allocated with their transmit power. Otherwise, if we can find an index i_0 which satisfies the condition $f_{i_0} \leq \Gamma \leq f_{i_0+1}$, then, for the SUs with index $k \leq i_0$, the transmit power $\bar{P}_k$ will be allocated, while for the SUs with index $k > i_0$, the transmit powers will be less than their transmit powers. Therefore, the interference power introduced by the SUs with index $k \leq i_0$ can be removed because the powers allocated to these SUs are already known, and the power allocation problem becomes

$$\max_{\boldsymbol{p}} \sum_{j=i_0+1}^{K} \log\left(1 + \frac{d_j p_j}{\sigma_j^2}\right) \tag{2.13}$$

$$\text{subject to: } \sum_{j=i_0+1}^{K} g_j p_j \leq \Gamma - \sum_{k=1}^{i_0} g_k \bar{P}_k. \tag{2.14}$$

If $\Gamma \leq f_1$, the T-parameter for all SUs will not reach the lowest t_1, and thus i_0 in (2.14) is set to be zero. The power allocation solution to (2.13) under (2.14) can be derived through modifying the conventional water filling formula.

2.3.2 Multiple PU Constraints

We now consider the scenario with multiple PUs. We start with the two-PU case, for which the optimization problem is formulated as follows:

$$\max_{\boldsymbol{p}} \sum_{i=1}^{K} \log\left(1 + \frac{p_i d_i}{\sigma_i^2}\right) \tag{2.15}$$

$$\text{subject to: } \sum_{i=1}^{K} g_{1,i} p_i \leq \Gamma_1, \text{ and } \sum_{i=1}^{K} g_{2,i} p_i \leq \Gamma_2, \tag{2.16}$$

$$p_i \leq \bar{P}_i, \;\; i = 1, 2, ..., K.$$

Obviously, for any k, if $\sum_{i=1}^{K} g_{k,i} \bar{P}_i \leq \Gamma_k$, then the kth interference power constraint becomes redundant and can be removed. Without loss of generality, assume that no interference constraint is redundant. In a general case, using the KKT approach to solve the above problem will encounter the difficulty in determining $(K+2)$ Lagrange

multipliers. In the following, we decouple the original problem into the following two sub-problems:

1. Sub-problem 1 (SP1):

$$\max_{\boldsymbol{p}} \sum_{i=1}^{K} \log\left(1+\frac{p_i d_i}{\sigma_i^2}\right)$$
$$\text{subject to: } \sum_{i=1}^{K} g_{1,i}p_i \leq \Gamma_1,\ p_i \leq \bar{P}_i,\ i=1,2,...,K.$$

2. Sub-problem 2 (SP2):

$$\max_{\boldsymbol{p}} \sum_{i=1}^{K} \log\left(1+\frac{p_i d_i}{\sigma_i^2}\right)$$
$$\text{subject to: } \sum_{i=1}^{K} g_{2,i}p_i \leq \Gamma_2,\ p_i \leq \bar{P}_i,\ i=1,2,...,K.$$

Clearly, each sub-problem can be solved through the CML water-filling algorithm proposed in Section 2.3.1. Let $\boldsymbol{p}^{(1)}$ be the optimal power allocation vector for SP1, where $p_i^{(1)}$ denotes its ith entry, and $\boldsymbol{p}^{(2)}$ is the optimal power allocation vector corresponding to SP2, where $p_i^{(2)}$ denotes its ith entry. The following lemmas describe the relationship between the globally optimal solution and the optimal solutions, $\boldsymbol{p}^{(1)}$ and $\boldsymbol{p}^{(2)}$, to the sub-problems. We assume that $\boldsymbol{p}^{(1)} \neq \boldsymbol{p}^{(2)}$.

Lemma 2.1 *The two inequalities,* $\sum_{i=1}^{K} g_{2,i}p_i^{(1)} < \Gamma_2$ *and* $\sum_{i=1}^{K} g_{1,i}p_i^{(2)} < \Gamma_1$*, cannot be satisfied simultaneously.*

Lemma 2.2 *If* $\sum_{i=1}^{K} g_{1,i}p_i^{(2)} \leq \Gamma_1$*, then* $\boldsymbol{p}^{(2)}$ *is the globally optimal solution. Similarly, if* $\sum_{i=1}^{K} g_{2,i}p_i^{(1)} \leq \Gamma_2$*, then* $\boldsymbol{p}^{(1)}$ *is the globally optimal solution.*

Lemma 2.3 *If the two inequalities,* $\sum_{i=1}^{K} g_{2,i}p_i^{(1)} > \Gamma_2$ *and* $\sum_{i=1}^{K} g_{1,i}p_i^{(2)} > \Gamma_1$*, are satisfied simultaneously, then the globally optimal power vector must simultaneously satisfy the interference constraints given in* (2.16) *with equality.*

The proofs can be found in Appendices A.1, A.2, and A.3, respectively. For Lemma 2.3, according to the KKT conditions and the Lagrange function, the power allocation formula can be written as

$$p_i = \left[\frac{1}{\lambda_1 g_{1,i} + \lambda_2 g_{2,i} + \nu_i} - \frac{\sigma_i^2}{d_i} \right]^+, \; i = 1, ..., K, \tag{2.17}$$

where λ_1, λ_2, and ν_is are the Lagrange multipliers. Similar to Theorem 2.1, since the transmission powers are upper bounded by the transmit powers, we do not need to compute each ν_i, and the power allocation formula (2.17) can be simplified as

$$p_i = \begin{cases} \bar{P}_i, & \text{if } (\lambda_1 g_{1,i} + \lambda_2 g_{2,i})^{-1} - \sigma_i^2 d_i^{-1} > \bar{P}_i, \\ \left[(\lambda_1 g_{1,i} + \lambda_2 g_{2,i})^{-1} - \sigma_i^2 d_i^{-1} \right]^+, & \text{otherwise.} \end{cases} \tag{2.18}$$

for $i = 1, \cdots, K$. The parameters λ_1 and λ_2 can be obtained by substituting p_i of (2.18) into the following complementary slackness conditions:

$$\lambda_1 \left(\Gamma_1 - \sum_{i=1}^{K} g_{1,i} p_i \right) = 0,$$
$$\lambda_2 \left(\Gamma_2 - \sum_{i=1}^{K} g_{2,i} p_i \right) = 0,$$

Using Lemmas 1, 2, and 3, a recursive decoupled power allocation algorithm, RDPA-2, for the two-PU case is shown in Table 2.1. It starts with the sub-problems with one interference power constraint and K transmit power constraints, and tests each solution in a sequential manner. After obtaining a power vector for a sub-problem, the algorithm checks whether it satisfies the other interference power constraint. If the answer is yes, then exit; otherwise, continue. If neither of the two solutions is globally optimal, then solve the original two-constraint problem to obtain the optimal solution.

Finally, let us examine the case with N $(N > 2)$ PUs. When the N constraints hold with equality simultaneously, similar to (2.18), the optimal power allocation for SU_i is given by

$$p_i = \begin{cases} \bar{P}_i, & \text{if } (\sum_{n=1}^{N} \lambda_n g_{n,i})^{-1} - \sigma_i^2 d_i^{-1} > \bar{P}_i, \\ \left[(\sum_{n=1}^{N} \lambda_n g_{n,i})^{-1} - \sigma_i^2 d_i^{-1} \right]^+, & \text{otherwise.} \end{cases} \tag{2.19}$$

Table 2.1: Recursive Decoupled Power Allocation Algorithm for Two PUs (RDPA-2).

RDPA-2 Algorithm
1. For SP1, use CML water-filling to derive $\boldsymbol{p}^{(1)}$. If $\boldsymbol{p}^{(1)}$ satisfies SP2's constraint, then exit; otherwise, continue.
2. For SP2, use CML water-filling to derive $\boldsymbol{p}^{(2)}$. If $\boldsymbol{p}^{(2)}$ satisfies SP1's constraint, then exit; otherwise, continue.
3. Use (2.18) to compute the optimal power vector.

where λ_n is the Lagrange multiplier for the interference power constraint of the PU$_n$.

Extending the idea of the search procedure for RDPA-2, a generalized algorithm, RDPA-N, is proposed to derive the optimal power allocation for the N-PU case. This algorithm is detailed in Table 2.2. As we can see, it starts with removing noneffective interference power constraints. Suppose that only m effective interference constraints remain. Same as the RDPA-2 algorithm, the RDPA-N algorithm starts with the sub-problems with a single constraint. When reaching to the case with i constraints, the algorithm selects i out of the m constraints, and there are C_m^i combinations. For each combination, the solution to the sub-problem is used to check whether this solution also satisfies the other $(m-i)$ constraints. If yes, the solution is globally optimal, and exit; otherwise, continue. The worse case scenario in terms of complexity occurs when the m constraints hold with equality simultaneously.

2.4 SINR Balancing Problem

Fairness is an important metric to evaluate the network performance, and therefore it often needs to be considered in the network design. Motivated by this, we consider the SINR balancing problem formulated in Section 2.2. We first unify the expressions

Table 2.2: Recursive Decoupled Power Allocation Algorithm for N PUs (RDPA-N).

RDPA-N Algorithm

1. Initialization: $i \leftarrow 0$, $m \leftarrow N$, and the N interference constraints form
   the constraint set (CS)
2. repeat
   $i \leftarrow i + 1$
   If $\sum_{k=1}^{K} g_{i,k}\bar{P}_k \leq \Gamma_i$, remove PU$_i$'s interference constraint from the CS,
   and set $m \leftarrow m - 1$
3. until $i = N$
4. Initialization: $i \leftarrow 0$
5. repeat
   $i \leftarrow i + 1$, $j \leftarrow 0$
   From the m constraints, form i-constraint CSs $S_k^{(i)}$, $k = 1, \cdots, C_m^i$.
   repeat
   $j \leftarrow j + 1$
   For CS $S_j^{(i)}$, use RDPA-i algorithm to compute the optimal power vector $\boldsymbol{p}$.
   Check whether $\boldsymbol{p}$ satisfies the other $(m - i)$ constraints,
   if yes, exit; otherwise, continue.
   until $j = C_m^i$
6. until $i = m - 1$
7. Use (2.19) by setting $N = m$ to obtain the optimal power allocation.

of transmit power and interference power constraints depicted in (2.5) using the single expression $\tilde{\boldsymbol{g}}_l^T \boldsymbol{p} \leq P^{(l)},\ l = 1, \cdots, N+K$, where

$$\tilde{\boldsymbol{g}}_l = \begin{cases} \boldsymbol{e}_l, & l = 1, \cdots, K, \\ \boldsymbol{g}_{l-K}, & l = K+1, \cdots, K+N, \end{cases} \quad \text{and}$$

$$P^{(l)} = \begin{cases} \bar{P}_l, & l = 1, \cdots, K, \\ \Gamma_{l-K}, & l = K+1, \cdots, K+N, \end{cases}$$

with $\boldsymbol{e}_l$ defining the lth column of $\boldsymbol{I}_M$. Thus, (2.4) and (2.5) can be rewritten as

$$\max_{\boldsymbol{U},\boldsymbol{p}} \min_{1 \leq i \leq K} \frac{\text{SINR}_i(\boldsymbol{u}_i, \boldsymbol{p})}{\gamma_i} \tag{2.20}$$

$$\text{subject to: } \tilde{\boldsymbol{g}}_l^T \boldsymbol{p} \leq P^{(l)},\ \ l = 1, \cdots, N+K. \tag{2.21}$$

In the above problem, $N_r \geq K$ is not required. To obtain an insight on how to solve (2.20) subject to (2.21), we first consider the case with two constraints which are, without loss of generality, due to the interference power constraints from two PUs. The above problem becomes

$$\max_{\boldsymbol{U},\boldsymbol{p}} \min_{1 \leq i \leq K} \frac{\text{SINR}_i(\boldsymbol{u}_i, \boldsymbol{p})}{\gamma_i} \tag{2.22}$$

$$\text{subject to: } \sum_{i=1}^{K} g_{1,i} p_i \leq \Gamma_1 \text{ and } \sum_{i=1}^{K} g_{2,i} p_i \leq \Gamma_2.$$

Following the similar arguments in Section 2.3.2, we decompose this two-constraint optimization problem into the following two single-constraint sub-problems:

- Sub-Problem 3 (SP3): The SINR balancing problem with the first interference constraint is described as

$$\max_{\boldsymbol{U},\boldsymbol{p}} \min_{1 \leq i \leq K} \frac{\text{SINR}_i(\boldsymbol{u}_i, \boldsymbol{p})}{\gamma_i} \tag{2.23}$$

$$\text{subject to: } \sum_{i=1}^{K} g_{1,i} p_i \leq \Gamma_1. \tag{2.24}$$

- Sub-Problem 4 (SP4): The SINR balancing problem with the second interference constraint is described as

$$\max_{\boldsymbol{U},\boldsymbol{p}} \min_{1\le i\le K} \frac{\text{SINR}_i(\boldsymbol{u}_i,\boldsymbol{p})}{\gamma_i} \tag{2.25}$$

$$\text{subject to: } \sum_{i=1}^{K} g_{2,i}p_i \le \Gamma_2. \tag{2.26}$$

The SINR balancing problem under a single sum-power constraint was investigated in [72]. In the following, we develop a similar method to solve the single interference constraint problem, and derive the optimal solution of (2.20) under (2.21) by examining its relationship with the optimal solutions to SP3 and SP4.

2.4.1 Solution to the Single Constraint Sub-Problem

Without loss of generality, we consider SP3. Similar to the SINR balancing problem under the sum power constraint [72], an iterative algorithm is adopted to obtain the optimal power allocation and beamforming matrix. In each iteration, two steps are involved. In the first step, the beamforming matrix $\boldsymbol{U}$ is fixed, and the optimal power vector $\boldsymbol{p}$ is identified. In the second step, we fix the updated power vector $\boldsymbol{p}$, and find the corresponding optimal beamforming matrix $\boldsymbol{U}$. One key property for the iterative algorithm is that, for a given beamforming matrix $\boldsymbol{U}$, the optimal power vector must satisfy the following two necessary conditions:

$$\frac{\text{SINR}_i(\boldsymbol{u}_i,\boldsymbol{p})}{\gamma_i} = C_1(\boldsymbol{U},\Gamma_1), \text{ for } i = 1,\cdots,K, \tag{2.27}$$

and

$$\sum_{i=1}^{K} g_{1,i}p_i = \Gamma_1. \tag{2.28}$$

Alternatively speaking, the optimal power allocation leads to the balanced SINR for all SUs, and it satisfies the constraint (2.24) with equality. $C_1(\boldsymbol{U},\Gamma_1)$ in (2.27) is called the balanced SINR level for the SUs, for the given beamforming matrix $\boldsymbol{U}$.

The first step in each iteration is to determine the optimal power allocation $\boldsymbol{p}$ for a fixed beamforming matrix $\boldsymbol{U}$. Let $\boldsymbol{D} = \text{diag}((\gamma_1/(\boldsymbol{u}_1^H \boldsymbol{R}_1 \boldsymbol{u}_1)), \cdots, (\gamma_K/(\boldsymbol{u}_K^H \boldsymbol{R}_K \boldsymbol{u}_K)))$. According the definition of $\text{SINR}_i(\boldsymbol{u}_i, \boldsymbol{p})$ in (2.3), (2.27) can be rewritten as

$$\frac{1}{C_1(\boldsymbol{U}, \Gamma_1)} \boldsymbol{p} = \boldsymbol{D}\boldsymbol{\Psi}^T(\boldsymbol{U})\boldsymbol{p} + \boldsymbol{D}\boldsymbol{q}, \tag{2.29}$$

where $\boldsymbol{q} = \left[\sigma^2 \boldsymbol{I}_K + \boldsymbol{Q}_p\right] \mathbf{1}_K$ with $\boldsymbol{Q}_p = \text{diag}\{(\sum_{n=1}^N \check{p}_n \boldsymbol{u}_1^H \check{\boldsymbol{R}}_n \boldsymbol{u}_1, \cdots, \sum_{n=1}^N \check{p}_n \boldsymbol{u}_K^H \check{\boldsymbol{R}}_n \boldsymbol{u}_K)\}$, and

$$[\boldsymbol{\Psi}(\boldsymbol{U})]_{ik} = \begin{cases} \boldsymbol{u}_k^H \boldsymbol{R}_i \boldsymbol{u}_k, & k \neq i, \\ 0, & k = i. \end{cases}$$

Moreover, (2.28) can be rewritten as

$$\frac{1}{C_1(\boldsymbol{U}, \Gamma_1)} = \frac{1}{\Gamma_1} \boldsymbol{g}_1^T \boldsymbol{D}\boldsymbol{\Psi}^T(\boldsymbol{U})\boldsymbol{p} + \frac{1}{\Gamma_1} \boldsymbol{g}_1^T \boldsymbol{D}\boldsymbol{q}, \tag{2.30}$$

where $\boldsymbol{g}_1 = [g_{1,1}, ..., g_{1,K}]^T$. Eqs. (2.30) and (2.29) can be merged into a matrix eigenvector equation:

$$\frac{1}{C_1(\boldsymbol{U}, \Gamma_1)} \begin{bmatrix} \boldsymbol{p} \\ 1 \end{bmatrix} = \boldsymbol{\Phi}_1(\boldsymbol{U}, \Gamma_1) \begin{bmatrix} \boldsymbol{p} \\ 1 \end{bmatrix}.$$

We define matrix $\boldsymbol{\Phi}_1(\boldsymbol{U}, \Gamma_1)$ as

$$\boldsymbol{\Phi}_1(\boldsymbol{U}, \Gamma_1) = \begin{bmatrix} \boldsymbol{D}\boldsymbol{\Psi}^T(\boldsymbol{U}) & \boldsymbol{D}\boldsymbol{q} \\ \frac{1}{\Gamma_1} \boldsymbol{g}_1^T \boldsymbol{D}\boldsymbol{\Psi}^T(\boldsymbol{U}) & \frac{1}{\Gamma_1} \boldsymbol{g}_1^T \boldsymbol{D}\boldsymbol{q} \end{bmatrix},$$

and define $\tilde{\boldsymbol{p}} = [\boldsymbol{p}^T, 1]^T$. It has been shown in [51] that, for a given $\boldsymbol{U}$, the optimal power allocation corresponds to the unique positive eigenvector of matrix $\boldsymbol{\Phi}_1(\boldsymbol{U}, \Gamma_1)$.

We next consider the second step in each iteration. For the power allocation vector $\boldsymbol{p}$ determined in the first step, using the MMSE criterion, the uplink beamforming vector $\boldsymbol{u}_i$ for SU_i can be updated as:

$$\boldsymbol{u}_i = \alpha_i \Big(\sum_{k \neq i} p_k \boldsymbol{R}_k + \sigma^2 \boldsymbol{I}_{N_r} + \sum_{n=1}^N \check{p}_n \check{\boldsymbol{R}}_n \Big)^{-1} \boldsymbol{h}_i,$$

where α_i is chosen such that $||\boldsymbol{u}_i||^2 = 1$, and $i = 1, \cdots, K$. In [72], the convergence of the iterative algorithm has been proved under the sum-power constraint, where $\boldsymbol{g}_1 = \mathbf{1}_K$, and $\Gamma_1 = P_{\max}$. It is straightforward to prove the convergence of the iterative algorithm for the case where $\boldsymbol{g}_1 \neq \mathbf{1}_K$.

2.4.2 Relationship Between the Multi-Constraint Problem and Single-Constraint Sub-Problems

In this subsection, we will show that the two-constraint problem (2.22) can be completely decoupled into two single-constraint sub-problems. The main results are as follows:

Theorem 2.2 *Between the optimal solutions to the two decoupled single-constraint sub-problems, SP3 and SP4, there is one and only one solution that is the globally optimal solution to the two-constraint problem* (2.22)*.*

To prove the above theorem, we start with considering the computation of the optimal power allocation for a given beamforming matrix. Now the sub-problems SP3 and SP4 can be transformed as:

- Sub-Problem 3' (SP3'): For a given beamforming matrix $\boldsymbol{U}$, the SINR balancing problem with the first interference constraint is described as

$$\max_{\boldsymbol{p}} \min_{1 \leq i \leq K} \frac{\text{SINR}_i(\boldsymbol{u}_i, \boldsymbol{p})}{\gamma_i}$$
$$\text{subject to:} \quad \sum_{i=1}^{K} g_{1,i} p_i \leq \Gamma_1.$$

- Sub-Problem 4' (SP4'): For a given beamforming matrix $\boldsymbol{U}$, the SINR balancing

problem with the second interference constraint is described as

$$\max_{\boldsymbol{p}} \min_{1\le i\le K} \frac{\text{SINR}_i(\boldsymbol{u}_i, \boldsymbol{p})}{\gamma_i}$$
$$\text{subject to: } \sum_{i=1}^{K} g_{2,i} p_i \le \Gamma_2.$$

For a given beamforming matrix $\boldsymbol{U}$, suppose that $\boldsymbol{p}^{(1)} = \left[p_1^{(1)}, \cdots, p_K^{(1)}\right]^T$ and $\boldsymbol{p}^{(2)} = \left[p_1^{(2)}, \cdots, p_K^{(2)}\right]^T$ are the optimal power vectors for SP3' and SP4', respectively, and $C_1(\boldsymbol{U}, \Gamma_1)$ and $C_2(\boldsymbol{U}, \Gamma_2)$ are the corresponding balanced SINR levels. We next examine the relationship between $\boldsymbol{p}^{(1)}$ and $\boldsymbol{p}^{(2)}$. Fig. 2.3 depicts the so-called *admissible* power allocation region in which the two interference power constraints are both satisfied. In this figure, the interference power constraints are depicted as the two slant lines. □ and ◯ represent the optimal power allocation vectors for each sub-problem. The solutions to the two sub-problems yield four possible combinations displaying on the corresponding sub-figures of Fig. 2.3.

- Fig. 2.3 (a) shows that the optimal solution, $\boldsymbol{p}^{(1)}$, for SP3' satisfies the interference constraint of SP4', and that the optimal solution, $\boldsymbol{p}^{(2)}$, for SP4' satisfies the interference power constraint of SP3'.

- Fig. 2.3 (b) shows that the optimal solution, $\boldsymbol{p}^{(2)}$, for SP4' satisfies the interference power constraint of SP3', but the optimal solution, $\boldsymbol{p}^{(1)}$, for SP3' does not satisfy the interference constraint of SP4.

- Fig. 2.3 (c) shows that the optimal solution, $\boldsymbol{p}^{(1)}$, for SP3' satisfies the interference constraint of SP4', but the optimal solution, $\boldsymbol{p}^{(2)}$, for SP4' does not satisfy the interference constraint of SP3'.

- Fig. 2.3 (d) shows that the optimal solution, $\boldsymbol{p}^{(1)}$, for SP3' does not satisfy the interference constraint of SP4', and that the optimal solution, $\boldsymbol{p}^{(2)}$, for SP4' does not satisfy the interference power constraint of SP3' either.

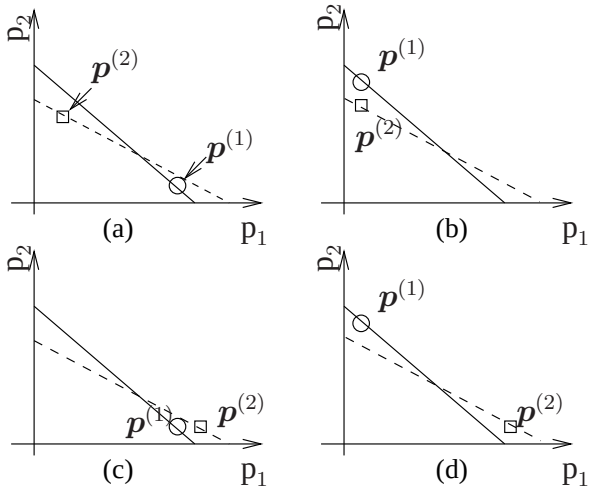

Figure 2.3: The relationship between the optimal solutions to the single constraint subproblems, SP3' and SP4'. The solid slant line represents the interference constraint for PU_1, and the dash slant line represents the constraint for PU_2. $\boldsymbol{p}^{(1)}$, denoted by ◯, indicates the optimal power allocation for SP3'. $\boldsymbol{p}^{(2)}$, denoted by □, represents the optimal power allocation for SP4'.

The following lemmas are used to describe the relationship between $\boldsymbol{p}^{(1)}$ and $\boldsymbol{p}^{(2)}$.

Lemma 2.4 *For a given beamforming matrix $\boldsymbol{U}$, it is infeasible that the two inequalities $\sum_{i=1}^{K} g_{2,i}p_i^{(1)} > \Gamma_2$ and $\sum_{i=1}^{K} g_{1,i}p_i^{(2)} > \Gamma_1$ hold simultaneously. In other words, the case illustrated in Fig. 2.3 (d) can never happen.*

Lemma 2.5 *For a given beamforming matrix $\boldsymbol{U}$, if $\boldsymbol{p}^{(1)}$ does not satisfy the interference constraint for SP4', i.e., $\sum_{i=1}^{K} g_{2,i}p_i^{(1)} > \Gamma_2$, then we have $C_1(\boldsymbol{U}, \Gamma_1) > C_2(\boldsymbol{U}, \Gamma_2)$. Similarly, if $\boldsymbol{p}^{(2)}$ does not satisfy the interference constraint for SP3', i.e., $\sum_{i=1}^{K} g_{1,i}p_i^{(2)} > \Gamma_1$, then we have $C_1(\boldsymbol{U}, \Gamma_1) < C_2(\boldsymbol{U}, \Gamma_2)$.*

Lemma 2.6 *For a given beamforming matrix $\boldsymbol{U}$, it is infeasible that the two inequalities $\sum_{i=1}^{K} g_{2,i}p_i^{(1)} < \Gamma_1$ and $\sum_{i=1}^{K} g_{1,i}p_i^{(2)} < \Gamma_1$ hold simultaneously. In other words, the case for Fig. 2.3 (a) can never happen.*

The proofs can be found in Appendices A.5, A.6, and A.7, respectively. Lemmas 2.4 and 2.6 state that the cases shown in Fig. 2.3 (a) and Fig. 2.3 (d) are not feasible. Thus, the relationship between $\boldsymbol{p}^{(1)}$ and $\boldsymbol{p}^{(2)}$ can only be the case described in either Fig. 2.3 (b) or Fig. 2.3 (c). Lemma 2.4 is an important property which helps to decouple the two constraints completely.

Based on the relationship between the solutions of SP3' and SP4', we proceed to analyze the relationship between the optimal solutions of SP3 and SP4. Assume that $\boldsymbol{p}_o^{(1)}$, $\boldsymbol{U}_o^{(1)}$, and $C_o^{(1)}(\Gamma_1)$ are the optimal power vector, the beamforming matrix, and the balanced SINR level for SP3, respectively, and $\boldsymbol{p}_o^{(2)}$, $\boldsymbol{U}_o^{(2)}$, and $C_o^{(2)}(\Gamma_2)$ are the optimal power vector, the beamforming matrix, and the balanced SINR level for SP4, respectively. We have the following lemma.

Lemma 2.7 *The two inequalities, $\boldsymbol{g}_2^T\boldsymbol{p}_o^{(1)} < \Gamma_2$ and $\boldsymbol{g}_1^T\boldsymbol{p}_o^{(2)} < \Gamma_1$, cannot be satisfied simultaneously.*

The proof can be found in Appendix A.8. We are now ready to provide the proof for Theorem 2.2.

Proof of Theorem 2.2: Suppose that $\hat{\boldsymbol{U}}$ and $\hat{\boldsymbol{p}}$ are the globally optimal beamforming matrix and the power allocation vector, respectively, and $\hat{C}$ is the optimal balanced SINR. First, we show that at least one solution, $\boldsymbol{p}_o^{(1)}$ or $\boldsymbol{p}_o^{(2)}$, is globally optimal solution. We next prove that it is impossible that both $\boldsymbol{p}_o^{(1)}$ and $\boldsymbol{p}_o^{(2)}$ are the optimal solutions of (2.22).

For the fixed beamforming matrix $\hat{\boldsymbol{U}}$, we solve the single-constraint power allocation problems of SP3' and SP4' separately. Let $\hat{\boldsymbol{p}}^{(1)}$ and $\hat{\boldsymbol{p}}^{(2)}$ be the optimal power vectors. According to Lemmas 2.4, 2.5, and 2.6, there is one power vector satisfying the two constraints. Without loss of generality, suppose that $\sum_{i=1}^{K} g_{2,i}\hat{p}_i^{(1)} \leq \Gamma_2$, and $\hat{\boldsymbol{p}}^{(1)}$ is the optimal power allocation for SP3' for the fixed $\hat{\boldsymbol{U}}$.

On the other hand, for the fixed power vector $\hat{\boldsymbol{p}}^{(1)}$, if there exists another beamforming matrix $\widetilde{\boldsymbol{U}}$ which can further optimize the SINR through MMSE, then it contradicts with the fact that $\hat{\boldsymbol{U}}$ is the optimal solution. Therefore, $\hat{\boldsymbol{p}} = \hat{\boldsymbol{p}}^{(1)}$ is the globally optimal solution.

We next consider sub-problem SP3. Since $\hat{\boldsymbol{U}}$ corresponds to the optimal MMSE solution for the fixed power vector $\hat{\boldsymbol{p}}^{(1)}$, and $\hat{\boldsymbol{p}}^{(1)}$ is the optimal power vector for SP3' under a fixed $\hat{\boldsymbol{U}}$, $\hat{\boldsymbol{U}}$ and $\hat{\boldsymbol{p}}^{(1)}$ are the optimal beamforming matrix and power allocation vector for SP3, i.e., $\hat{\boldsymbol{p}}^{(1)} = \boldsymbol{p}_o^{(1)}$ and $\hat{\boldsymbol{U}} = \boldsymbol{U}_o^{(1)}$, according to Theorem 2 in [72]. Since there is a unique solution for SP3 [76], $\boldsymbol{p}_o^{(1)} = \hat{\boldsymbol{p}}^{(1)} = \hat{\boldsymbol{p}}$ arrives, which means that the globally optimal solutions are $\boldsymbol{p}_o^{(1)}$ and $\boldsymbol{U}_o^{(1)}$.

Finally, according to Lemma 2.7, there is only one solution out of the two solutions, $\boldsymbol{p}_o^{(1)}$ and $\boldsymbol{p}_o^{(2)}$, satisfying the two constraints. ■

Theorem 2.2 suggests that the two-constraint SINR balancing problem (2.22) can be decoupled to two single-constraint sub-problems. These single-constraint sub-problems can be solved through the iterative algorithm discussed in Section 2.4.1. Be-

tween the two solutions to the sub-problems, there is one and only one solution that can satisfy the other constraint as well, and thus this solution is the globally optimal solution.

Using induction method, we can extend Theorem 2.2 to solve the SINR balancing problem (2.20) with $(N + K)$ constraints in (2.21).

Theorem 2.3 *The $(N + K)$-constraint SINR balancing problem can be decoupled into $(N + K)$ single-constraint sub-problems. Among these $(N + K)$ solutions of the sub-problems, there is one and only one solution that satisfies all other $(N + K - 1)$ constraints, and this is the optimal solution to the $(N + K)$-constraint SINR balancing problem.*

Theorem 2.3 indicates that there is only one dominant constraint. Thus, the optimal solution of the original $(N+K)$-constraint problem can be found from the optimal solutions of the $(N + K)$ single-constraint sub-problems. If an optimization problem with multiple constraints has such a property, we say that the multi-constraint optimization problem can be *completely decoupled*. Note that in the SINR balancing problem the interference power constraints and transmit power constraints can be equally treated. This property can greatly reduce the computational complexity since finding an optimal solution for a $(N + K)$-constraint problem is usually highly complex while finding the optimal solution to each single-constraint subproblem is much easier. Based on Theorem 2.3, we develop a decoupled multiple-constraint power allocation algorithm (DMCPA) to solve (2.20). This algorithm is detailed in Table 2.3. Note that the search of an optimal solution can be implemented in a sequential manner. It implies that, when a solution to a sub-problem is derived, we only need check whether this solution also satisfies all other $(N + K - 1)$ constraints. If yes, this solution is the globally optimal solution and exit; otherwise, continue to search the solutions for other sub-problems. The average complexity in searching is $(N + K)/2$ times the

Table 2.3: Decoupled Multiple-Constraint Power Allocation Algorithm (DMCPA).

DMCPA Algorithm
1. Initialization: $i \leftarrow 0$
2. repeat
$i \leftarrow i+1$
For sub-problem i, find the optimal beamforming matrix $\boldsymbol{U}_o^{(i)}$ and power vector $\boldsymbol{p}_o^{(i)}$.
Check whether $\boldsymbol{p}_o^{(i)}$ satisfies the other $(N+K-1)$ constraints, if yes, exit; otherwise, continue.
3. until $i = N+K$

complexity for solving the single constraint sub-problem.

Example 2.2 *We provide an example to illustrate the convergence behavior of the power vectors for the SINR balancing problem. We simulate the case where* $K = N_r = 2$ *under two interference power constraints. The thresholds for interference constraints,* Γ_1 *and* Γ_2*, are fixed as* 0 *dB and 0.8 dB, respectively, and the power gain vectors from the SUs to the PUs are* $\boldsymbol{g}_1 = [2, 2]$ *and* $\boldsymbol{g}_2 = [0.8, 2.4]$*, respectively. The convergence behavior of the algorithm and the power vector evolution for the SINR balancing problem are illustrated in Fig. 2.4. In this figure, each point represents a power allocation vector in an iterative step, and the arrow represents the direction of the power allocation evolution. Since each power allocation vector satisfies a constraint with equality, i.e., the vector is on the line corresponding to a constraint, the arrow also locates on the corresponding line. It can be observed from the figure that each sub-problem converges in a few iterative steps. Moreover, there is only one solution satisfying the other constraint. This matches well with Theorem 2.2.*

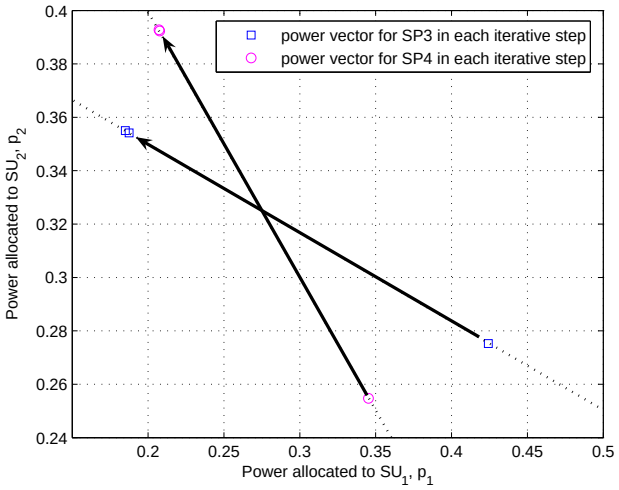

(a) Result 1

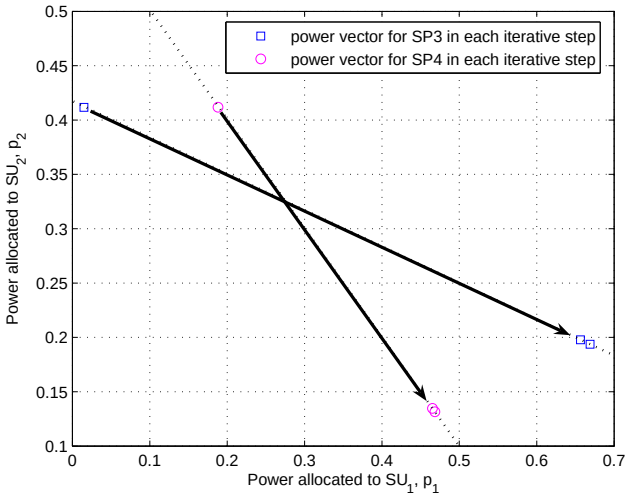

(b) Result 2

Figure 2.4: Two sample results show the convergence behavior of power vectors for SUs using the DMCPA algorithm. ◯ represents a power vector of an iterative step in solving SP3, and it satisfies PU_1's interference constraint. □ represents a power vector of an iterative step in solving SP4, and it satisfies PU_2's interference constraint. The arrows represent the directions of the power vector evolution.

2.5 Numerical Examples

Numerical examples are presented in this section to evaluate the performance of the proposed algorithms. In the examples, for simplicity, we assume that all SUs are at the same distance, l_1, to the BS, and the same distance, $l_2^{(n)}$, to PU$_n$. We also denote by $l_3^{(n)}$ the distance from PU$_n$ to the BS. When there is only one PU, we will drop off the superscripts and use notations l_2 and l_3. Suppose that the same path loss model can be used to describe the transmissions from the SUs to the BS and to the PUs, and from the PUs to the BS, and the path loss exponent is 4. The elements of matrix $\boldsymbol{H}$ are assumed to be circularly symmetric complex Gaussian (CSCG) RVs with mean zero and variance 1. By doing so, the power considered in this chapter is defined as the average received power at each receive antenna of the BS. Thus, $\check{\boldsymbol{h}}_n$ can be modelled as $\check{\boldsymbol{h}}_n = (l_1/l_3^{(n)})^2 \boldsymbol{a}_n$ where $\boldsymbol{a}_n$ is a $N_r \times 1$ vector whose elements are CSCG RVs with mean zero and variance 1, and the power gain factor from the SU$_i$ to the PU$_n$ can be modelled as $g_{n,i} = (l_1/l_2^{(n)})^4 |\alpha_{n,i}|^2$, where $\alpha_{n,i}$ is also modelled as CSCG with mean zero and variance 1. The noise power is set to be 1, and the power and interference power are defined in dB relative to the noise power. For all cases, we choose $\Gamma = 0$ dB and ignore the interference from the PUs to the BS of the SUs, unless it is specifically stated. When evaluating different schemes, we consider the performance of the average achievable sum-rate and average maximum SINR for CR SIMO-MAC calculated over 2000 block fading channels.

2.5.1 Sum-Rate Performance

We first consider the case with a single PU, and choose l_1 such that $\bar{P}_i = 20$ dB for each SU. Fig. 2.5 shows the average achievable sum-rate with respect to the value of l_2/l_1 for different combinations of K and N_r. It is seen that when the ratio l_2/l_1 is smaller than a threshold, the sum-rate increases as the ratio increases. This is due to the fact

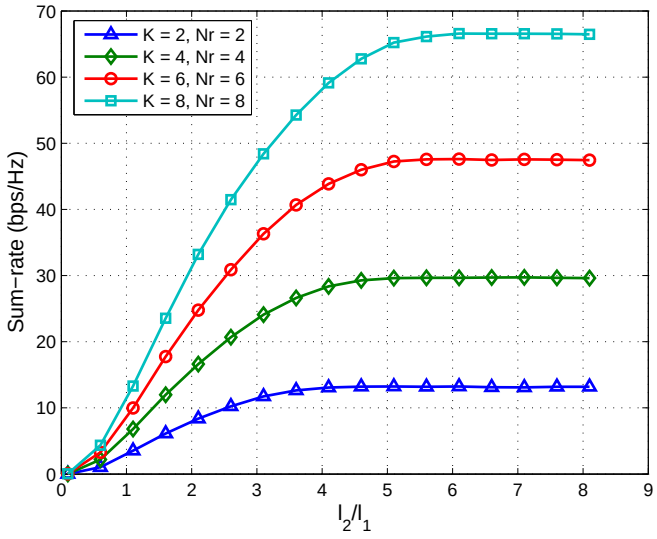

Figure 2.5: Achievable sum-rate vs the ratio of l_2/l_1 using the CML water filling algorithm for different numbers of K and N_r: one PU and $\bar{P}_i = 20$ dB.

that the interference constraint becomes less tight as the PU moves away from the SUs. However, when l_2/l_1 reaches a certain threshold (called turning point), the sum-rate will not further increase. This is because the transmit power constraint is the dominant constraint affecting the achievable sum-rate in the case that the PU is far away from the SUs. Furthermore, when the number of SU increases, the interference increases for a given distance, and thus the required distance for turning point happening increases.

We next evaluate the effect of the interference from the PU on the achievable sum-rate of the CR SIMO-MAC. Again, we consider a single PU. Fig. 2.6 shows the average achievable sum-rate with respect to various number K of SUs when $N_r = 6$, $l_2/l_1 = 4$, and $\check{p}_1 = 10$ dB. The distances from PU to the BS are chosen as $l_3/l_1 = 5, 4$ and 3, respectively. As can be seen, when K increases, the achievable sum-rate increases. Furthermore, when the PU moves further away from the BS, the effect of the PU's interference on the achievable sum-rate decreases.

We then consider the scenario when the feedback matrix $\boldsymbol{G}$ is imperfect. In this

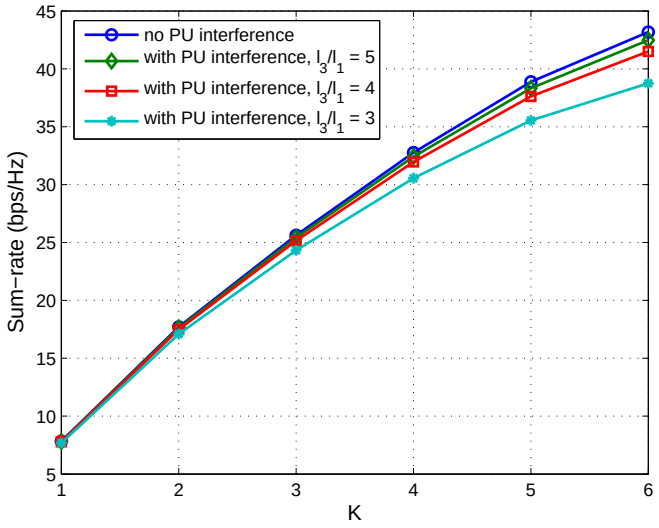

Figure 2.6: Effect of PU interference on the achievable sum-rate of the CR SIMO-MAC: one PU, $l_2/l_1 = 4$, $N_r = 6$, $\bar{P}_i = 20$ dB and $\check{p}_1 = 10$ dB.

example, when the estimated matrix $\boldsymbol{G}$ is modelled, the estimated fading coefficient $\hat{\alpha}_{n,i}$ is different from its exact value $\alpha_{n,i}$ by a CSCG RV $b\beta_{n,i}$, where $\beta_{n,i}$ is a CSCG RV with mean zero and variance 1. We choose $b = 0.1$. When the estimated matrix $\boldsymbol{G}$ is imperfect, the interference received at the PU may exceed the preset threshold, and thus we use outage probability to define how frequently this case happens. Furthermore, in order to reduce this outage probability, we propose a robust design method which chooses a smaller interference power threshold in the algorithms as compared to the exact threshold the PU can tolerate.

Fig.2.7 shows the achievable sum-rate versus l_2/l_1 for the case with perfect $\boldsymbol{G}$ and the cases with estimated $\boldsymbol{G}$ and various interference power threshold Γ used in robust algorithm design. It is seen that if the PU is far away from the BS ($l_2/l_1 > 6$), the achievable sum-rate is almost not affected by the estimated errors in $\boldsymbol{G}$ even if the interference power threshold is set to be 2 dB lower than the target. However, when the PU is closer to the BS, the achievable sum-rate will decrease if the interference power

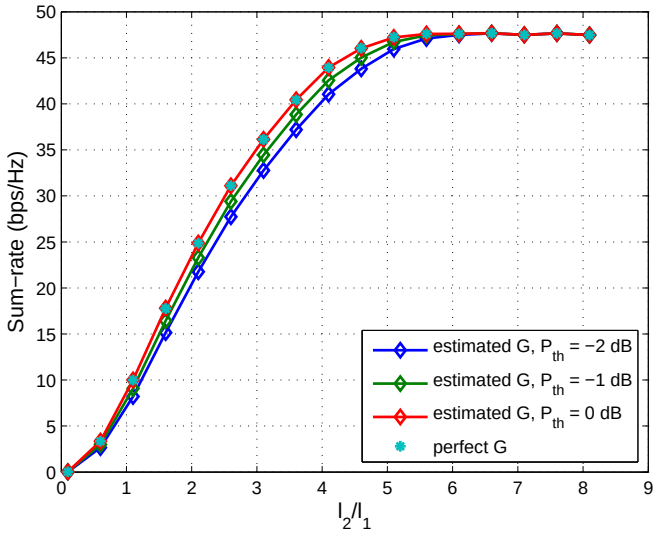

Figure 2.7: Achievable sum-rate vs the ratio of l_2/l_1 for perfect and estimated matrix $\boldsymbol{G}$: one PU, $N_r = K = 6$ and $\bar{P}_i = 20$ dB. Robust design with 1 dB and 2 dB margins are also considered.

threshold is set to be lower than the target. In Fig.2.8, we plot the outage probability for the case when $l_2/l_1 = 5$. It is seen that the outage probability can be as high as 20% if the algorithm uses the exact target (0 dB) as the algorithm input; however, if we use the robust design with 2 dB margin, the outage probability drops below 1%.

Fig. 2.9 shows the average achievable sum-rate versus transmit power, ranging from 0 dB to 30 dB, for $K = N_r = 4$ and different values of l_2/l_1. It can be seen that in low transmit power constraint region, average sum-rate increases as the transmit power increases, due to transmit power constraint dominates the final result. In the case where the transmit power is very high, the interference constraint is dominant, and therefore the sum-rate does not further increase with an increase of the transmit power.

In Fig. 2.10, we consider the two-PU case where $K = N_r = 3$ and $\bar{P}_i = 20$ dB. In this example, $l_2^{(2)}/l_1$ ranges from 0.1 to 4.6, and $l_2^{(1)}/l_1$ is fixed as 3. It can be

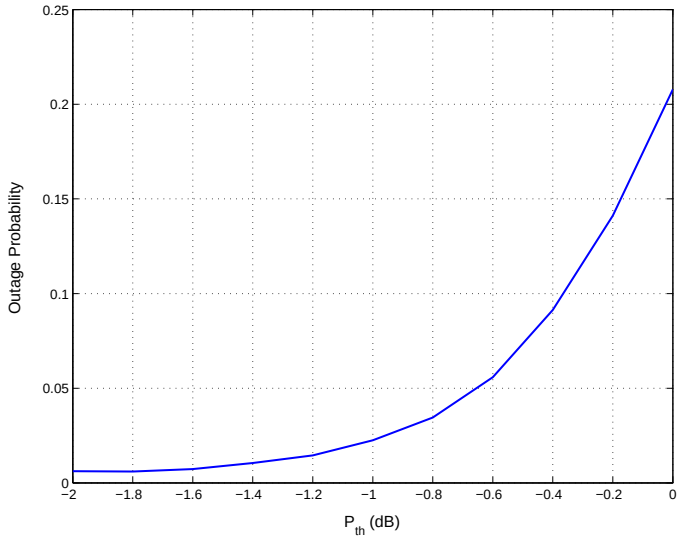

Figure 2.8: Outage probability for interference power to PU: one PU, $l_2/l_1 = 5$, $N_r = K = 6$ and $\bar{P}_i = 20$ dB.

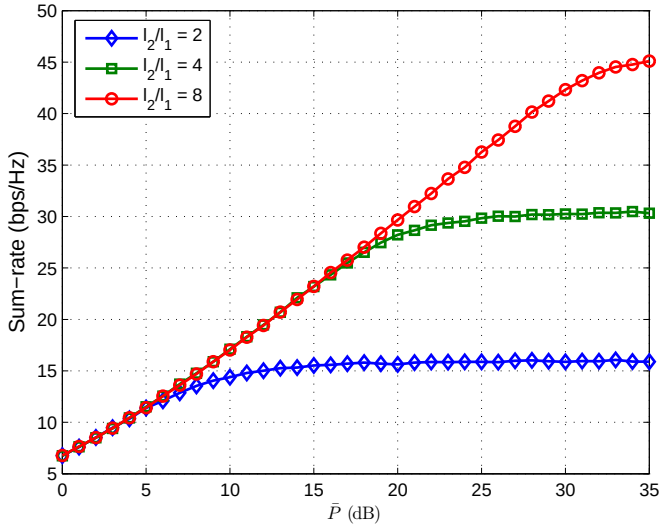

Figure 2.9: Achievable sum-rate vs transmit power using the CML water filling algorithm for different l_2/l_1: one PU and $K = N_r = 4$.

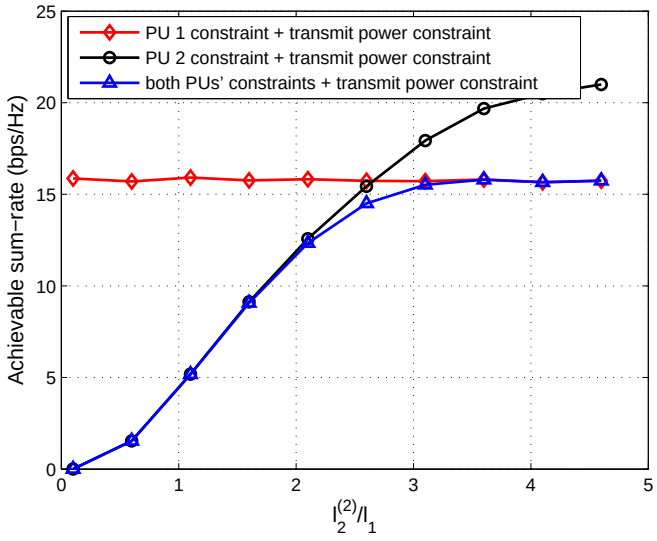

Figure 2.10: Achievable sum-rate vs the ratio of $l_2^{(2)}/l_1$ under different constraints: two PUs, $K = N_r = 3$, $l_2^{(1)}/l_1 = 3$ and $\bar{P}_i = 20$ dB.

observed from Fig. 2.10 that the achievable sum-rate under the interference constraint for PU_1 is a straight line, which can be explained by the fact that $l_2^{(1)}$ is a constant. We also observe that the sum-rate increases as $l_2^{(2)}/l_1$ increases under the interference constraint for PU_2. This is because the constraint becomes less tight when $l_2^{(2)}/l_1$ increases. Moreover, the achievable sum-rate under two constraints is always less than or equal to the achievable sum-rate under a single constraint. This is also reasonable, since the feasible region of two constraints is a subset of the feasible region of a single constraint.

2.5.2 SINR Balancing Performance

We now evaluate the performance of the proposed DMCPA under the sum-power and interference power constraints. For comparison, the method of [72] is also simulated for the case where a single sum-power constraint is considered. We choose $K = N_r = 3$, and set the target SINRs, $\gamma_1, \cdots, \gamma_K$, for SUs as 1. By doing so, we seek to

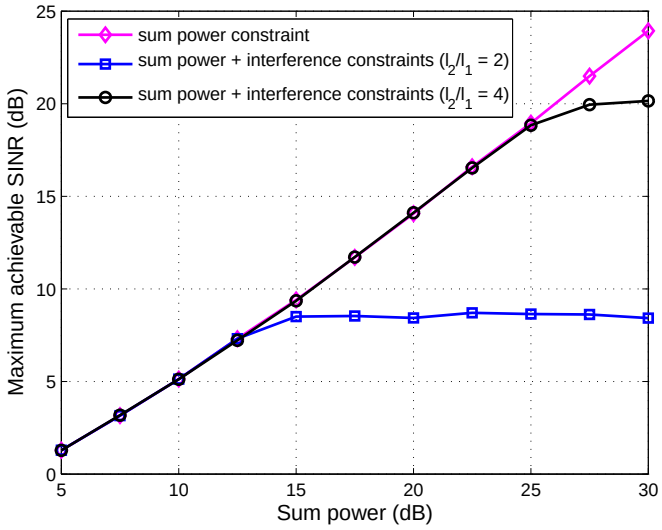

Figure 2.11: Maximum achievable SINR versus the sum-power using the DMCPA algorithm: one PU and $K = N_r = 3$.

maximize the minimal SINR among all the SUs, and thus all SUs will have the same achievable SINR.

Fig. 2.11 illustrates the maximum achievable SINR under a single sum-power constraint, as well as those with an additional interference power constraint for different values of l_2/l_1. It can been seen that when the PU is close to the SUs, the maximum achievable SINR in dB almost linearly increases with the sum-power in dB. When the sum-power reaches a large value, the achievable SINR saturates, due to the existence of the interference constraint, which does not allow the transmission power to further increase. Obviously, when the distance changes from $l_2/l_1 = 2$ to $l_2/l_1 = 4$, the sum-power associated with the turning point also increases.

Finally, we consider the case with two PUs, where the distance, $l_2^{(1)}$, between PU_1 and the SUs is half the distance, $l_2^{(2)}$, between PU_2 and the SUs. Fig. 2.12 shows the maximum achievable SINRs under each individual constraint (20 dB transmit power constraint, and 0 dB interference power constraint for each PU), as well as that un-

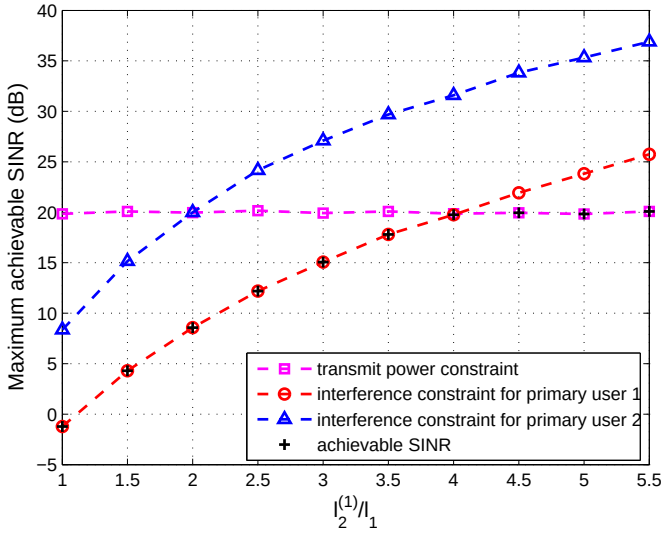

Figure 2.12: Maximum achievable SINR versus the ratio of $l_2^{(1)}/l_1$ using the DMCPA algorithm: two PUs, $K = N_r = 3$, $l_2^{(2)} = 2l_1^{(1)}$ and $\bar{P}_i = 20$ dB.

der all constraints. If only the transmit power constraint is considered, the maximum achievable SINR is around 20 dB. This implies that the linear MMSE receiver used at the BS can suppress the strong interference from the other SUs. The achievable SINR associated with the interference constraint for PU_2 is higher than that with the interference constraint for PU_1, since PU_2 is further away from the SUs. Finally, for a fixed distance, as we can see, the achievable SINR is just the minimum value of the three SINRs achieved under each individual constraint.

2.6 Conclusions

In this chapter, we have studied the problem of joint beamforming and power allocation for CR SIMO-MAC. Two optimization problems have been formulated: the sum-rate maximization problem and SINR balancing problem, both under the transmit power constraints as well as interference power constraints. For the sum-rate maximization

problem, ZF-DFE is used to decouple the SIMO-MAC, and a capped multi-level water-filling algorithm was proposed to maximize the achievable sum-rate of the SUs when a single PU is present. When multiple PUs exist, a recursive decoupled power allocation algorithm was proposed to derive the optimal power allocation solution. For the SINR balancing problem, it was shown that, using linear MMSE receivers, each of the interference constraints and transmit power constraints can be completely decoupled, and thus the multi-constraint optimization problem can be solved through finding the solutions to each single-constraint sub-problems. Numerical examples were presented to compare the performances of different schemes.

Chapter 3

Transmit Optimization for CR MIMO-BC

This chapter studies the capacity computation problem for spectrum sharing based CR MIMO-BC. By establishing a new BC-MAC duality, the problem is transformed into an equivalent capacity computation for the dual MIMO-MAC. Moreover, we develop an efficient subgradient based iterative algorithm to solve the equivalent problem and show that the developed algorithm converges to a globally optimal solution. This new BC-MAC duality can be extended to solve the capacity computation problem for the MIMO-BC with multiple linear constraints.

3.1 Introduction

In MIMO-BC, the BS equipped with multiple transmit antennas sends independent messages to each of multiple users, which are equipped with multiple receive antennas. In the past decade, a great deal of research has been focused on the characterization of optimal transmission schemes for MIMO-BC [33, 52, 77–80]. Due to the coupled structure of the transmitted signals, the optimization problems associated with the BC

are usually non-convex. The key technique used to overcome this difficulty is to transform the BC problem into a convex MAC problem via a so-called BC-MAC duality relationship. Under a single sum power constraint, the capacity region (or SINR region) of a BC is identical to that of a dual MAC under the same sum power constraint. This property is called the conventional BC-MAC duality [33, 77, 81, 82], which was first observed by Rashid-Rarrokhi *et al.* [33]. However, the conventional BC-MAC duality is not applicable only to the case with multiple power constraints. To solve this problem, a novel minimax BC-MAC duality is developed in [83], where the new equivalent MAC problem has a minimax formulation. Although the minimax duality results can handle the BC problem with per-antenna power constraints [79], only interior point algorithms can be applied to solve this minimax problem, and high-efficiency algorithms, such as the iterative water-filling algorithm [47], cannot be applied.

In this chapter, we consider the capacity computation problem for spectrum sharing based CR MIMO-BC, in which the BS is subject to the transmit power constraint as well as the interference power constraint. As discussed above, the conventional BC-MAC duality cannot be applied to MIMO-BC with multiple linear constraints. To handle this difficulty, we propose a generalized BC-MAC duality result that can solve MIMO-BC problems with multiple linear constraints. Moreover, a subgradient based algorithm is developed to solve the capacity computation problem for CR MIMO-BC.

The rest of the chapter is organized as follows. In Section 3.2, the system model of the CR MIMO-BC is introduced, and the capacity computation problem is formulated. In Section 3.3, we transform the capacity computation into its equivalent form, and introduce the general MAC-BC duality between a MIMO-BC and its dual MIMO-MAC. Section 3.4 presents an primal dual method based iterative to solve the capacity computation problem for the dual MIMO-MAC. Section 3.5 develops the complete algorithm to solve the capacity computation problem for CR MIMO-BC. Section 3.6 provides several numerical examples. Finally, Section 3.7 concludes the chapter.

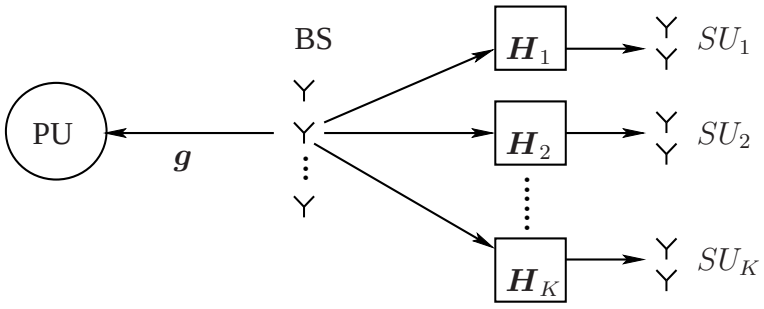

Figure 3.1: The system model for CR MIMO-BC. There are K SUs and one PUs. The BS has N_t transmit antennas, each SU is equipped with N_r receive antennas, and the PU is equipped with a single receive antenna.

3.2 System Model and Problem Formulation

Consider a spectrum sharing based CR MIMO-BC, where the BS is equipped with N_t transmit antennas and there are K SUs with N_r receive antennas. The CR MIMO-BC, as shown in Fig. 3.1, share the same spectrum with a single PU equipped with one transmit antenna[1]. The transmit-receive signal model from the BS to the ith SU denoted by SU$_i$, for $i = 1, \ldots, K$, can be expressed as

$$\boldsymbol{y}_i = \boldsymbol{H}_i \boldsymbol{x} + \boldsymbol{z}_i, \tag{3.1}$$

where $\boldsymbol{y}_i$ is the $N_r \times 1$ received signal vector, $\boldsymbol{H}_i$ is the $N_r \times N_t$ channel matrix from the BS to the SU$_i$, $\boldsymbol{x}$ is the $N_t \times 1$ transmitted signal vector, and $\boldsymbol{z}_i$ is the $N_r \times 1$ Gaussian noise vector with entries being independent identically distributed RVs with means zero and variances σ^2. Consider $\boldsymbol{g}$ as the $N_t \times 1$ channel gain vector between the transmitters of the BS and the PU. We further assume that $\boldsymbol{H}_i$ for $i = 1, \ldots, K$, and $\boldsymbol{g}$ remain constant during a transmission block and change independently from

[1]We consider a single PU case in the rest of this chapter for convenience of description. The results derived for the single PU case can be readily extended to the case with multiple PUs, which is discussed in Remark 3.4.

block to block, and $\boldsymbol{H}_i$ for $i = 1, \ldots, K$, and $\boldsymbol{g}$ are perfectly known to the BS and SU$_i$. To acquire channel matrices $\boldsymbol{H}_i$ and channel vector $\boldsymbol{g}$ at the BS of the SUs, transmission protocols need to be carefully designed to incorporate certain cooperation in terms of parameter feedback between the PU and the BS. As an example, the BS need transmit pilot symbols to allow the SUs and PU to obtain respective estimates of channel matrices $\boldsymbol{H}_i$ and channel vector $\boldsymbol{g}$. Such estimates are needed to be fed back to the BS via feedback channels.

We next consider the weighted sum rate maximization problem for CR MIMO-BC, which is also called capacity computation problem[2]. Mathematically, the problem is formulated as

$$\textbf{Main Problem } (\mathbf{Pa}): \max_{\{\boldsymbol{S}_i^{\mathrm{b}}\}_{i=1}^K:\, \boldsymbol{S}_i^{\mathrm{b}} \succeq 0} \sum_{i=1}^K w_i r_i^{\mathrm{b}} \quad \text{subject to: } \sum_{i=1}^K \boldsymbol{g}^H \boldsymbol{S}_i^{\mathrm{b}} \boldsymbol{g} \le \Gamma, \text{ and } \sum_{i=1}^K \mathrm{tr}(\boldsymbol{S}_i^{\mathrm{b}}) \le \bar{P}, \tag{3.2}$$

where r_i^{b} is the rate achieved by SU$_i$, w_i is the weight of SU$_i$, $\boldsymbol{S}_i^{\mathrm{b}} = \mathbb{E}[\boldsymbol{x}\boldsymbol{x}^H]$ denotes the $N_t \times N_t$ transmit covariance matrix for SU$_i$, $\boldsymbol{S}_i^{\mathrm{b}} \succeq 0$ indicates that $\boldsymbol{S}_i^{\mathrm{b}}$ is a semidefinite matrix, Γ denotes the interference threshold of the PU, and $\bar{P}$ denotes the sum power constraint at the BS. Compared with the capacity computation problem under a non-CR setting, the key difference is that in addition to the sum power constraint, an interference constraint is applied to the SUs in the CR MIMO-BC, i.e., the total received interference power $\sum_{i=1}^K \boldsymbol{g}^H \boldsymbol{S}_i^{\mathrm{b}} \boldsymbol{g}$ at the PU is below the threshold Γ.

Remark 3.1 *It has long been observed that the optimal sum rate for MIMO-BC with a single sum power constraint is equal to the optimal sum rate of the dual MIMO-MAC with the same sum power constraint [48, 52, 82]. We simply term this property as the*

[2]It is worth to note that any boundary point of the capacity regions of the MIMO-MAC and the MIMO-BC can be expressed as a weighted sum rate for a certain choice of weights [46] [84]. Thus, by varying the weights of the SUs in (**Pa**), the entire capacity region of the CR MIMO-BC can be obtained.

conventional BC-MAC duality. However, the conventional BC-MAC duality can only be applied to the case with a single sum power constraint (even not applicable to an arbitrary linear power constraint). Hence, the additional interference power constraint in ($\mathbf{Pa}$*) makes the existing duality cannot be applied. In this chapter, we proposed a new BC-MAC duality result which generalizes the previous results as special cases.*

3.3 Equivalence and Duality

Evidently, the MIMO-BC capacity computation problem under either a non-CR or a CR setting is a non-convex optimization problem and is difficult to solve directly. Under a single sum power constraint, the capacity computation problem for MIMO-BC can be transformed to its dual MIMO-MAC problem, which is convex and can be solved in an efficient manner [77]. In the CR setting, the problem ($\mathbf{Pa}$) has not only a sum power constraint but also an interference constraint. The imposed multiple constraints render difficulty to formulate an efficiently solvable dual problem. To overcome the difficulty, we first transform this multi-constrained capacity computation problem ($\mathbf{Pa}$) into its equivalent problem which has a single constraint with multiple auxiliary variables, and next develop a duality between a MIMO-BC and a dual MIMO-MAC in the case where the multiple auxiliary variables are fixed.

3.3.1 An Equivalent MIMO-BC Capacity Computation Problem

In the following, by exploiting Theorem 4 in [85], we present an equivalent form of ($\mathbf{Pa}$)

Theorem 3.1 *Problem (*$\mathbf{Pa}$*) shares the same optimal solution with*

$$\textbf{\textit{Equivalent Problem}}\ (\mathbf{Pb}): \min_{q_t\geq 0,\ q_u\geq 0} \max_{\{\boldsymbol{S}_i^b\}_{i=1}^K:\ \boldsymbol{S}_i^b\succeq 0} \sum_{i=1}^{K} w_i r_i^b \tag{3.3}$$

$$\textit{subject to: } q_t\big(\sum_{i=1}^{K} \boldsymbol{g}^H \boldsymbol{S}_i^b \boldsymbol{g} - \Gamma\big) + q_u\big(\sum_{i=1}^{K} tr(\boldsymbol{S}_i^b) - \bar{P}\big) \leq 0, \quad (3.4)$$

where q_t and q_u are the auxiliary dual variables for the respective interference constraint and sum power constraint.

Finding an efficiently solvable dual problem for $(\mathbf{Pb})$ directly is still difficult. However, as we show later, when q_t and q_u are fixed as constants, $(\mathbf{Pb})$ reduces to a simplified form, which we can solve by applying the following duality result.

3.3.2 CR BC-MAC Duality

For fixed q_t and q_u, $(\mathbf{Pb})$ reduces to the following form

$$\textbf{CR MIMO-BC Problem } (\mathbf{Pc}): \max_{\{\boldsymbol{S}_i^{\mathrm{b}}\}_{i=1}^K:\, \boldsymbol{S}_i^{\mathrm{b}} \succeq 0} \sum_{i=1}^{K} w_i r_i^{\mathrm{b}} \quad (3.5)$$

$$\text{subject to: } q_t \sum_{i=1}^{K} \boldsymbol{g}^H \boldsymbol{S}_i^{\mathrm{b}} \boldsymbol{g} + q_u \sum_{i=1}^{K} \mathrm{tr}(\boldsymbol{S}_i^{\mathrm{b}}) \leq P, \quad (3.6)$$

where $P := q_t\Gamma + q_u\bar{P}$. Since q_t and q_u are fixed, P is a constant in $(\mathbf{Pc})$. The constraint (3.6) is not a single sum power constraint, and thus the duality result established in [77] is not applicable to $(\mathbf{Pc})$. Therefore, we formulate the following new dual MAC problem.

Theorem 3.2 *The dual MAC problem of $(\mathbf{Pc})$ is*

$$\textbf{\textit{CR MIMO-MAC Problem}} \ (\mathbf{Pd}): \max_{\{\boldsymbol{S}_i^{m}\}_{i=1}^K:\, \boldsymbol{S}_i^{m} \succeq 0} \sum_{i=1}^{K} w_i r_i^{m} \quad (3.7)$$

$$\textit{subject to: } \sum_{i=1}^{K} tr(\boldsymbol{S}_i^{m})\sigma^2 \leq P, \quad (3.8)$$

where r_i^{m} is the rate achieved by the ith user of the dual MAC, and $\boldsymbol{S}_i^{\mathrm{m}}$ is the transmit covariance matrix of the ith user, and the noise covariance at the BS is $q_t\boldsymbol{g}\boldsymbol{g}^H + q_u\boldsymbol{I}_{N_t}$.

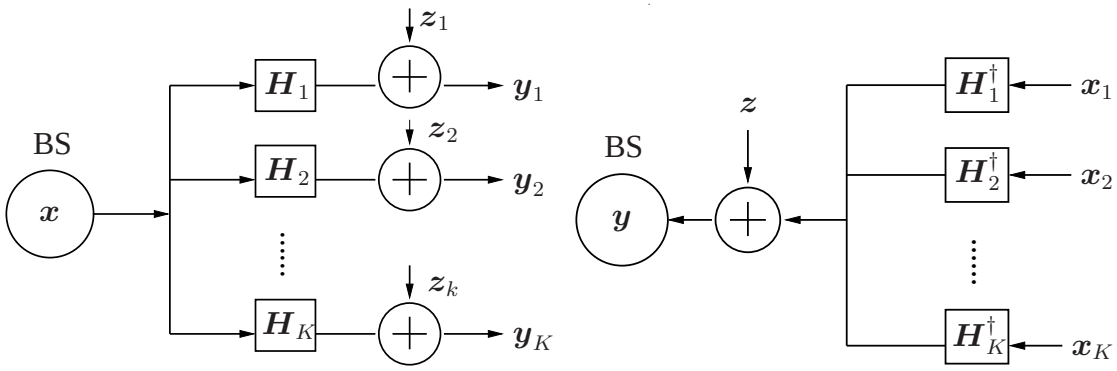

BC, $\boldsymbol{z}_i \sim \mathcal{N}(0, \sigma^2 \boldsymbol{I}_{N_r})$, Dual MAC, $\boldsymbol{z} \sim \mathcal{N}(0, q_t \boldsymbol{R}_o + q_u \boldsymbol{I}_{N_t})$,

$q_t \sum_{i=1}^K \boldsymbol{g}^\dagger \boldsymbol{S}_i^{\mathrm{b}} \boldsymbol{g} + q_u \sum_{i=1}^K \mathrm{tr}(\boldsymbol{S}_i^{\mathrm{b}}) \leq P$ $\sum_{i=1}^K \mathrm{tr}(\boldsymbol{S}_i^{\mathrm{m}})\sigma^2 \leq P,\ \boldsymbol{R}_o = \boldsymbol{g}\boldsymbol{g}^H$

Figure 3.2: The system models for $(\mathbf{Pc})$ and $(\mathbf{Pd})$, where q_t and q_u are constant, and $\boldsymbol{R}_o = \boldsymbol{g}\boldsymbol{g}^\dagger$.

Remark 3.2 *According to Theorem 3.2, for fixed q_t and q_u, the optimal weighted sum rate of the dual MAC is equal to the optimal weighted sum rate of the primal BC. From the formulation perspective, this duality result is quite similar to the conventional duality in [52] [82] [48]. However, as shown in Fig. 3.2, one thing needs to highlight is that the noise covariance matrix of the dual MAC is a function of the auxiliary variable q_t and q_u, instead of the identity matrix [48]. This difference comes from the constraint* (3.6)*, which is not a sum power constraint as in [48]. Note that when $q_t = 0$, the duality result reduces to the conventional BC-MAC duality in [48]. Compared with the minimax duality in [79], our duality result has a simpler format.*

As illustrated in Fig. 3.2, Theorem 3.2 describes a capacity computation problem for a dual MIMO-MAC. To prove this theorem, we first examine the relation between the SINR regions of the MIMO-BC and the dual MIMO-MAC. Based on this relation, we will show that the achievable rate regions of the MIMO-BC and the dual MIMO-

MAC are the same.

In the sequel, we first describe the definition of the SINR for the MIMO-BC. It has been shown in [67] that the dirty paper coding (DPC) [86] is a capacity achieving scheme. Each set of the transmit covariance matrix determined by DPC scheme defines a set of transmit and receive beamforming vectors, and each pair of these transmit and receive beamforming vectors forms a data stream. In a beamforming perspective, the BS transmitter have $N_t \times K$ beamformers, $\boldsymbol{u}_{i,j}$, for $i = 1, \cdots, K$, and $j = 1, \cdots, N_t$. Therefore, the transmit signal can be represented as

$$\boldsymbol{x} = \sum_{i=1}^{K} \sum_{j=1}^{N_t} x_{i,j} \boldsymbol{u}_{i,j},$$

where $x_{i,j}$ is a scalar representing the data stream transmitted in this beamformer, and $\mathbb{E}[x_{i,j}^2] = p_{i,j}$ denotes the power allocated to this beamformer. At SU_i, the receive beamformer corresponding to $\boldsymbol{u}_{i,j}$ is denoted by $\boldsymbol{v}_{i,j}$. The transmit beamformer $\boldsymbol{u}_{i,j}$ and the power $p_{i,j}$ can be obtained via the eigenvalue decomposition of $\boldsymbol{S}_i^{\text{b}}$, i.e., $\boldsymbol{S}_i^{\text{b}} = \boldsymbol{U}_i^H \boldsymbol{P}_i \boldsymbol{U}_i$, where $\boldsymbol{U}_i$ is a unitary matrix, and $\boldsymbol{P}_i$ is a diagonal matrix. The transmit beamformer $\boldsymbol{u}_{i,j}$ is the jth column of $\boldsymbol{U}_i$, and $p_{i,j}$ is the jth diagonal entry of $\boldsymbol{P}_i$. With these notations, we express the $\text{SINR}_{i,j}^{\text{b}}$ as

$$\text{SINR}_{i,j}^{\text{b}} = \frac{p_{i,j} |\boldsymbol{u}_{i,j}^H \boldsymbol{H}_i^H \boldsymbol{v}_{i,j}|^2}{\sum_{k=i+1}^{K} \sum_{l=1}^{N_r} p_{k,l} |\boldsymbol{u}_{k,l}^H \boldsymbol{H}_i^H \boldsymbol{v}_{i,j}|^2 + \sum_{l=j+1}^{N_r} p_{i,l} |\boldsymbol{u}_{i,l}^H \boldsymbol{H}_i^H \boldsymbol{v}_{i,j}|^2 + \sigma^2}. \quad (3.9)$$

It can be observed from (3.9) that the DPC scheme is applied. This can be interpreted as follows. The signal from SU_1 is first encoded with the signals from other SUs being treated as interference. The signal from SU_2 is next encoded by using the DPC scheme. Signals from the other SUs will be encoded sequentially in a similar manner. For the data streams within SU_i, the data stream 1 is also encoded first while the other data streams are treated as the interference. The data stream 2 is encoded next. In a similar manner, the other data streams will be sequentially encoded. The encoding order is

assumed to be arbitrary at this moment, and the optimal encoding order $(\mathbf{Pb})$ will be discussed in Section 3.4.

To explore the relation of the SINR regions of the dual MAC and the BC, we formulate the following optimization problem

$$\begin{aligned} \min_{\{\boldsymbol{S}_i^{\mathrm{b}}\}_{i=1}^K:\, \boldsymbol{S}_i^{\mathrm{b}} \succeq 0} \; & q_t \sum_{i=1}^{K} \boldsymbol{g}^H \boldsymbol{S}_i^{\mathrm{b}} \boldsymbol{g} + q_u \sum_{i=1}^{K} \mathrm{tr}(\boldsymbol{S}_i^{\mathrm{b}}) - P \\ \text{subject to: } & \mathrm{SINR}_{i,j}^{\mathrm{b}} \geq \gamma_{i,j}, \end{aligned} \tag{3.10}$$

where $\gamma_{i,j}$ denotes the SINR threshold of the jth data stream within the SU_i for the BC. Note that the objective function in (3.10) is a function of signal covariance matrices and the constraints are SINR constraints for the CR MIMO-BC.

It has been shown in [79] and [50] that the *non-convex* BC sum power minimization problem under the SINR constraints can be solved efficiently via its dual MAC problem, which is a convex optimization problem. By following a similar line of thinking, the problem in (3.10) can be efficiently solved via its dual MAC problem. Similar to the primal MIMO-BC, the dual MIMO-MAC depicted in Fig. 3.2 consists of K users each with N_r transmit antennas, and one BS with N_t receive antennas. By transposing the channel matrix and interchanging the input and output signals, we obtain the dual MIMO-MAC from the primal MIMO-BC. For the covariance matrices $\boldsymbol{S}_i^{\mathrm{m}}$ of the dual MIMO-MAC, we apply the eigenvalue decomposition,

$$\boldsymbol{S}_i^{\mathrm{m}} = \boldsymbol{V}_i \boldsymbol{\Lambda}_i \boldsymbol{V}_i^H = \sum_{j=1}^{N_r} q_{i,j} \boldsymbol{v}_{i,j} \boldsymbol{v}_{i,j}^H, \tag{3.11}$$

where $\boldsymbol{v}_{i,j}$ is the jth column of $\boldsymbol{V}_i$, and $q_{i,j}$ is the jth diagonal entry of $\boldsymbol{\Lambda}_i$. For user i, $\boldsymbol{v}_{i,j}$ is the transmit beamforming vector of the jth data stream, the power allocated to the jth data stream equals $q_{i,j}$, and the receive beamforming vector of the jth data stream at the BS is $\boldsymbol{u}_{i,j}$. The SINR of the dual MIMO-MAC is given by

$$\mathrm{SINR}_{i,j}^{\mathrm{m}} = \frac{q_{i,j} |\boldsymbol{u}_{i,j}^H \boldsymbol{H}_i^H \boldsymbol{v}_{i,j}|^2}{\boldsymbol{u}_{i,j}^H \left(\sum_{k=1}^{i-1} \sum_{l=1}^{N_r} q_{k,l} \boldsymbol{H}_k^H \boldsymbol{v}_{k,l} \boldsymbol{v}_{k,l}^H \boldsymbol{H}_k + \sum_{l=1}^{j-1} q_{i,l} \boldsymbol{H}_i^H \boldsymbol{v}_{i,l} \boldsymbol{v}_{i,l}^H \boldsymbol{H}_i + \boldsymbol{R}_w \right) \boldsymbol{u}_{i,j}}, \tag{3.12}$$

where $\boldsymbol{R}_w := q_t\boldsymbol{R}_o + q_u\boldsymbol{I}_{N_t}$ is the noise covariance matrix of the MIMO-MAC with $\boldsymbol{R}_o := \boldsymbol{g}\boldsymbol{g}^H$. In the dual MIMO-MAC, $\boldsymbol{R}_w$ depends on q_t and q_u defined in (3.10) whereas the noise covariance matrix in the primal MIMO-BC is an identity matrix. It can be observed from (3.12) that the successive interference cancelation (SIC) scheme is used in this dual MIMO-MAC, and the decoding order is the reverse encoding order of the primal BC. The signal from SU_K is first decoded with the signals from other users being treated as interference. After decoded at the BS, the signals from SU_K will be subtracted from the received signal. The signal from SU_{K-1} is next decoded, and so on. Again, the data streams within a SU can be decoded in a sequential manner.

For the dual MIMO-MAC, we consider the following minimization problem similar to the problem (3.10)

$$\begin{aligned} &\min_{\{\boldsymbol{S}_i^{\mathrm{m}}\}_{i=1}^K:\, \boldsymbol{S}_i^{\mathrm{m}}\succeq 0} \sum_{i=1}^K \mathrm{tr}(\boldsymbol{S}_i^{\mathrm{m}})\sigma^2 - P \\ &\text{subject to: } \mathrm{SINR}_{i,j}^{\mathrm{m}} \geq \gamma_{i,j}. \end{aligned} \tag{3.13}$$

The following theorem describes the relation between the problems (3.10) and (3.13).

Theorem 3.3 *For fixed q_t and q_u, the MIMO-MAC problem* (3.13) *is dual to the MIMO-BC problem* (3.10)*.*

$Proof:$ The constraints in (3.10) can be rewritten as

$$\frac{p_{i,j}|\boldsymbol{u}_{i,j}^H\boldsymbol{H}_i^H\boldsymbol{v}_{i,j}|^2}{\gamma_{i,j}} \geq \sum_{k=i+1}^K\sum_{l=1}^{N_r} p_{k,l}|\boldsymbol{u}_{k,l}^H\boldsymbol{H}_i^H\boldsymbol{v}_{i,j}|^2 + \sum_{l=j+1}^{N_r} p_{i,l}|\boldsymbol{u}_{i,l}^H\boldsymbol{H}_i^H\boldsymbol{v}_{i,j}|^2 + \sigma^2. \tag{3.14}$$

Thus, the Lagrange function of the problem (3.10) is

$$\begin{aligned} &L_1(\boldsymbol{S}_1^{\mathrm{b}},\ldots,\boldsymbol{S}_K^{\mathrm{b}},\lambda_{i,j}) \\ =&q_t\sum_{i=1}^K \boldsymbol{g}^H\boldsymbol{S}_i^{\mathrm{b}}\boldsymbol{g} + q_u\sum_{i=1}^K \mathrm{tr}(\boldsymbol{S}_i^{\mathrm{b}}) - P - \sum_{i=1}^K\sum_{j=1}^{N_r}\lambda_{i,j}\Big(\frac{p_{i,j}|\boldsymbol{u}_{i,j}^H\boldsymbol{H}_i^H\boldsymbol{v}_{i,j}|^2}{\gamma_{i,j}} \\ &-\sum_{k=i+1}^K\sum_{l=1}^{N_r} p_{k,l}|\boldsymbol{u}_{k,l}^H\boldsymbol{H}_i^H\boldsymbol{v}_{i,j}|^2 - \sum_{l=j+1}^{N_r} p_{i,l}|\boldsymbol{u}_{i,l}^H\boldsymbol{H}_i^H\boldsymbol{v}_{i,j}|^2 - \sigma^2\Big) \end{aligned} \tag{3.15}$$

$$= \sum_{i=1}^{K}\sum_{j=1}^{N_r} \lambda_{i,j}\sigma^2 - P - \sum_{i=1}^{K}\sum_{j=1}^{N_r} p_{i,j}\boldsymbol{u}_{i,j}^H \Big(\frac{\lambda_{i,j}\boldsymbol{H}_i^H \boldsymbol{v}_{i,j}\boldsymbol{v}_{i,j}^H \boldsymbol{H}_i}{\gamma_{i,j}} - \sum_{k=1}^{i-1}\sum_{l=1}^{N_r} \lambda_{k,l}\boldsymbol{H}_k^H \boldsymbol{v}_{k,l}\boldsymbol{v}_{k,l}^H \boldsymbol{H}_k - \sum_{l=1}^{j-1} \lambda_{i,l}\boldsymbol{H}_i^H \boldsymbol{v}_{i,l}\boldsymbol{v}_{i,l}^H \boldsymbol{H}_i - \boldsymbol{R}_w \Big) \boldsymbol{u}_{i,j}, \quad (3.16)$$

where $\lambda_{i,j}$ is the Lagrangian multiplier. Eq. (3.16) is obtained by applying the eigenvalue decomposition to $\boldsymbol{S}_i^{\mathrm{b}}$ and rearranging the terms in (3.15). The optimal objective value of (3.10) is

$$\max_{\lambda_{i,j}} \min_{\boldsymbol{S}_1^{\mathrm{b}},\ldots,\boldsymbol{S}_K^{\mathrm{b}}} L_1(\boldsymbol{S}_1^{\mathrm{b}},\ldots,\boldsymbol{S}_K^{\mathrm{b}},\lambda_{i,j}). \quad (3.17)$$

On the other hand, the Lagrange function of the problem (3.13) is

$$L_2(\boldsymbol{S}_1^{\mathrm{m}},\ldots,\boldsymbol{S}_K^{\mathrm{m}},\delta_{i,j}) = \sum_{i=1}^{K}\sum_{j=1}^{N_r} q_{i,j}\sigma^2 - P - \sum_{i=1}^{K}\sum_{j=1}^{N_r} \delta_{i,j}\boldsymbol{u}_{i,j}^H \Big(\frac{q_{i,j}\boldsymbol{H}_i^H \boldsymbol{v}_{i,j}\boldsymbol{v}_{i,j}^H \boldsymbol{H}_i}{\gamma_{i,j}} - \sum_{k=1}^{i-1}\sum_{l=1}^{N_r} q_{k,l}\boldsymbol{H}_k^H \boldsymbol{v}_{k,l}\boldsymbol{v}_{k,l}^H \boldsymbol{H}_k - \sum_{l=1}^{j-1} q_{i,l}\boldsymbol{H}_i^H \boldsymbol{v}_{i,l}\boldsymbol{v}_{i,l}^H \boldsymbol{H}_i - \boldsymbol{R}_w \Big) \boldsymbol{u}_{i,j}, \quad (3.18)$$

where $\delta_{i,j}$ is the Lagrangian multiplier. Eq. (3.18) is also obtained by applying eigenvalue decomposition to $\boldsymbol{S}_i^m$. The optimal objective value of (3.13) is

$$\max_{\delta_{i,j}} \min_{\boldsymbol{S}_1^{\mathrm{m}},\ldots,\boldsymbol{S}_K^{\mathrm{m}}} L_2(\boldsymbol{S}_1^{\mathrm{m}},\ldots,\boldsymbol{S}_K^{\mathrm{m}},\delta_{i,j}). \quad (3.19)$$

Note that if we choose $q_{i,j} = \lambda_{i,j}$, $\delta_{i,j} = p_{i,j}$, and the same beamforming vectors $\boldsymbol{u}_{i,j}$ and $\boldsymbol{v}_{i,j}$ for both problems, (3.16) and (3.18) become identical. This means that the optimal solutions of (3.17) and (3.19) are the same. ■

Theorem 3.3 implies that under the SINR constraints, the problems (3.10) and (3.13) can achieve the same objective value, which is a function of the transmit covariance matrices. On the other hand, under the corresponding constraints on the signal covariance matrix, the achievable SINR regions of the MIMO-BC and its dual MIMO-MAC are the same. Mathematically, we define the respective achievable SINR regions for the primal MIMO-BC and the dual MIMO-MAC as follows.

Definition 3.1 *A SINR vector $\boldsymbol{\gamma} = (\gamma_{1,1},\ldots,\gamma_{1,N_t},\ldots,\gamma_{K,N_t})$ is said to be achievable for the primal BC if and only if there exists a set of $\boldsymbol{S}_1^b,\ldots,\boldsymbol{S}_K^b$ such that $q_t \sum_{i=1}^{K} \boldsymbol{g}^H \boldsymbol{S}_i^b \boldsymbol{g}$*

$+ q_u \sum_{i=1}^{K} tr(\boldsymbol{S}_i^b) - P \leq C$ *for a constant* C *and the corresponding SINR*$_{i,j}^b \geq \gamma_{i,j}$*. An achievable BC SINR region denoted by* $\mathcal{R}_{BC}$*, is a set containing all the BC achievable* $\boldsymbol{\gamma}$*.*

Definition 3.2 *A SINR vector* $\boldsymbol{\gamma} = (\gamma_{1,1}, \ldots, \gamma_{1,N_t}, \ldots, \gamma_{K,N_t})$ *is said to be achievable for the dual MAC if and only if there exists a set of* $\boldsymbol{S}_1^m, \ldots, \boldsymbol{S}_K^m$ *such that* $\sum_{i=1}^{K} tr(\boldsymbol{S}_i^m)\sigma^2 - P \leq C$ *for a constant* C *and the corresponding SINR*$_{i,j}^m \geq \gamma_{i,j}$*. An achievable MAC SINR region denoted by* $\mathcal{R}_{MAC}$*, is a set containing all the MAC achievable* $\boldsymbol{\gamma}$*.*

In the following corollary, we will show $\mathcal{R}_{\mathrm{M}AC} = \mathcal{R}_{\mathrm{BC}}$.

Corollary 3.1 *For fixed* q_t *and* q_u*, and a constant* C*, the MIMO-BC under the constraint* $q_t \sum_{i=1}^{K} \boldsymbol{g}^H \boldsymbol{S}_i^b \boldsymbol{g} + q_u \sum_{i=1}^{K} tr(\boldsymbol{S}_i^b) - P \leq C$ *and the dual MIMO-MAC under the constraint* $\sum_{i=1}^{K} tr(\boldsymbol{S}_i^m)\sigma^2 - P \leq C$ *achieve the same SINR region.*

$Proof$: For any $\boldsymbol{\gamma} \in \mathcal{R}_{\mathrm{M}AC}$, by Definition 3.2, there exists a set of $\boldsymbol{S}_1^m, \ldots, \boldsymbol{S}_K^m$ such that $\sum_{i=1}^{K} \mathrm{tr}(\boldsymbol{S}_i^{\mathrm{m}})\sigma^2 - P \leq C$ and the corresponding $\mathrm{SINR}_{i,j}^{\mathrm{m}} \geq \gamma_{i,j}$. It can be readily concluded from Theorem 3.3 that there exists a set of $\boldsymbol{S}_1^b, \ldots, \boldsymbol{S}_K^b$ such that $q_t \sum_{i=1}^{K} \boldsymbol{g}^H \boldsymbol{S}_i^{\mathrm{b}} \boldsymbol{g} + q_u \sum_{i=1}^{K} \mathrm{tr}(\boldsymbol{S}_i^{\mathrm{b}}) - P \leq C$ and the corresponding $\mathrm{SINR}_{i,j}^{\mathrm{b}} \geq \gamma_{i,j}$. This implies $\boldsymbol{\gamma} \in \mathcal{R}_{\mathrm{BC}}$. Since $\boldsymbol{\gamma}$ is an arbitrary element in $\mathcal{R}_{\mathrm{MAC}}$, we have $\mathcal{R}_{\mathrm{M}AC} \subseteq \mathcal{R}_{\mathrm{BC}}$. In a similar manner, we have $\mathcal{R}_{\mathrm{BC}} \subseteq \mathcal{R}_{\mathrm{M}AC}$. The proof follows. ■

We are now in the position to prove Theorem 3.2.

Proof of Theorem 3.2: According to Corollary 3.1, if $C = 0$, then under the constraint $q_t \sum_{i=1}^{K} \boldsymbol{g}^H \boldsymbol{S}_i^{\mathrm{b}} \boldsymbol{g} + q_u \sum_{i=1}^{K} \mathrm{tr}(\boldsymbol{S}_i^{\mathrm{b}}) \leq P$ for the BC and the constraint $\sum_{i=1}^{K} \mathrm{tr}(\boldsymbol{S}_i^{\mathrm{m}})\sigma^2 \leq P$ for the dual MAC, the two channels have the same SINR region. Since the achievable rates of user i in the MIMO-MAC and the MIMO-BC are $r_i^m = \sum_{j=1}^{N_r} \log(1 + \mathrm{SINR}_{i,j}^m)$ and $r_i^b = \sum_{j=1}^{N_r} \log(1 + \mathrm{SINR}_{i,j}^b)$, the rate regions of the two channels are the same. Therefore, Theorem 3.2 follows. ■

Note that due to the additional interference constraint, $(\mathbf{Pb})$ cannot be solved by using the established duality result in [82] and [48], in which only a single sum power constraint was considered. Our duality result in Theorem 3.2 can be thought as an extension of the duality results in [82] [48] to a multiple linear constraint case. Moreover, as will be shown in the following section, our duality result formulates a MIMO-MAC problem $(\mathbf{Pd})$, which can be efficiently solved.

3.4 Dual MAC Capacity Computation Problem

In this section, we propose an efficient algorithm to solve $(\mathbf{Pd})$. With the SIC scheme, the achievable rate of the kth user in the dual MIMO-MAC is given by

$$r_k^m = \log \frac{|\boldsymbol{R}_w + \sum_{j=1}^{k} \boldsymbol{H}_j \boldsymbol{S}_j^{\mathrm{m}} \boldsymbol{H}_j^H|}{|\boldsymbol{R}_w + \sum_{j=1}^{k-1} \boldsymbol{H}_j \boldsymbol{S}_j^{\mathrm{m}} \boldsymbol{H}_j^H|}. \tag{3.20}$$

For the MIMO-MAC, the *equally* weighted sum rate maximization is irrespective of the decoding order. However, in general the weighted sum rate maximization in the MIMO-MAC is affected by the decoding order. We thus need to consider the optimal decoding order of the SIC for the dual MIMO-MAC, and further need to consider the corresponding optimal encoding order of the DPC for the primal BC.

Let π be the optimal decoding order, which is a permutation on the SU index set $\{1, \cdots, K\}$. It follows from [84] that the optimal user decoding order π for $(\mathbf{Pd})$ is the order such that $w_{\pi(1)} \geq w_{\pi(2)} \geq \cdots \geq w_{\pi(K)}$ is satisfied. The following lemma presents the optimal decoding order of the SIC for the data streams within a SU.

Lemma 3.1 *The optimal data stream decoding order for a particular SU is arbitrary.*

The proof can be found in Appendix B.1. Due to the duality between the MIMO-BC and the MIMO-MAC, for $(\mathbf{Pc})$, the optimal encoding order for the DPC is the reverse of π. Because of the arbitrary encoding order for the data streams within a SU,

if we choose a different encoding order for the BC, the MAC-to-BC mapping algorithm can give different results which yield the same objective value. Hence, the matrix $\boldsymbol{S}_i^{\mathrm{b}}$ achieving the optimal objective value are not unique. With no loss of generality, we assume $w_1 \geq w_2 \geq \cdots \geq w_K$ for notational convenience.

According to (3.20), the objective function of $(\mathbf{Pd})$ can be rewritten as

$$f(\boldsymbol{S}_1^{\mathrm{m}}, \cdots, \boldsymbol{S}_K^{\mathrm{m}}) := \sum_{i=1}^{K} \Delta_i \log |\boldsymbol{R}_w + \sum_{j=1}^{i} \boldsymbol{H}_j \boldsymbol{S}_j^{\mathrm{m}} \boldsymbol{H}_j^H|, \tag{3.21}$$

where $\Delta_i := w_i - w_{i+1}$, and $w_{K+1} := 0$. Clearly, $(\mathbf{Pd})$ is a convex problem, which can be solved through standard convex optimization software packages directly. However, the standard convex optimization software does not exploit the special structure of the problem, and thus is computationally expensive. In the following, we develop a primal dual method based algorithm [87] to solve this problem.

We next rewrite $(\mathbf{Pd})$ as

$$\max_{\{\boldsymbol{S}_i^{\mathrm{m}}\}_{i=1}^K:\, \boldsymbol{S}_i^{\mathrm{m}} \succeq 0} f(\boldsymbol{S}_1^{\mathrm{m}}, \cdots, \boldsymbol{S}_K^{\mathrm{m}}) \;\text{ subject to: } \sum_{i=1}^{K} \mathrm{tr}(\boldsymbol{S}_i^{\mathrm{m}}) \leq P. \tag{3.22}$$

Recall that the positive semi-definiteness of $\boldsymbol{S}_i^{\mathrm{m}}$ is equivalent to the positiveness of the eigenvalues of $\boldsymbol{S}_i^{\mathrm{m}}$, i.e., $q_{i,j} \geq 0$. Correspondingly, the Lagrange function is

$$L(\boldsymbol{S}_1^{\mathrm{m}}, \cdots, \boldsymbol{S}_K^{\mathrm{m}}, \lambda, \delta_{i,j}) = f(\boldsymbol{S}_1^{\mathrm{m}}, \cdots, \boldsymbol{S}_K^{\mathrm{m}}) - \lambda\big(\sum_{i=1}^{K} \mathrm{tr}(\boldsymbol{S}_i^{\mathrm{m}}) - P\big) + \sum_{i=1}^{K}\sum_{j=1}^{M_i} \delta_{i,j} q_{i,j}, \tag{3.23}$$

where λ and $\delta_{i,j}$ are Lagrangian multipliers. According to the KKT conditions of (3.22), we have

$$\frac{\partial f(\boldsymbol{S}_1^{\mathrm{m}}, \cdots, \boldsymbol{S}_K^{\mathrm{m}})}{\partial \boldsymbol{S}_i^{\mathrm{m}}} - \lambda \boldsymbol{I}_{N_r} + \sum_{j=1}^{M_i} \delta_{i,j} \boldsymbol{E}_{i,j} = 0, \tag{3.24}$$

$$\lambda\big(\sum_{i=1}^{K} \mathrm{tr}(\boldsymbol{S}_i^{\mathrm{m}}) - P\big) = 0, \tag{3.25}$$

$$\delta_{i,j} q_{i,j} = 0, \tag{3.26}$$

where $\boldsymbol{E}_{i,j} := \partial q_{i,j}/\partial \boldsymbol{S}_i^{\mathrm{m}}$. Notice that it is not necessary to compute the actual value of $\delta_{i,j}$ and $\boldsymbol{E}_{i,j}$, because if $\delta_{i,j} \neq 0$, then $q_{i,j} = 0$. Thus, the semi-definite constraint turns into $q_{i,j} = [q_{i,j}]^+$. Thus, we can assume $\delta_{i,j} = 0$.

The dual objective function of (3.22) is

$$g(\lambda) = \max_{\{\boldsymbol{S}_i^{\mathrm{m}}\}_{i=1}^K:\ \boldsymbol{S}_i^{\mathrm{m}} \geq 0} L(\boldsymbol{S}_1^{\mathrm{m}}, \cdots, \boldsymbol{S}_K^{\mathrm{m}}, \lambda). \tag{3.27}$$

Because the problem (3.22) is convex, it is equivalent to the following minimization problem

$$\min_{\lambda}\ g(\lambda)\ \text{ subject to: }\ \lambda \geq 0. \tag{3.28}$$

We outline the algorithm to solve the problem (3.28). We choose an initial λ and compute the value of $g(\lambda)$ (3.27), and then update λ according to the descent direction of $g(\lambda)$. The process repeats until the algorithm converges.

It is easy to observe that all the users share the same λ, and thus λ can be viewed as a water level in the water filling principle [47]. Once λ is fixed, the unique optimal set $\{\boldsymbol{S}_1^{\mathrm{m}}, \ldots, \boldsymbol{S}_K^{\mathrm{m}}\}$ can be obtained through the gradient ascent algorithm. In each iterative step, $\boldsymbol{S}_i^{\mathrm{m}}$ is updated sequentially according to its gradient direction of (3.23). Denote by $\boldsymbol{S}_i^{\mathrm{m}}(n)$ the matrix $\boldsymbol{S}_i^{\mathrm{m}}$ at the nth iteration step. The gradient of each step is determined by

$$\nabla^{(n)}_{\boldsymbol{S}_i^m} L := \frac{\partial f\big(\boldsymbol{S}_1^{\mathrm{m}}(n), \cdots, \boldsymbol{S}_{i-1}^{\mathrm{m}}(n), \boldsymbol{S}_i^{\mathrm{m}}(n-1), \ldots, \boldsymbol{S}_K^{\mathrm{m}}(n-1)\big)}{\partial \boldsymbol{S}_i^{\mathrm{m}}(n-1)} - \lambda \boldsymbol{I}_{N_r}. \tag{3.29}$$

Thus, $\boldsymbol{S}_i^{\mathrm{m}}(n)$ can be updated according to

$$\boldsymbol{S}_i^{\mathrm{m}}(n) = \Big[\boldsymbol{S}_i^{\mathrm{m}}(n-1) + t\nabla^{(n)}_{\boldsymbol{S}_k^m} L\Big]^+,$$

where t is the step size, and the notation $[\boldsymbol{A}]^+$ is defined as $[\boldsymbol{A}]^+ := \sum_j [\lambda_j]^+ \boldsymbol{v}_j \boldsymbol{v}_j^H$ with λ_j and $\boldsymbol{v}_j$ being the jth eigenvalue and the corresponding eigenvector of $\boldsymbol{A}$ re-

spectively. The gradient in (3.29) can be readily computed as

$$\frac{\partial f(\boldsymbol{S}_1^{\mathrm{m}}, \cdots, \boldsymbol{S}_K^{\mathrm{m}})}{\partial \boldsymbol{S}_k^{\mathrm{m}}} = \sum_{j=k}^{K} \Delta_j \left(\boldsymbol{H}_k \boldsymbol{F}_j (\boldsymbol{S}_1^{\mathrm{m}}, \cdots, \boldsymbol{S}_K^{\mathrm{m}})^{-1} \boldsymbol{H}_k^H \right), \tag{3.30}$$

where $\boldsymbol{F}_j(\boldsymbol{S}_1^{\mathrm{m}}, \cdots, \boldsymbol{S}_K^{\mathrm{m}}) := \boldsymbol{R}_w + \sum_{i=1}^{j} \boldsymbol{H}_i^H \boldsymbol{S}_i^{\mathrm{m}} \boldsymbol{H}_i$. We next need to determine the optimal λ. Since the Lagrange function $g(\lambda)$ is convex over λ, the optimal λ can be obtained through the one-dimensional search. However, because $g(\lambda)$ is not necessarily differentiable, the gradient algorithm cannot be applied. Alternatively, the subgradient method can be used to find the optimal solution. In each iterative step, λ is updated according to the subgradient direction.

Lemma 3.2 *The subgradient of $g(\lambda)$ is $P - \sum_{i=1}^{K} tr(\boldsymbol{S}_i^m)$, where $\lambda \geq 0$, and $\boldsymbol{S}_i^m$, $i = 1, \ldots, K$, are the corresponding optimal covariance matrices for a fixed λ in* (3.27)*.*

The proof can be found in Appendix B.2. Lemma 3.2 indicates that the value of λ should increase, if $\sum_{i=1}^{K} \mathrm{tr}(\boldsymbol{S}_i^{\mathrm{m}}) > P$, and vice versa. We now present our DIPA algorithm for solving $(\mathbf{Pd})$ in table 3.1. The following theorem shows the convergence property of the DIPA algorithm.

Theorem 3.4 *The DIPA algorithm converges to an optimal set of the MAC transmit covariance matrices.*

$Proof:$ The DIPA algorithm consists of the inner and outer loops. The inner loop is to compute $\boldsymbol{S}_i^{\mathrm{m}}$ for $i = 1, \cdots, K$. In each iterative step of the inner loop, we update $\boldsymbol{S}_i^{\mathrm{m}}$ by fixing other $\boldsymbol{S}_j^{\mathrm{m}}$ with $j \neq i$, and compute the corresponding gradient. The inner loop uses the gradient ascent algorithm, which converges to the optimal value due to its nondecreasing property and the convexity of the objective function. The outer loop is to compute the optimal Lagrangian multiplier λ in (3.28). Due to the convexity of the dual objective function [53], there is a unique λ achieving the optimal solution in (3.28). Hence, one dimensional line bisection search [47,78] is guaranteed to converge to its optimal solution. ■

Table 3.1: Decoupled Iterative Power Allocation (DIPA) Algorithm.

DIPA Algorithm
1. Initialize $\lambda_{\min}$ and $\lambda_{\max}$;
2. repeat
$\lambda = (\lambda_{\min} + \lambda_{\max})/2$
repeat, initialize $\boldsymbol{S}_1^{\mathrm{m}}(0), \cdots, \boldsymbol{S}_K^{\mathrm{m}}(0)$, $n = 1$
for $i = 1, \cdots, K$,
$\boldsymbol{S}_i^{\mathrm{m}}(n) = \left[\boldsymbol{S}_i^{\mathrm{m}}(n-1) + t\nabla_{Q_i^m}^{(n)} L\right]^+$,
end for,
$n \leftarrow n + 1$,
until $\boldsymbol{S}_k^{\mathrm{m}}$ for $k = 1, \cdots, K$ converge, i.e., $\|\nabla_{\boldsymbol{S}_i^m}^{(n)} L\|^2 \leq \hat{\epsilon}$ for a small preset $\hat{\epsilon}$.
if $\sum_{i=1}^K \mathrm{tr}(\boldsymbol{S}_i^{\mathrm{m}}) > P$, then $\lambda_{\min} = \lambda$, elseif $\sum_{i=1}^K \mathrm{tr}(\boldsymbol{S}_i^{\mathrm{m}}) < P$, then $\lambda_{\max} = \lambda$;
3. until $\lvert\lambda_{\min} - \lambda_{\max}\rvert \leq \epsilon$

Remark 3.3 *In the previous work on the sum rate maximization [47, 77, 78], the covariance matrix of each user is the same as the single user water-filling covariance matrix in a point-to-point link with multiuser interference being treated as noise [34]. However, for the weighted sum rate maximization problem, the optimal solution does not possess a water-filling structure. Thus, our DIPA algorithm does not obey the water-filling principle. In Section 3.6, Example 1 compares the water-filling algorithm with the DIPA algorithm.*

In the dual MIMO-MAC, according to (3.11), the transmit beamforming vectors $\boldsymbol{v}_{i,j}$ can be obtained by the eigenvalue decomposition. The corresponding receive beamforming vector at the BS, $\boldsymbol{u}_{i,j}$, is obtained by using the MMSE algorithm. Throughout the proof of Theorem 3.3, we can see that when the same optimal solutions are achieved the primal BC and the dual MAC share the same beamforming vectors $\boldsymbol{u}_{i,j}$ and $\boldsymbol{v}_{i,j}$, and achieve the same SINR region, i.e., $\text{SINR}_{i,j}^{\text{b}} = \text{SINR}_{i,j}^{\text{m}}$. Based on this observation, we can compute the power allocated to the BC beamforming direction $\boldsymbol{u}_{i,j}$, $p_{i,j}$, and obtain the signal covariance matrix, $\boldsymbol{S}_i^{\text{b}} = \sum_{j=1}^{N_r} p_{i,j}\boldsymbol{u}_{i,j}\boldsymbol{u}_{i,j}^H$. The MAC-to-BC covariance matrix mapping allows us to obtain the optimal BC covariance matrices for ($\mathbf{Pc}$) by solving ($\mathbf{Pd}$).

3.5 A Complete Solution to ($\mathbf{Pa}$)

We are now ready to present a complete algorithm to solve ($\mathbf{Pb}$). The Lagrangian dual objective function of ($\mathbf{Pb}$) can be rewritten as follows

$$g(q_t, q_u) = \max_{\{\boldsymbol{S}_i^{\text{b}}\}_{i=1}^K : \boldsymbol{S}_i^{\text{b}} \geq 0} \sum_{i=1}^{K} w_i r_i^{\text{b}}, \tag{3.31}$$

where the maximization is subject to the constraint $q_t\big(\sum_{i=1}^K \boldsymbol{g}^H \boldsymbol{S}_i^{\mathrm{b}}\boldsymbol{g} - \Gamma\big) + q_u\big(\sum_{i=1}^K \mathrm{tr}(\boldsymbol{S}_i^{\mathrm{b}}) - \bar{P}\big) \leq 0$. **(Pb)** is equivalent to the following problem

$$\min_{q_t, q_u} g(q_t, q_u), \quad \text{subject to: } q_t \geq 0 \text{ and } q_u \geq 0.$$

Applying the BC-MAC duality in Section 3.3.2 and the DIPA algorithm in Section 3.4, $g(q_t, q_u)$ can be obtained. The remaining task is to determine the optimal q_t and q_u. Since $g(q_t, q_u)$ is not necessarily differentiable, we search the optimal q_t and q_u through the subgradient algorithm; that is, in each iterative step, we update the vector $[q_t, q_u]$ according to the subgradient direction $\boldsymbol{s} = [s_1, s_2]$ of $g(q_t, q_u)$.

Lemma 3.3 *The subgradient of* $g(q_t, q_u)$ *is* $\big[\Gamma - \sum_{i=1}^K \boldsymbol{g}^H \boldsymbol{S}_i^b \boldsymbol{g}, \bar{P} - \sum_{i=1}^K tr(\boldsymbol{S}_i^b)\big]$, *where* $q_t \geq 0, q_u \geq 0$, *and* $\boldsymbol{S}_i^b, i = 1, \ldots, K$, *are the corresponding optimal covariance matrices for the problem* (3.31).

The proof of Lemma 3.3 is similar to that of Lemma 3.2, and is omitted here. It has been shown in [88] that with a constant step size, the subgradient algorithm converges to a value that is within a small range of the optimal value, i.e.,

$$\lim_{n\to\infty} |q_t^{(n)} - q_t^*| < \epsilon, \text{ and, } \lim_{n\to\infty} |q_u^{(n)} - q_u^*| < \epsilon, \tag{3.32}$$

where q_t^* and q_u^* denote the optimal values, and $q_t^{(n)}$ and $q_u^{(n)}$ denote the values of q_t and q_u at the nth step of the subgradient algorithm, respectively. This implies that the subgradient method finds an ϵ-suboptimal point within a finite number of steps. The number ϵ is a decreasing function of the step size.

We next describe the algorithm to solve **(Pb)** in table 3.2. As a summary, the flow chart of the SIPA algorithm is depicted in Fig. 3.3. We shows that the SIPA algorithm converges to the optimal solution of **(Pa)** in the following theorem.

Theorem 3.5 *The SIPA algorithm converges to the globally optimal solution of* **(Pa)**.

Table 3.2: Subgradient Iterative Power Allocation (SIPA) Algorithm.

SIPA Algorithm
1. Initialization: $q_t^{(1)}$, $q_u^{(1)}$, $n = 1$;
2. repeat
Find the optimal solution of the dual MAC ($\mathbf{Pd}$) through the DIPA algorithm;
Find the solution of the BC problem (3.31) through the MAC-to-BC mapping;
Update $q_t^{(n)}$ and $q_u^{(n)}$ through a subgradient algorithm $q_t^{(n+1)} = q_t^{(n)} + t(\sum_{i=1}^K \boldsymbol{g}^\dagger \boldsymbol{S}_i^{\mathrm{b}} \boldsymbol{g} - \Gamma)$, and $q_u^{(n+1)} = q_u^{(n)} + t(\sum_{i=1}^K \mathrm{tr}(\boldsymbol{S}_i^{\mathrm{b}}) - \bar{P})$, where t denotes the step size of the subgradient algorithm;
$n \leftarrow n + 1$;
3. Stop when $\lvert q_t^{(n)}(\sum_{i=1}^K \boldsymbol{g}^\dagger \boldsymbol{S}_i^{\mathrm{b}} \boldsymbol{g} - \Gamma)\rvert \leq \epsilon$ and $\lvert q_u^{(n)}(\sum_{i=1}^K \mathrm{tr}(\boldsymbol{S}_i^{\mathrm{b}}) - \bar{P})\rvert \leq \epsilon$ are satisfied simultaneously,

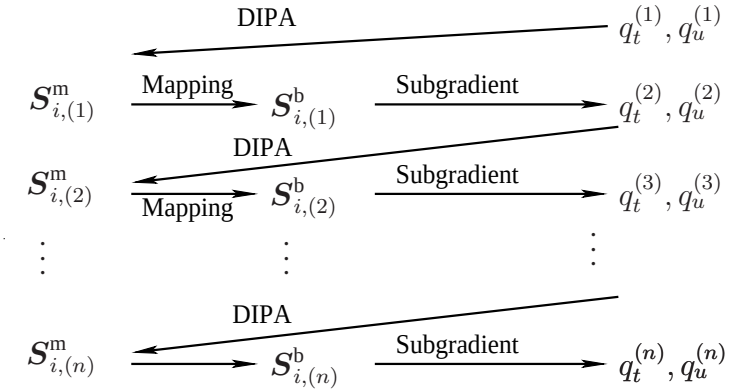

Figure 3.3: The flow chart for the SIPA algorithm, where $\boldsymbol{S}_{i,(n)}^{\mathrm{b}}$ and $\boldsymbol{S}_{i,(n)}^{\mathrm{n}}$ denote the transmit covariance matrices of SU_i for the BC and MAC at the nth step, respectively.

$Proof:$ The Lagrange function of **(Pa)** is given by

$$L(\boldsymbol{S}_1^{\mathrm{b}},\ldots,\boldsymbol{S}_K^{\mathrm{b}},\lambda_1,\lambda_2)=\sum_{i=1}^{K}w_i r_i^{\mathrm{b}}-\lambda_1\big(\sum_{i=1}^{K}\boldsymbol{g}^H\boldsymbol{S}_i^{\mathrm{b}}\boldsymbol{g}-\Gamma\big)-\lambda_2\big(\sum_{i=1}^{K}\mathrm{tr}(\boldsymbol{S}_i^{\mathrm{b}})-\bar{P}\big), \tag{3.33}$$

and the Lagrange function of **(Pb)** is given by

$$L_1(\boldsymbol{S}_1^{\mathrm{b}},\ldots,\boldsymbol{S}_K^{\mathrm{b}},\lambda,q_t,q_u)=\sum_{i=1}^{K}w_i r_i^{\mathrm{b}}-\lambda\big(q_t\big(\sum_{i=1}^{K}\boldsymbol{g}^H\boldsymbol{S}_i^{\mathrm{b}}\boldsymbol{g}-\Gamma\big)-q_u\big(\sum_{i=1}^{K}\mathrm{tr}(\boldsymbol{S}_i^{\mathrm{b}})-\bar{P}\big)\big). \tag{3.34}$$

Let $\bar{q}_t$, $\bar{q}_u$, $\bar{\lambda}$, and $\bar{\boldsymbol{S}}_i$ be the optimal values of $L_1(\boldsymbol{S}_1^{\mathrm{b}},\ldots,\boldsymbol{S}_K^{\mathrm{b}},\lambda,q_t,q_u)$, when the algorithm converges. We thus have

$$\frac{\partial L_1(\boldsymbol{S}_1^{b},\ldots,\boldsymbol{S}_K^{b},\lambda,q_t,q_u)}{\partial \boldsymbol{S}_i^{\mathrm{b}}}\Big|_{\{\bar{\boldsymbol{S}}_i^{b}\}_{i=1}^{K},\bar{\lambda},\bar{q}_t,\bar{q}_u}=0,$$

$|\bar{q}_t(\sum_{i=1}^{K}\boldsymbol{g}^H\bar{\boldsymbol{S}}_i\boldsymbol{g}-\Gamma)|=0$, and $|\bar{q}_u(\sum_{i=1}^{K}\mathrm{tr}(\bar{\boldsymbol{S}}_i)-\bar{P})|=0$. This means that $\bar{\boldsymbol{S}}_i$ is a locally optimal solution.

According to (3.33), if we select $\tilde{\lambda}_1=\bar{\lambda}\bar{q}_t$, $\tilde{\lambda}_2=\bar{\lambda}\bar{q}_u$, and $\tilde{\boldsymbol{S}}_i=\bar{\boldsymbol{S}}_i$, then $\tilde{\lambda}_1$, $\tilde{\lambda}_2$, and $\tilde{\boldsymbol{S}}_i$ satisfy the KKT conditions of **(Pa)** and thus are the locally optimal variables.

Suppose that there exists an optimal set of $\hat{\lambda}_1$, $\hat{\lambda}_2$, and $\hat{\boldsymbol{S}}_i$ such that $L(\hat{\boldsymbol{S}}_1,\ldots,\hat{\boldsymbol{S}}_K,\hat{\lambda}_1,\hat{\lambda}_2)>L(\tilde{\boldsymbol{S}}_1,\ldots,\tilde{\boldsymbol{S}}_K,\tilde{\lambda}_1,\tilde{\lambda}_2)$. Clearly, this optimal set of $\hat{\lambda}_1$, $\hat{\lambda}_2$, and $\hat{\boldsymbol{S}}_i$ satisfy the KKT conditions of **(Pa)**. In the sequel, we will derive a contradiction.

First, we can write

$$L(\tilde{\boldsymbol{S}}_1,\cdots,\tilde{\boldsymbol{S}}_K,\tilde{\lambda}_1,\tilde{\lambda}_2)\geq L(\hat{\boldsymbol{S}}_1,\cdots,\hat{\boldsymbol{S}}_K,\tilde{\lambda}_1,\tilde{\lambda}_2). \tag{3.35}$$

Suppose that the inequality (3.35) does not hold, i.e., $L(\tilde{\boldsymbol{S}}_1,\cdots,\tilde{\boldsymbol{S}}_K,\tilde{\lambda}_1,\tilde{\lambda}_2)<L(\hat{\boldsymbol{S}}_1,\cdots,\hat{\boldsymbol{S}}_K,\tilde{\lambda}_1,\tilde{\lambda}_2)$. Then, according to the BC-MAC duality in Section 3.3.2, an objective value of **(Pd)** which is larger than $L(\tilde{\boldsymbol{S}}_1,\cdots,\tilde{\boldsymbol{S}}_K,\tilde{\lambda}_1,\tilde{\lambda}_2)$, can be found for the fixed $\bar{q}_t$ and $\bar{q}_u$. However, from Theorem 3.4, the DIPA algorithm converges the optimal solution. It is a contradiction.

Secondly, according to the KKT conditions of (**Pa**), we have

$$\hat{\lambda}_1\big(\sum_{i=1}^{K}\boldsymbol{g}^H\hat{\boldsymbol{S}}_i^{\mathrm{b}}\boldsymbol{g}-\Gamma\big)=0,\hat{\lambda}_2\big(\sum_{i=1}^{K}\mathrm{tr}(\hat{\boldsymbol{S}}_i^{\mathrm{b}})-\bar{P}\big)=0. \tag{3.36}$$

We thus can write:

$$L(\hat{\boldsymbol{S}}_1,\cdots,\hat{\boldsymbol{S}}_K,\tilde{\lambda}_1,\tilde{\lambda}_2)\geq L(\hat{\boldsymbol{S}}_1,\cdots,\hat{\boldsymbol{S}}_K,\hat{\lambda}_1,\hat{\lambda}_2). \tag{3.37}$$

Combining (3.37) and (3.35), we have

$$L(\tilde{\boldsymbol{S}}_1,\cdots,\tilde{\boldsymbol{S}}_K,\tilde{\lambda}_1,\tilde{\lambda}_2)\geq L(\hat{\boldsymbol{S}}_1,\cdots,\hat{\boldsymbol{S}}_K,\hat{\lambda}_1,\hat{\lambda}_2). \tag{3.38}$$

This contradicts with our previous assumption. Hence the proof is complete. ■

Remark 3.4 *The algorithm can be extended to the multiple PU case in the following manner. Assume that there are N PUs. (**Pb**) becomes*

$$\begin{aligned}&\min_{q_{t,j}\geq 0,q_u\geq 0}\ \max_{\{\boldsymbol{S}_i^b\}_{i=1}^K:\ \boldsymbol{S}_i^b\succeq 0}\ \sum_{i=1}^{K}w_i r_i^b,\\ &\textit{subject to:}\ \sum_{j=1}^{N}q_{t,j}\big(\sum_{i=1}^{K}\boldsymbol{g}_j^H\boldsymbol{S}_i^b\boldsymbol{g}_j-\Gamma_{t,j}\big)+q_u\big(\sum_{i=1}^{K}tr(\boldsymbol{S}_i^b)-\bar{P}\big)\leq 0,\end{aligned} \tag{3.39}$$

where $q_{t,j}$ is the auxiliary variable for the jth PU, $\boldsymbol{g}_j$ is the channel response from the BS to the jth PU, and $\Gamma_{t,j}$ is the interference threshold of the jth PU. The role of auxiliary variables $q_{t,j}$ is similar to that of q_t in the single PU case. It is thus straightforward to modify the SIPA algorithm to solve the problem for the multiple PU case. Moreover, it should be noted that the multiple interference constraints of the problem (3.39) *can be transformed to the per-antenna power constraints [79] by setting $\boldsymbol{g}_j$, $j=1,\cdots,N_t$, to be the jth column of the identity matrix. Not limited by the sum rate maximization problem with interference power constraints, the method proposed in this chapter can be easily applied to solve the transmitter optimization problem (e.g. beamforming optimization) for MIMO-BC with multiple arbitrary linear power constraints.*

3.6 Numerical Examples

In this section, we provide the numerical examples to show the effectiveness of the proposed algorithm. In the examples, for simplicity, we assume that the BS is at the same distance, l_1, to all SUs, and the same distance, $l_2^{(n)}$, to PU$_n$. In the single PU case, we will drop the superscript and simply use notation l_2. Suppose that the same path loss model can be used to describe the transmissions from the BS to the SUs and to the PUs, and the path loss exponent is 4. The elements of matrix $\boldsymbol{H}$ are assumed to be CSCG RVs with mean zero and variance 1, and $\boldsymbol{g}$ can be modeled as $\boldsymbol{g} = (l_1/l_2)^2\boldsymbol{a}_n$, where $\boldsymbol{a}_n$ is a $N_t \times 1$ vector whose elements are CSCG RVs with mean zero and variance 1. The noise covariance matrix at the BS is assumed to be the identity matrix, and the sum power and interference power are defined in dB relative to the noise power, and Γ is chosen to be 0 dB. For all cases, we choose $l_1 = l_2$, except for explicitly stated.

In Fig. 3.4, we examine the validity of the DIPA algorithm. In this example, we choose $K = 1$ (a single SU case), $N_t = 4$, $N_r = 4$, and $\bar{P} = 10$ dB. It is well known that the optimal transmit covariance matrix can be obtained through the water-filling principle [34]. As can be observed from Fig. 3.4, in several iterations, the DIPA algorithm converges to the optimal solution obtained by using the water-filling principle.

In Fig. 3.5, we show the convergence property of the DIPA algorithm. In this example, we choose $K = 20$ and $\bar{P} = 10$ dB. It can be observed from this figure that the algorithm converges to the optimal solution within several iteration steps.

In Figs. 3.6 and 3.7, we consider a CR MIMO-BC with $K = 5$, $N_t = 5$, $N_r = 3$, and $\bar{P} = 13$ dB. In this example, the SUs with $w_1 = 5$ and $w_i = 1,\ i = 2, \ldots, K$ are assumed to share the same spectrum band with two PUs. Fig. 3.6 plots the weighted sum rate versus the number of iterations of the SIPA algorithm for step sizes $t = 0.1$ and $t = 0.01$. As can be seen from the figure, the step size affects the accuracy and

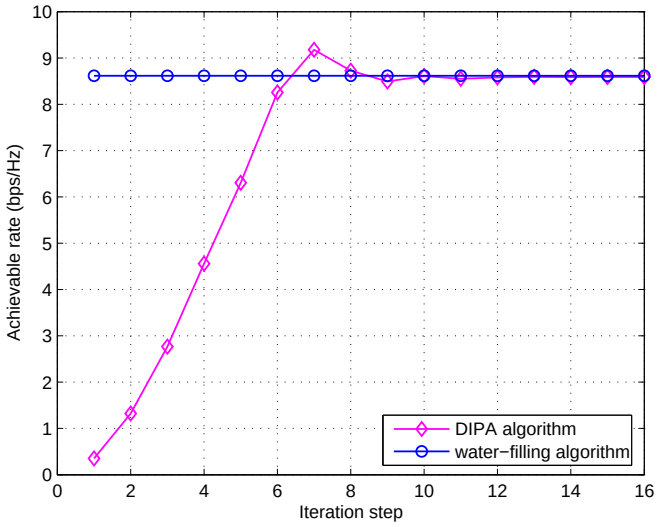

Figure 3.4: Comparison of the optimal achievable rates obtained by the DIPA and the water-filling algorithm in a MIMO channel ($N_t = N_r = 4$, $K = 1$ and $\bar{P}$=10 dB).

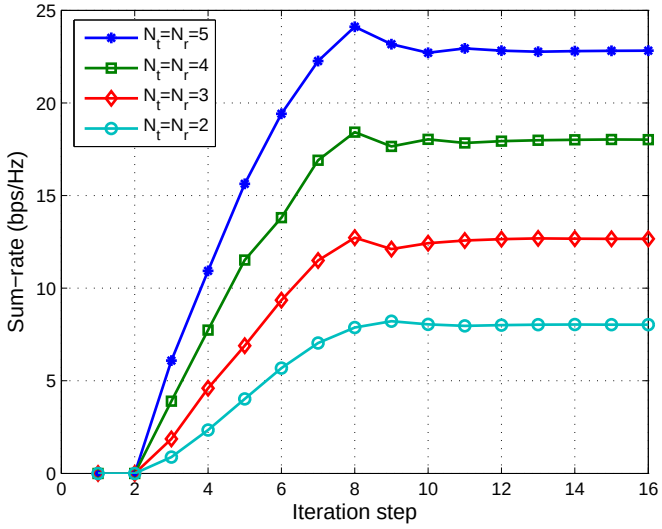

Figure 3.5: Convergence behavior of the DIPA algorithm ($K = 20$ and $\bar{P} = 10$ dB).

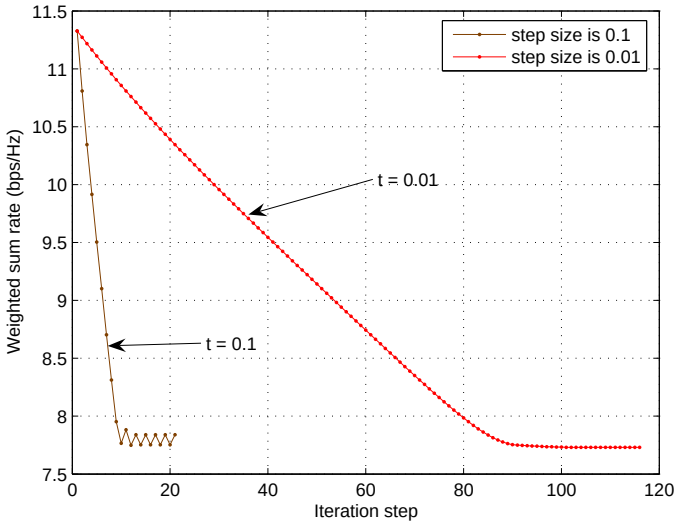

Figure 3.6: Convergence behavior of the SIPA algorithm ($N_t = 5$, $K = 5$, $N_r = 3$, $w_1 = 5$, and $w_i = 1$, for $i \neq 1$).

convergence speed of the algorithm. Fig. 3.7 plots the sum power at the BS and the interference power at the PUs versus the number of iterations. It can be seen from the figure that the sum power and the interference power approach to $\bar{P} = 13$ dB and $\Gamma = 0$ dB respectively when the SIPA algorithm converges. This implies that the sum power and interference constraints are satisfied with equalities when the SIPA algorithm converges.

Fig. 3.8 plots the achievable sum rates versus the sum power in the single PU case and the case with no PU. We choose $K = 5$, $N_t = 5$, and $N_r = 3$. As can be seen from Fig. 3.8, in the low sum power regime, the achievable sum rate in the case with no PU is quite close to the one in the single PU case while in the high sum power regime, the achievable sum rate in the case with no PU is much higher than the one in the single PU case. This is because the additional constraint reduces the degrees of freedom of the system.

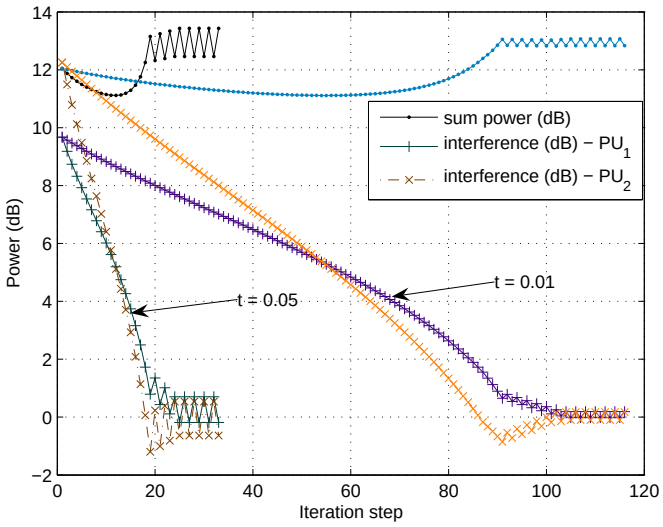

Figure 3.7: The convergence behavior of the sum power at the BS and the interference at the PU for the SIPA algorithm ($N_t = 5$, $K = 5$, $N_r = 3$, $w_1 = 5$, and $w_i = 1$ with $i \neq 1$).

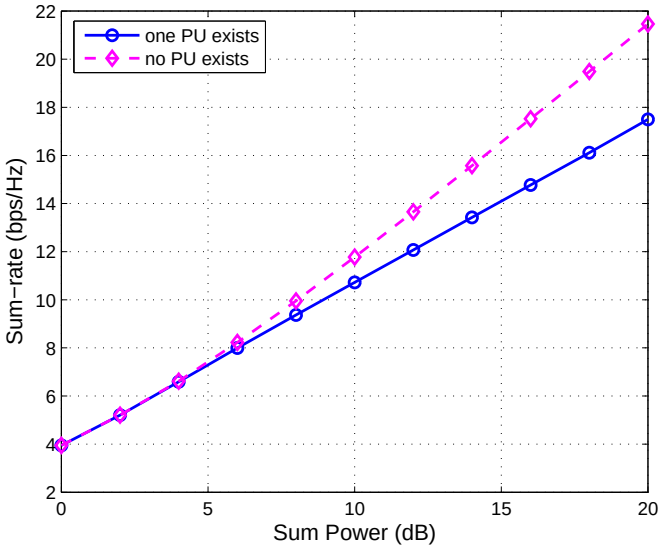

Figure 3.8: Achievable sum rates versus sum power in the single PU case and the case with no PU ($N_t = 5$, $K = 5$, $N_r = 3$).

3.7 Conclusions

In this chapter, we have developed a new BC-MAC duality result, which can be viewed as an extension of existing duality results developed under either a sum power constraint or per-antenna power constraints. Exploiting this duality result, we have proposed an efficient algorithm to solve the capacity computation problem for the CR MIMO-BC. Furthermore, we have shown that the proposed algorithm converges to the globally optimal solution.

Chapter 4

Robust Designs for CR MISO Channels

In Chapter 2 and Chapter 3, it is assumed that the CSI of the CR networks is perfectly known at the SU transmitter (SU-Tx). However, due to the loose cooperation between the SU and the PU, it is more practical to assume that only partial CSI is available at the SU-Tx. This chapter considers a spectrum sharing based CR MISO channel, in which the SU has multiple transmit antennas and a single receive antenna and the PU has a single receive antenna. With the partial CSI and a prescribed transmit power constraint, our design objective is to determine the transmit covariance matrix that maximizes the rate of the SU while keeping the interference power to the PU below a threshold for all the possible channel realizations within an uncertainty set. This problem is first transformed into the second order cone programming (SOCP) problem and then solved via a standard interior point algorithm. Next, an analytical solution with much reduced complexity is developed from a geometric perspective. It is shown that both algorithms obtain the same optimal solution.

4.1 Introduction

In non-CR settings, the study of multi-antenna systems with partial CSI has received considerable attention in the past decade [49, 89]. Specifically, the paper [49] considered the case in which the receiver has perfect CSI but the transmitter has only partial CSI (mean feedback or covariance feedback). It was proved in [49] that the optimal transmission directions are the same as those of the eigenvectors of the channel covariance matrix. However, the optimal power allocation solution was not given in an analytical form. A universal optimality condition for beamforming was explored in [90], and quantized feedback was studied in [91].

In CR settings, power allocation strategies have been developed for MAC [68] and for point-to-point MIMO channels [36]. Particularly, the solution developed in [36] can be viewed as cognitive beamforming since the SU-Tx forms its main beam direction with awareness of its interference to the PU. A closed-form method has been provided for CR MISO channel in [36]. However, both papers [68] and [36] assumed that perfect CSI of the link from the SU-Tx to the PU is available at the SU-Tx.

In this chapter, we consider a spectrum sharing based CR MISO channel, in which the SU network is a MISO channel and the PU is equipped with a single receive antenna. We assume that the CSI of the SU link is perfectly known at the SU-Tx. However, owing to loose cooperation between the SU and the PU, only the mean and covariance of the channel between the SU-Tx and the PU is available at the SU-Tx. With this partial CSI, our design objective is, for a given transmit power constraint, to determine the transmit covariance matrix that maximizes the rate of the SU while keeping the interference power to the PU below a threshold for all the possible channel realizations within an uncertainty set. We term this design problem the robust cognitive beamforming design problem. This problem is formulated as a semi-infinite programming (SIP) problem, and solved by two methods proposed in this chapter.

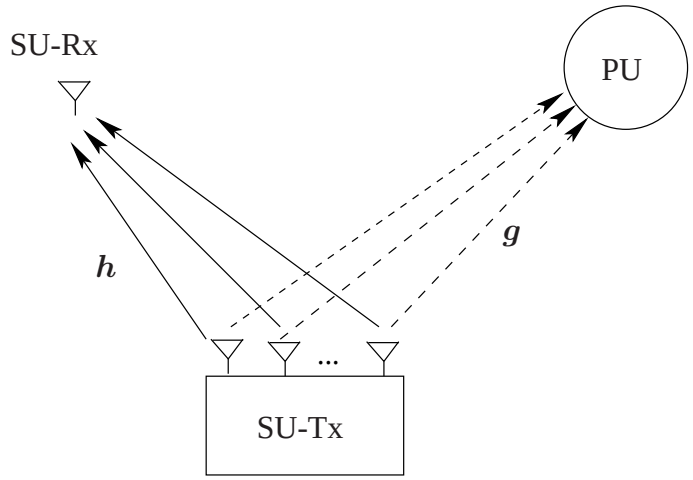

Figure 4.1: The system model for CR MISO channel. There are a N-antenna SU-Tx, a single antenna SU-Rx, and a single antenna PU.

The rest of this chapter is organized as follows. Section 4.2 describes the system model for CR MISO channel, and the problem formulation of the robust cognitive beamforming design. Section 4.3 presents several important lemmas that are used to develop the algorithms. Two different algorithms, the SOCP based solution and the analytical solution, are developed in Section 4.5 and Section 4.4, respectively. Section 4.6 presents numerical examples, and finally, Section 4.7 concludes the chapter.

4.2 System Model and Problem Formulation

Consider a CR MISO channel, where the SU-Tx is equipped with N transmit antennas and there are one SU receiver (SU-Rx) with a single receive antenna. The CR MISO channel, as shown in Fig. 4.1, share the same spectrum with a single PU equipped with one transmit antenna. The transmit-receive signal model from the SU-Tx to the SU-Rx can be expressed as

$$y = \boldsymbol{h}^H \boldsymbol{x} + n, \tag{4.1}$$

where y denotes the the received signal, $\boldsymbol{x}$ and $\boldsymbol{h}$ denote the $N \times 1$ transmitted vector and the $N \times 1$ channel response vector from the SU-Tx to the SU-Rx, respectively, and n is Gaussian noise with zero mean and unit variance. Suppose that the PU has one receive antenna. The channel response from the SU-Tx to the PU is denoted by an $N \times 1$ vector $\boldsymbol{g}$. Further, assume that the SU-Tx has perfect CSI for its own link, i.e., $\boldsymbol{h}$ is perfectly known at the SU-Tx. However, due to the loose cooperation between the SU and the PU, only the mean ($\boldsymbol{g}_0$) and the covariance matrix ($\boldsymbol{R}$) of $\boldsymbol{g}$ is assumed to be available at the SU-Tx[1]. In previous work [49, 92–94], imperfect CSI has been considered in two extreme cases in a non-CR setting. One is the mean feedback case, i.e., $\boldsymbol{R} = \sigma^2 \boldsymbol{I}$, where σ^2 can be viewed as the variance of the estimation error; and the other is the covariance feedback case, i.e., $\boldsymbol{g}_0$ is a zero vector. In this chapter, we study the case where the SU-Tx knows both the mean and covariance of $\boldsymbol{g}$ in a CR setting.

The objective of this chapter is to determine the optimal transmit covariance matrix such that the information rate of the SU link is maximized while the QoS of the PU is guaranteed under a robust design scenario, i.e., the instantaneous interference power for the PU should remain below a given threshold for all the $\boldsymbol{g}$ in the uncertain region. Mathematically, the problem is formulated as follows:

$$\begin{aligned} \textbf{Robust design problem } (\mathbf{P1}): \quad & \max_{\boldsymbol{S} \geq 0} \ \log(1 + \boldsymbol{h}^H \boldsymbol{S} \boldsymbol{h}) \\ \text{subject to}: \ & \text{tr}(\boldsymbol{S}) \leq \bar{P}, \\ & \boldsymbol{g}^H \boldsymbol{S} \boldsymbol{g} \leq \Gamma \text{ for } (\boldsymbol{g} - \boldsymbol{g}_0)^H \boldsymbol{R}^{-1} (\boldsymbol{g} - \boldsymbol{g}_0) \leq \epsilon, \end{aligned} \tag{4.2}$$

where $\boldsymbol{S} = \mathbb{E}[\boldsymbol{x}\boldsymbol{x}^H]$ is the transmit covariance matrix, $\boldsymbol{S} \geq 0$ denotes that $\boldsymbol{S}$ is a positive semi-definite matrix, $\bar{P}$ is the transmit power contraint, Γ is the interference

[1]Due to the cognitive property, we assume that the SU can obtain the pilot signal from the PU, and has the knowledge of the transmit power of the PU. Thus, the SU can detect the channel from the PU to the SU. Moreover, since the SU shares the same spectrum with the PU, based on the channel from the PU to the SU, the statistics of the channel from the SU to the PU can be obtained [92]. Therefore, we can assume that $\boldsymbol{g}_0$ and $\boldsymbol{R}$ are known to the SU.

threshold of the PU, and ϵ is a positive constant. The parameter ϵ characterizes the uncertainty of $\boldsymbol{g}$ at the SU. According to the definition of the uncertainty in [95], $\mathbf{P1}$ belongs to a type of ellipsoid uncertainty problem, i.e., the uncertain parameter $\boldsymbol{g}$ is confined in a range of an ellipsoid $\mathcal{H}(\epsilon)$, where $\mathcal{H}(\epsilon) : \{\boldsymbol{g}|(\boldsymbol{g}-\boldsymbol{g}_0)^H\boldsymbol{R}^{-1}(\boldsymbol{g}-\boldsymbol{g}_0) \leq \epsilon\}$. Thus, the optimal solution of $(\mathbf{P1})$ can guarantee the interference power constraint for all the $\boldsymbol{g} \in \mathcal{H}(\epsilon)$, and thus the robustness of $\mathbf{P1}$ is in the *worst case* sense [53], i.e., in the worst case channel realization, the interference constraint should also be satisfied. If the primary transmission does not exist, then the interference constraint is excluded, and thus the problem reduces to a trivial beamforming problem. Hence, we only focus on the case where both PU and SU transmission exist.

Remark 4.1 *An important observation is that the objective function in ($\mathbf{P1}$) remains invariant when $\boldsymbol{h}$ undergoes an arbitrary phase rotation. Without loss of generality, we assume, in the sequel, that $\boldsymbol{h}$ and $\boldsymbol{g}_0$ have the same phase, i.e., Im$\{\boldsymbol{h}^H\boldsymbol{g}_0\} = 0$. Therefore, we can define the angle between $\boldsymbol{h}$ and $\boldsymbol{g}_0$ as $\alpha := acos\Big(\frac{\boldsymbol{h}^H\boldsymbol{g}_0}{|\boldsymbol{h}^H||\boldsymbol{g}_0|}\Big)$.*

Since $(\mathbf{P1})$ has a finite number of decision variable $\boldsymbol{S}$, and is subjected to an infinite number of constraints with respect to the compact set $\mathcal{H}(\epsilon)$, $(\mathbf{P1})$ is an SIP problem [96]. One obvious approach for an SIP problem is to transform it into an equivalent problem with finite constraints. However, there is no universal algorithm to determine the finite constraints from the infinite constraint set such that the transformed problem has the same solution as the original SIP problem. In the following section, we first study several important properties of $(\mathbf{P1})$, which can be used to transform the SIP problem into its equivalent finite constraint counterpart.

4.3 Properties of The Optimal Solution

The maximization $(\mathbf{P1})$ is a convex optimization problem, and thus has a unique optimal solution. The following lemma presents a key property of the optimal solution of $(\mathbf{P1})$.

Lemma 4.1 *The optimal covariance matrix $\boldsymbol{S}$ for $(\mathbf{P1})$ is a rank-1 matrix.*

The proof can be found in Appendix C.1.

Remark 4.2 *Lemma 4.1 indicates that beamforming is the optimal transmission strategy for $(\mathbf{P1})$, and the optimal transmit covariance matrix can be expressed as $\boldsymbol{S}_{opt} = p_{opt}\boldsymbol{v}_{opt}\boldsymbol{v}_{opt}^H$, where p_{opt} is the optimal transmit power and $\boldsymbol{v}_{opt}$ is the optimal beamforming vector with $\|\boldsymbol{v}_{opt}\| = 1$. Therefore, the ultimate objective of $(\mathbf{P1})$ is to determine p_{opt} and $\boldsymbol{v}_{opt}$.*

The following Lemma presents a closed-form solution for an optimization problem, which will be used in the sequel.

Lemma 4.2 *For the problem*

$$\max_{\boldsymbol{h}} p\boldsymbol{g}^H\boldsymbol{v}\boldsymbol{v}^H\boldsymbol{g}, \text{ subject to: } (\boldsymbol{g}-\boldsymbol{g}_0)^H\boldsymbol{R}^{-1}(\boldsymbol{g}-\boldsymbol{g}_0) \leq \epsilon, \tag{4.3}$$

where p, $\boldsymbol{v}$, and $\boldsymbol{g}_0$ are constant, the optimal solution is

$$\boldsymbol{g}_{max} = \boldsymbol{g}_0 + \sqrt{\frac{\epsilon}{\boldsymbol{v}^H\boldsymbol{R}\boldsymbol{v}}}\alpha\boldsymbol{R}\boldsymbol{v}, \text{where } \alpha = \boldsymbol{v}^H\boldsymbol{g}_0/|\boldsymbol{v}^H\boldsymbol{g}_0|. \tag{4.4}$$

The proof can be found in Appendix C.2. Based on Lemma 4.1 and Lemma 4.2, a necessary and sufficient condition for the optimal solution of $(\mathbf{P1})$ is presented as follows.

Lemma 4.3 *A necessary and sufficient condition for $\boldsymbol{S}_{opt}$ to be the globally optimal solution of ($\mathbf{P1}$) is that there exists an $\boldsymbol{g}_{opt}$ such that*

$$\boldsymbol{S}_{opt} = \arg\max_{\boldsymbol{S},p} \log(1+\boldsymbol{h}^H\boldsymbol{S}\boldsymbol{h}),\ \textit{subject to}:\ tr(\boldsymbol{S}) \le p,\ 0 \le p \le \bar{P},\ \boldsymbol{g}_{opt}^H\boldsymbol{S}\boldsymbol{g}_{opt} \le \Gamma, \tag{4.5}$$

where

$$\boldsymbol{g}_{opt} = \arg\max_{\boldsymbol{h}} \boldsymbol{g}^H\boldsymbol{S}_{opt}\boldsymbol{g},\ \textit{for}\ (\boldsymbol{g}-\boldsymbol{g}_0)^H\boldsymbol{R}^{-1}(\boldsymbol{g}-\boldsymbol{g}_0) \le \epsilon. \tag{4.6}$$

The proof can be found in Appendix C.3.

Remark 4.3 *The vector $\boldsymbol{g}_{opt}$ is a key element for all $\boldsymbol{g}:\ (\boldsymbol{g}-\boldsymbol{g}_0)^H\boldsymbol{R}^{-1}(\boldsymbol{g}-\boldsymbol{g}_0) \le \epsilon$, in the sense that, for the optimal solution, the constraint $\boldsymbol{g}_{opt}^H\boldsymbol{S}\boldsymbol{g}_{opt} \le \Gamma$ dominates the whole interference constraints, i.e., all the other interference constraints are inactive. However, $\boldsymbol{g}_{opt}$ can be viewed as an implicit variable for the problem* (4.5)*, and the optimal $\boldsymbol{S}$ and $\boldsymbol{g}_{opt}$ cannot be obtained separately. It is worth noting that the problem* (4.5) *has the same form as the problem discussed in [36], in which the CSI on the link of the SU and the link between SU-Tx and PU are perfectly known at the SU-Tx. However, unlike the problem in [36], $\boldsymbol{g}_{opt}$ in* (4.5) *is an unknown variable.*

In the following lemma, the optimal beamforming vector $\boldsymbol{v}_{\text{opt}}$ is shown to lie in a two-dimensional (2-D) space spanned by $\boldsymbol{g}_0$ and the projection of $\boldsymbol{h}$ into the null space of $\boldsymbol{g}_0$. Define $\hat{\boldsymbol{g}}_{//} = \boldsymbol{g}_0/\|\boldsymbol{g}_0\|$ and $\hat{\boldsymbol{g}}_{\perp} = \boldsymbol{g}_{\perp}/\|\boldsymbol{g}_{\perp}\|$, where $\boldsymbol{g}_{\perp} = \boldsymbol{h} - (\hat{\boldsymbol{g}}_{//}^H\boldsymbol{h})\hat{\boldsymbol{g}}_{//}$. Hence, we have $\boldsymbol{h} = a_{h_s}\hat{\boldsymbol{g}}_{//} + b_{h_s}\hat{\boldsymbol{g}}_{\perp}$ with $a_{h_s}, b_{h_s} \in \mathbb{R}$.

Lemma 4.4 *The optimal beamforming vector $\boldsymbol{v}_{opt}$ is of the form $a_v\hat{\boldsymbol{g}}_{//} + b_v\hat{\boldsymbol{g}}_{\perp}$ with $a_v, b_v \in \mathbb{R}$.*

The proof can be found in Appendix C.4.

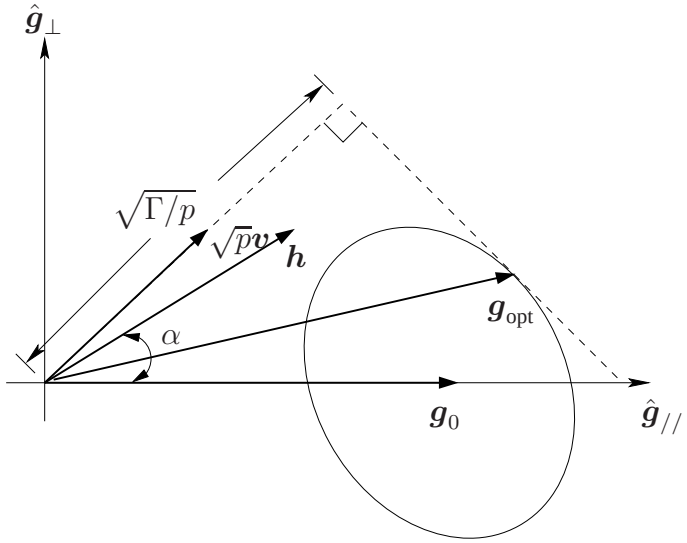

Figure 4.2: The geometric explanation of Lemma 4.4. The ellipse is the projection of $\boldsymbol{g} = \{\boldsymbol{g} | (\boldsymbol{g} - \boldsymbol{g}_0)^H \boldsymbol{R}^{-1} (\boldsymbol{g} - \boldsymbol{g}_0) = \epsilon\}$ on the plane spanned by $\hat{\boldsymbol{g}}_{//}$ and $\hat{\boldsymbol{g}}_\perp$.

Remark 4.4 *According to Lemma 4.4, we can search for the optimal beamforming vector $\boldsymbol{v}_{opt}$ on the 2-D space spanned by $\hat{\boldsymbol{g}}_{//}$ and $\hat{\boldsymbol{g}}_\perp$, which simplifies the search process significantly. As depicted in Fig. 4.2, ($\mathbf{P1}$) is transformed into the problem of determining the beamforming vector $\boldsymbol{v}_{opt}$ in the 2-D space and the corresponding power p_{opt}. Combining Lemma 4.3 and Lemma 4.4, it is easy to conclude that $\boldsymbol{g}_{opt}$ lies in the space spanned by $\hat{\boldsymbol{g}}_{//}$ and $\hat{\boldsymbol{g}}_\perp$.*

4.4 Second Order Cone Programming Solution

In this section, we solve ($\mathbf{P1}$) via a standard interior point algorithm [46, 53, 97]. We first transform the SIP problem into a finite constraint problem, and further transform it into a standard SOCP form, which can be solved by using a standard software package such as SeDuMi [98]. One key observation is that if $\max_{\boldsymbol{h} \in \mathcal{H}(\epsilon)} \boldsymbol{g}^H \boldsymbol{S} \boldsymbol{g} \leq \Gamma$, i.e., the worst case interference constraint of satisfied, then the interference constraint of $\mathbf{P1}$

holds. Combining this observation with Lemma 4.1, $(\mathbf{P1})$ can be transformed as:

$$\begin{aligned} \textbf{Equivalent problem } (\mathbf{P2}): \quad & \max_{p\geq 0, \|\boldsymbol{v}\|=1} \log(1+p\boldsymbol{h}^H\boldsymbol{v}\boldsymbol{v}^H\boldsymbol{h}) \\ & \text{subject to : } p\leq \bar{P},\ \max_{\boldsymbol{h}\in\mathcal{H}(\epsilon)} p\boldsymbol{g}^H\boldsymbol{v}\boldsymbol{v}^H\boldsymbol{g}\leq \Gamma. \end{aligned} \tag{4.7}$$

It is clear that maximizing $\log(1+p\boldsymbol{h}^H\boldsymbol{v}\boldsymbol{v}^H\boldsymbol{h})$ is equivalent to maximizing $|\sqrt{p}\boldsymbol{h}^H\boldsymbol{v}|$. By defining $\boldsymbol{w}=\sqrt{p}\boldsymbol{v}$, the objective function can be rewritten as $|\boldsymbol{h}^H\boldsymbol{w}|$. Similarly, the interference power can be expressed as $|\boldsymbol{g}^H\boldsymbol{w}|^2$. Thus, problem $\mathbf{P2}$ can be further transformed to

$$\begin{aligned} & \max_{\boldsymbol{w}} |\boldsymbol{h}^H\boldsymbol{w}| \\ & \text{subject to : } \|\boldsymbol{w}\|\leq\sqrt{P},\ \max_{\boldsymbol{h}\in\mathcal{H}(\epsilon)} |\boldsymbol{g}^H\boldsymbol{w}|\leq\sqrt{\Gamma}. \end{aligned} \tag{4.8}$$

According to the definition of $\mathcal{H}(\epsilon)$, we can rewrite the worst-case constraint in (4.8) as

$$\max_{\boldsymbol{h}\in\mathcal{H}(\epsilon)} |\boldsymbol{g}^H\boldsymbol{w}| = \max_{\boldsymbol{h}_1\in\mathcal{H}_1(\epsilon)} |(\boldsymbol{g}_0+\boldsymbol{g}_1)^H\boldsymbol{w}|\leq\sqrt{\Gamma}, \tag{4.9}$$

where $\boldsymbol{g}=\boldsymbol{g}_0+\boldsymbol{g}_1$, the vector $\boldsymbol{g}_1$ is a variable, and $\mathcal{H}_1(\epsilon):\{\boldsymbol{g}_1|\boldsymbol{g}_1^H\boldsymbol{R}^{-1}\boldsymbol{g}_1\leq\epsilon\}$. By applying the triangle inequality, the interference power can be transformed as follows:

$$|(\boldsymbol{g}_0+\boldsymbol{g}_1)^H\boldsymbol{w}| \leq |\boldsymbol{g}_0^H\boldsymbol{w}|+|\boldsymbol{g}_1^H\boldsymbol{w}|\leq|\boldsymbol{g}_0^H\boldsymbol{w}|+\sqrt{\epsilon}\|\boldsymbol{Q}\boldsymbol{w}\|, \tag{4.10}$$

where $\boldsymbol{Q}=\boldsymbol{\Delta}^{-1/2}\boldsymbol{U}$ with $\boldsymbol{\Delta}$ and $\boldsymbol{U}$ being obtained by the eigenvalue decomposition of $\boldsymbol{R}^{-1}$ as $\boldsymbol{R}^{-1}=\boldsymbol{U}^H\boldsymbol{\Delta}\boldsymbol{U}$. The last inequality in (4.10) is obtained by solving the problem $\max_{\boldsymbol{g}_1\in\mathcal{H}_1(\epsilon)} |\boldsymbol{g}_1^H\boldsymbol{w}|$ (refer to Lemma 4.2). Moreover, since the arbitrary phase rotation of $\boldsymbol{w}$ does not change the value of the objective function or the constraints, according to Remark 4.1 and Lemma 4.4, we can assume that $\boldsymbol{w}$, $\boldsymbol{h}$, and $\boldsymbol{g}_0$ have the same phase, i.e.,

$$\text{Re}\{\boldsymbol{w}^H\boldsymbol{h}\}\geq 0,\ \text{Im}\{\boldsymbol{w}^H\boldsymbol{g}_0\}=0,\ \text{and Im}\{\boldsymbol{w}^H\boldsymbol{h}\}=0. \tag{4.11}$$

Hence, the interference constraint can be transformed into two second order cone inequalities as follows

$$\sqrt{\epsilon}\|\boldsymbol{Q}\boldsymbol{w}\| + \boldsymbol{g}_0^H\boldsymbol{w} \leq \sqrt{\Gamma}, \text{ and } \sqrt{\epsilon}\|\boldsymbol{Q}\boldsymbol{w}\| - \boldsymbol{g}_0^H\boldsymbol{w} \leq \sqrt{\Gamma}. \tag{4.12}$$

By combining (4.8), (4.12), with (4.11), $(\mathbf{P1})$ is transformed into the standard SOCP problem as follows

$$\begin{aligned} &\max_{\boldsymbol{w}} \boldsymbol{h}^H\boldsymbol{w} \\ &\text{subject to :} \|\boldsymbol{w}\| \leq \sqrt{P}, \text{Im}\{\boldsymbol{w}^H\boldsymbol{g}_0\} = 0, \\ &\qquad \sqrt{\epsilon}\|\boldsymbol{Q}\boldsymbol{w}\| + \boldsymbol{g}_0^H\boldsymbol{w} \leq \sqrt{\Gamma}, \sqrt{\epsilon}\|\boldsymbol{Q}\boldsymbol{w}\| - \boldsymbol{g}_0^H\boldsymbol{w} \leq \sqrt{\Gamma}. \end{aligned} \tag{4.13}$$

Since the parameters $\boldsymbol{h}$ and $\boldsymbol{g}_0$, and the variable $\boldsymbol{w}$ in (4.13) have complex values, we first convert them to its corresponding real-valued form in order to simplify the solution. Define $\tilde{\boldsymbol{w}} := [\text{Re}\{\boldsymbol{w}\}^T, \text{Im}\{\boldsymbol{w}\}^T]^T$, $\tilde{\boldsymbol{g}}_0 := [\text{Re}\{\boldsymbol{g}_0\}^T, \text{Im}\{\boldsymbol{g}_0\}^T]^T$, $\tilde{\boldsymbol{g}}_s := [\text{Re}\{\boldsymbol{h}\}^T, \text{Im}\{\boldsymbol{h}\}^T]^T$, $\check{\boldsymbol{g}}_0 := [\text{Im}\{\boldsymbol{g}_0\}^T, -\text{Re}\{\boldsymbol{g}_0\}^T]^T$, and $\tilde{\boldsymbol{Q}} := \begin{bmatrix} \text{Re}\{\boldsymbol{Q}\} & -\text{Im}\{\boldsymbol{Q}\} \\ \text{Im}\{\boldsymbol{Q}\} & \text{Re}\{\boldsymbol{Q}\} \end{bmatrix}$.

We then can rewrite the standard SOCP problem (4.13) as

$$\begin{aligned} &\max_{\tilde{\boldsymbol{w}}} \tilde{\boldsymbol{g}}_s^H\tilde{\boldsymbol{w}} \\ &\text{subject to :} \ \|\tilde{\boldsymbol{w}}\| \leq \sqrt{P}, \check{\boldsymbol{g}}_0^H\tilde{\boldsymbol{w}} = 0, \\ &\qquad \sqrt{\epsilon}\|\tilde{\boldsymbol{Q}}\tilde{\boldsymbol{w}}\| + \tilde{\boldsymbol{g}}_0^H\tilde{\boldsymbol{w}} \leq \sqrt{\Gamma}, \sqrt{\epsilon}\|\tilde{\boldsymbol{Q}}\tilde{\boldsymbol{w}}\| - \tilde{\boldsymbol{g}}_0^H\tilde{\boldsymbol{w}} \leq \sqrt{\Gamma}. \end{aligned} \tag{4.14}$$

Problem (4.14) can be solved by a standard interior point program SeDuMi [98], which has a polynomial complexity. In the next section, we develop an analytical algorithm to solve $(\mathbf{P1})$, which reduces the complexity of the interior point based algorithm substantially.

4.5 An Analytical Solution

In this section, we present a geometric approach to $(\mathbf{P1})$. We begin by studying a special case, the mean feedback case, i.e., $\boldsymbol{R} = \sigma^2\boldsymbol{I}$. Due to its special geometric

structure, the mean feedback case problem can be solved via a closed-form algorithm. We next show that $(\mathbf{P1})$ can be transformed into an optimization problem similar to the mean feedback case. Based on the closed-form solution derived for the mean feedback case, the analytical solution to $(\mathbf{P1})$ with a general form of a covariance matrix $\boldsymbol{R}$ is presented in Subsection 4.5.2.

4.5.1 Mean Feedback Case

Based on the observation in Lemma 4.1 and the definition of the mean feedback, the special case of $(\mathbf{P1})$ with mean feedback can be written as follows.

$$\begin{aligned} \textbf{Mean feedback problem (P3):} \max_{p\geq 0, \|\boldsymbol{v}\|=1} \; & \log(1+p\boldsymbol{h}^H\boldsymbol{v}\boldsymbol{v}^H\boldsymbol{h}) \\ \text{subject to :} \; & p \leq \bar{P}, \\ & p\boldsymbol{g}^H\boldsymbol{v}\boldsymbol{v}^H\boldsymbol{g} \leq \Gamma, \text{for } \|\boldsymbol{g}-\boldsymbol{g}_0\|^2 \leq \epsilon\sigma^2. \end{aligned} \tag{4.15}$$

Problem $\mathbf{P3}$ has two constraints, i.e., the transmit power constraint and the interference constraint. Similar to the idea in [68], the two-constraint problem is decoupled into two single-constraint subproblems:

$$\textbf{Subproblem 1 (SP1):} \max_{p\geq 0, \|\boldsymbol{v}\|=1} \quad \log(1+p\boldsymbol{h}^H\boldsymbol{v}\boldsymbol{v}^H\boldsymbol{h}) \tag{4.16}$$

$$\text{subject to :} \quad p \leq \bar{P}. \tag{4.17}$$

$$\textbf{Subproblem 2 (SP2):} \max_{p\geq 0, \|\boldsymbol{v}\|=1} \quad \log(1+p\boldsymbol{h}^H\boldsymbol{v}\boldsymbol{v}^H\boldsymbol{h}) \tag{4.18}$$

$$\text{subject to :} \quad p\boldsymbol{g}^H\boldsymbol{v}\boldsymbol{v}^H\boldsymbol{g} \leq \Gamma, \text{ for } \|\boldsymbol{g}-\boldsymbol{g}_0\|^2 \leq \epsilon\sigma^2. \tag{4.19}$$

In the sequel, we present the algorithm to obtain the optimal power p_{opt} and the optimal beamforming vector $\boldsymbol{v}_{\text{opt}}$ for both subproblems in subsection 4.5.1.1, and describe the relationship between the subproblems and problem $\mathbf{P3}$ in subsection 4.5.1.2.

4.5.1.1 Solution to subproblems

For $\mathbf{SP1}$, the optimal power is constrained by the transmit power constraint, and thus $p_{\text{opt}} = P$. Moreover, since there does not exist any constraints on the beamforming direction, it is obvious that the optimal beamforming direction is equal to $\boldsymbol{h}$, i.e., $\boldsymbol{v}_{\text{opt}} = \boldsymbol{h}/\|\boldsymbol{h}\|$. Thus, the optimal covariance matrix $\boldsymbol{S}_{\text{opt}}$ for $\mathbf{SP1}$ is $\bar{P}\boldsymbol{h}\boldsymbol{h}^H/\|\boldsymbol{h}\|^2$. In the following, we focus on the solution to $\mathbf{SP2}$.

$\mathbf{SP2}$ has infinitely many interference constraints, and thus is an SIP problem too. By following a similar line of thinking as in Lemma 4.3, $\mathbf{SP2}$ can be transformed into an equivalent problem that has finite constraints as follows.

Lemma 4.5 $\mathbf{SP2}$ *and the following optimization problem:*

$$\max_{p\geq 0, \|\boldsymbol{v}\|=1} \log(1+p\boldsymbol{h}^H\boldsymbol{v}\boldsymbol{v}^H\boldsymbol{h}),\ \textit{subject to}:\ p\boldsymbol{g}_{opt}^H\boldsymbol{v}\boldsymbol{v}^H\boldsymbol{g}_{opt} \leq \Gamma, \tag{4.20}$$

where $\boldsymbol{g}_{opt} = \boldsymbol{g}_0 + \sqrt{\epsilon}\sigma\boldsymbol{v}$*, have the same optimal solution.*

The proof can be found in Appendix C.5. Since $\mathbf{SP2}$ can be viewed as a special case of $\mathbf{P1}$ by setting $\bar{P} = \infty$, it is evident from Lemma 4.4 that the optimal solution $\boldsymbol{v}$ of problem (4.20) lies in the plane spanned by $\hat{\boldsymbol{g}}_{//}$ and $\hat{\boldsymbol{g}}_{\perp}$, i.e., the optimal $\boldsymbol{v}$ found in this 2-D space is also the globally optimal solution of the original problem $\mathbf{SP2}$. We next apply a geometric approach to search the optimal solution, i.e., by restricting our search space to a 2-D space. As shown in Fig. 4.3, we define the angle between $\boldsymbol{v}$ and $\boldsymbol{g}_0$ as β. It is easy to observe that $0 \leq \alpha \leq \pi/2$[2]. Since $\boldsymbol{v}$ lies in a 2-D space, $\boldsymbol{v}$ can be uniquely identified by the angle β. Hence, we need only to search for the optimal angle β_{opt}. By exploiting the relationship between p, $\boldsymbol{v}$, and β, the two-variable optimization problem (4.20) can be further transformed into an optimization problem with a single variable β, which can be readily solved.

[2]Note that we can always replace $\boldsymbol{h}$ by $-\boldsymbol{h}$ without affecting the final result of $\mathbf{SP2}$. Therefore, if $\alpha \geq \pi/2$, we can have a new equivalent problem by replacing $\boldsymbol{h}$ with $-\boldsymbol{h}$. The inequality $\alpha \leq \pi/2$ holds for the new problem.

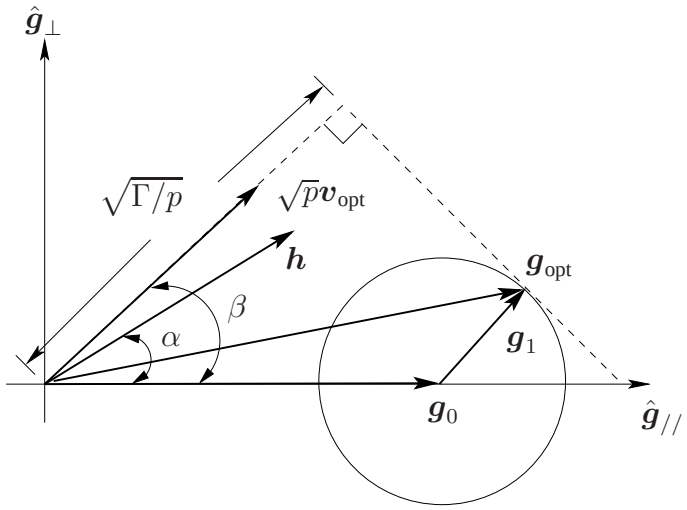

Figure 4.3: The geometric explanation of problem $\mathbf{P3}$. The circle is the projection of $\boldsymbol{g} = \{\boldsymbol{g} | \|\boldsymbol{g} - \boldsymbol{g}_0\|^2 = \epsilon\}$ on the plane spanned by $\hat{\boldsymbol{g}}_{//}$ and $\hat{\boldsymbol{g}}_{\perp}$.

By observing Fig. 4.3, the angle between $\boldsymbol{h}$ and $\boldsymbol{v}$ is $\beta - \alpha$, and hence the objective function of (4.20) can be expressed as

$$\max_{\|\boldsymbol{v}\|=1} \log(1 + p\boldsymbol{h}^H \boldsymbol{v}\boldsymbol{v}^H \boldsymbol{h}) = \max_{\beta} \log\Big(1 + p\|\boldsymbol{h}\|^2 \cos^2(\beta - \alpha)\Big). \tag{4.21}$$

Clearly, the maximum rate is achieved if the following function

$$f(\beta) := p\|\boldsymbol{h}\|^2 \cos^2(\beta - \alpha) \tag{4.22}$$

is maximized.

Moreover, it can be proved by contradiction that the interference constraint is satisfied with equality, i.e., $\boldsymbol{g}_{\text{opt}}^H \boldsymbol{S} \boldsymbol{g}_{\text{opt}} = \Gamma$. Thus, we have

$$p\boldsymbol{g}_{\text{opt}}^H \boldsymbol{v}\boldsymbol{v}^H \boldsymbol{g}_{\text{opt}} = p(\boldsymbol{g}_0 + \sqrt{\epsilon}\sigma\boldsymbol{v})^H \boldsymbol{v}\boldsymbol{v}^H (\boldsymbol{g}_0 + \sqrt{\epsilon}\sigma\boldsymbol{v}) = p\big(\|\boldsymbol{g}_0\| \cos\beta + \sqrt{\epsilon}\sigma\big)^2 = \Gamma. \tag{4.23}$$

Hence, the interference constraint is transformed into

$$p = \frac{\Gamma}{\big(\|\boldsymbol{g}_0\| \cos\beta + \sqrt{\epsilon}\sigma\big)^2}. \tag{4.24}$$

By substituting (4.24) into (4.22), we have

$$f(\beta) = p\|\boldsymbol{h}\|^2 \cos^2(\beta - \alpha) = \frac{\|\boldsymbol{h}\|^2 \Gamma \cos^2(\beta - \alpha)}{\left(\|\boldsymbol{g}_0\| \cos(\beta) + \sqrt{\epsilon}\sigma\right)^2}. \tag{4.25}$$

Thus, the optimal β_{opt} can be expressed as

$$\beta_{\text{opt}} = \arg\max f(\beta) = \arg\max \frac{\|\boldsymbol{h}\|^2 \Gamma \cos^2(\beta - \alpha)}{\left(\|\boldsymbol{g}_0\| \cos(\beta) + \sqrt{\epsilon}\sigma\right)^2}. \tag{4.26}$$

The problem of (4.26) is a single variable optimization problem. It is easy to observe that the feasible region for β is $[\alpha, \pi/2]$. According to the sufficient and necessary condition for the optimal solution of an optimization problem, β_{opt} lies either on the border of the region (α or $\pi/2$) or on the point which satisfies $\partial f(\beta)/\partial\beta = 0$. Since

$$\frac{\partial f(\beta)}{\partial \beta} = \frac{2\|\boldsymbol{h}\|^2 \Gamma \cos(\beta - \alpha)\Big(\sin\alpha - \sin(\beta - \alpha)\sqrt{\epsilon}\sigma/\|\boldsymbol{g}_0\|\Big)}{\|\boldsymbol{g}_0\|^2\big(\cos\beta + \sqrt{\epsilon}\sigma/\|\boldsymbol{g}_0\|\big)^3}, \tag{4.27}$$

we can obtain a locally optimal solution $\beta_1 = \sin^{-1}\left(\frac{\|\boldsymbol{g}_0\|\sin\alpha}{\sqrt{\epsilon}\sigma}\right) + \alpha$ by solving the equation $\partial f(\beta)/\partial\beta = 0$. In the case when $\frac{\|\boldsymbol{g}_0\|\sin\alpha}{\sqrt{\epsilon}\sigma} > 1$, $f(\beta)$ is a non-decreasing function. Hence, the optimal β is $\pi/2$, and we define $f(\beta_1) = -\infty$ for this case. Therefore, the globally optimal solution is

$$\beta_{\text{opt}} = \arg\max(f(\alpha), f(\pi/2), f(\beta_1)). \tag{4.28}$$

The optimal power p_{opt} can be further obtained by substituting β_{opt} into (4.24). According to the definition of β and Lemma 4.4, we have

$$\boldsymbol{v}_{\text{opt}} = a_v \hat{\boldsymbol{g}}_{//} + b_v \hat{\boldsymbol{g}}_{\perp}, \tag{4.29}$$

where $a_v = \cos(\beta_{\text{opt}})$ and $b_v = \sin(\beta_{\text{opt}})$. In summary, $\mathbf{SP2}$ can be solved by Algorithm 1 as described in Table 4.1.

4.5.1.2 Optimal solution to problem $\mathbf{P3}$

In the preceding subsection, we presented the optimal solutions for the two subproblems. We now turn our attention to the relationship between problem $\mathbf{P3}$ and the subproblems, and present the complete algorithm to solve problem $\mathbf{P3}$. Since the convex

Table 4.1: The algorithm for SP2.

Algorithm 1
1. Compute β_{opt} through (4.28),
2. Compute p_{opt} according to (4.24),
3. Compute $\boldsymbol{v}_{\text{opt}}$ according to (4.29),
4. $\boldsymbol{S}_{\text{opt}} = p_{\text{opt}}\boldsymbol{v}_{\text{opt}}\boldsymbol{v}_{\text{opt}}^H$.

optimization problem $\mathbf{P3}$ has two constraints, the optimal solution can be classified into three cases depending on the activeness of the constraints: 1) only the transmit power constraint is active; 2) only the interference constraint is active; and 3) both constraints are active. Relying on this classification, the relationship between the solutions of problem $\mathbf{P3}$ and the two subproblems is described as follows.

Theorem 4.1 *If the optimal solution $\boldsymbol{S}_1$ of $\mathbf{SP1}$ satisfies the constraint of $\mathbf{SP2}$, then $\boldsymbol{S}_1$ is the optimal solution of problem $\mathbf{P3}$. If the optimal solution $\boldsymbol{S}_2$ of $\mathbf{SP2}$ satisfies the constraint of $\mathbf{SP1}$, then $\boldsymbol{S}_2$ is the optimal solution of problem $\mathbf{P3}$. Otherwise, the optimal solution of problem $\mathbf{P3}$ simultaneously satisfies the transmit power constraint and $\boldsymbol{g}_{opt}^H\boldsymbol{S}\boldsymbol{g}_{opt} \leq \Gamma$ with equality.*

The proof can be found in Appendix C.6.

Remark 4.5 *To apply Theorem 4.1, we need to test whether $\boldsymbol{S}_1$ and $\boldsymbol{S}_2$ satisfy both constraints. The condition that $\boldsymbol{S}_1$ satisfies the interference constraint is*

$$P_{int} \leq \Gamma, \text{where } P_{int} = \max_{\boldsymbol{h}} \boldsymbol{g}^H\boldsymbol{S}_1\boldsymbol{g}, \text{ for } \|\boldsymbol{g} - \boldsymbol{g}_0\|^2 \leq \epsilon\sigma^2, \tag{4.30}$$

where P_{int} can be obtained by applying Lemma 4.2. The condition that $\boldsymbol{S}_2$ satisfies the transmit power constraint is $tr(\boldsymbol{S}_2) \leq \bar{P}$.

Table 4.2: The algorithm for problem $\mathbf{P3}$ in the case where two constraints are satisfied simultaneously.

Algorithm 2
1. Compute β_{opt} through (4.33),
2. Based on (4.29), compute $\boldsymbol{v}_{\text{opt}}$,
3. $\boldsymbol{S}_{\text{opt}} = \bar{P}\boldsymbol{v}_{\text{opt}}\boldsymbol{v}_{\text{opt}}^H$.

We next discuss the method for finding the solution in the case where neither $\boldsymbol{S}_1$ nor $\boldsymbol{S}_2$ is the optimal solution of problem $\mathbf{P3}$. Similarly to the method in the preceding subsection, we solve this case from a geometric perspective. According to Theorem 4.1, in the case in which neither $\boldsymbol{S}_1$ nor $\boldsymbol{S}_2$ is the feasible solution, the optimal covariance $\boldsymbol{S}_{\text{opt}}$ must satisfy both constraints with equality, i.e.,

$$p_{\text{opt}} = \bar{P}, \text{ and } p_{\text{opt}}\boldsymbol{g}_{\text{opt}}^H\boldsymbol{v}_{\text{opt}}\boldsymbol{v}_{\text{opt}}^H\boldsymbol{g}_{\text{opt}} = \Gamma. \tag{4.31}$$

Combining these two equalities, we have

$$\bar{P}\big(\|\boldsymbol{g}_0\|\cos(\beta) + \sqrt{\epsilon}\sigma\big)^2 = \Gamma. \tag{4.32}$$

Thus,

$$\beta_{\text{opt}} = \arccos\Big(\frac{\sqrt{\Gamma/P} - \sqrt{\epsilon}\sigma}{\|\boldsymbol{g}_0\|}\Big). \tag{4.33}$$

Based on β_{opt}, we can obtain $\boldsymbol{v}_{\text{opt}}$ from (4.29). We summarize the procedure called Algorithm 2, which solves the case where both constraints are active for problem $\mathbf{P3}$, in Table 4.2. Furthermore, we are now ready to present the complete algorithm, namely Algorithm 3, to solve problem $\mathbf{P3}$ in Table 4.3.

In Algorithm 3, we obtain the optimal solutions to $\mathbf{SP1}$ and $\mathbf{SP2}$ and the optimal solution to the case where both constraints are active separately. According to Theorem 4.1, the final solution obtained in Algorithm 3 is thus the optimal solution of problem $\mathbf{P3}$.

Table 4.3: The complete algorithm for problem $\mathbf{P3}$.

Algorithm 3
1. Compute the optimal solution $\boldsymbol{S}_1 = \bar{P}\boldsymbol{h}\boldsymbol{h}^H/\|\boldsymbol{h}\|^2$ for $\mathbf{SP1}$,
2. Compute the optimal solution $\boldsymbol{S}_2$ for $\mathbf{SP2}$ via Algorithm 1,
3. If $\boldsymbol{S}_1$ satisfies the interference constraint, then $\boldsymbol{S}_1$ is the optimal solution,
4. Elsif $\boldsymbol{S}_2$ satisfies the transmit power constraint, then $\boldsymbol{S}_2$ is the optimal solution,
5. Otherwise compute the optimal solution via Algorithm 2.

4.5.2 The Analytical Method for $(\mathbf{P1})$

In the preceding subsection, the mean feedback problem $\mathbf{P3}$ is solved via a closed-form algorithm. Unlike problem $\mathbf{P3}$, $(\mathbf{P1})$ has a non-identity-matrix covariance feedback. To exploit the closed-form algorithm, we first transform $(\mathbf{P1})$ into a problem with the mean feedback form as follows.

$$\begin{aligned} \textbf{Equivalent problem } (\mathbf{P4}): \max_{p,\bar{\boldsymbol{v}}} \ & \log(1 + p\bar{\boldsymbol{g}}_s^H \bar{\boldsymbol{v}}\bar{\boldsymbol{v}}^H \bar{\boldsymbol{g}}_s) \\ \text{subject to}: \ & p\|\boldsymbol{\Delta}^{1/2}\bar{\boldsymbol{v}}\|^2 \le \bar{P}, \\ & p\bar{\boldsymbol{g}}^H \bar{\boldsymbol{v}}\bar{\boldsymbol{v}}^H \bar{\boldsymbol{g}} \le \Gamma, \ \text{for } \|\bar{\boldsymbol{g}} - \bar{\boldsymbol{g}}_0\|^2 \le \epsilon, \end{aligned} \tag{4.34}$$

where $\boldsymbol{R}^{-1} = \boldsymbol{U}^H\boldsymbol{\Delta}\boldsymbol{U}$ obtained by eigen-decomposing $\boldsymbol{R}^{-1}$, $\bar{\boldsymbol{g}} := \boldsymbol{\Delta}^{1/2}\boldsymbol{U}\boldsymbol{g}$, $\bar{\boldsymbol{g}}_0 := \boldsymbol{\Delta}^{1/2}\boldsymbol{U}\boldsymbol{g}_0$, $\bar{\boldsymbol{g}}_s := \boldsymbol{\Delta}^{1/2}\boldsymbol{U}\boldsymbol{h}$, and $\bar{\boldsymbol{v}} := \boldsymbol{\Delta}^{-1/2}\boldsymbol{U}\boldsymbol{v}$. By substituting these definitions into (4.34), it can be observed that the achieved rates and constraints of both $(\mathbf{P1})$ and $\mathbf{P4}$ are equivalent. Thus, the optimal solution of $\mathbf{P1}$ can be obtained by solving its equivalent problem $\mathbf{P4}$. Moreover, the optimal beamforming vector $\bar{\boldsymbol{v}}_{\text{opt}}$ of problem $\mathbf{P4}$ can be easily transformed into the optimal solution $\boldsymbol{v}_{\text{opt}}$ for $(\mathbf{P1})$ by letting $\boldsymbol{v}_{\text{opt}} = \boldsymbol{U}^H\boldsymbol{\Delta}^{1/2}\bar{\boldsymbol{v}}_{\text{opt}}$. Note that it is not necessary that $\|\bar{\boldsymbol{v}}\| = 1$ in (4.34).

In the preceding subsection, decoupling the multiple constraint problem into several single constraint subproblems facilitates the analysis and simplifies the process of

solving the problem. For problem $\mathbf{P4}$, it can also be decoupled into two subproblems as follows.

$$\textbf{Subproblem 3 (SP3):} \max_{p,\bar{\boldsymbol{v}}} \ \log(1 + p\bar{\boldsymbol{g}}_s^H \bar{\boldsymbol{v}}\bar{\boldsymbol{v}}^H \bar{\boldsymbol{g}}_s) \tag{4.35}$$

$$\text{subject to :} \ \ p\|\boldsymbol{\Delta}^{1/2}\bar{\boldsymbol{v}}\|^2 \leq \bar{P}. \tag{4.36}$$

$$\textbf{Subproblem 4 (SP4):} \max_{p,\bar{\boldsymbol{v}}} \ \log(1 + p\bar{\boldsymbol{g}}_s^H \bar{\boldsymbol{v}}\bar{\boldsymbol{v}}^H \bar{\boldsymbol{g}}_s) \tag{4.37}$$

$$\text{subject to :} \ \ p\bar{\boldsymbol{g}}^H \bar{\boldsymbol{v}}\bar{\boldsymbol{v}}^H \bar{\boldsymbol{g}} \leq \Gamma \text{ for } \|\bar{\boldsymbol{g}} - \bar{\boldsymbol{g}}_0\|^2 \leq \epsilon. \tag{4.38}$$

It is easy to observe that $\mathbf{SP3}$ is equivalent to $\mathbf{SP1}$, and the optimal transmit covariance matrix of $\mathbf{SP3}$ can be obtained in the same way as that for $\mathbf{SP1}$. Moreover, $\mathbf{SP4}$ is the same as $\mathbf{SP2}$, and thus it can be solved by Algorithm 1 discussed in Subsection 4.5.1.1.

The relationship between problem $\mathbf{P4}$ and subproblems $\mathbf{SP3}$ and $\mathbf{SP4}$ is similar to the one between $\mathbf{P3}$ and corresponding subproblems as depicted in Theorem 4.1, i.e., if either optimal solution of $\mathbf{SP3}$ or $\mathbf{SP4}$ satisfies both constraints, then it is the globally optimal solution; otherwise, the optimal solution satisfies both constraints with equalities. We hereafter need to consider only the case in which the solutions of both subproblems are not feasible for problem $\mathbf{P4}$. For this case, the two equality constraints can be written as follows.

$$\|\boldsymbol{\Delta}^{1/2}\bar{\boldsymbol{v}}\| = 1, \text{ and } \max\left(\bar{\boldsymbol{g}}^H \bar{\boldsymbol{v}}\bar{\boldsymbol{v}}^H \bar{\boldsymbol{g}}\right) = \frac{\Gamma}{\bar{P}}, \text{ for } \|\bar{\boldsymbol{g}} - \bar{\boldsymbol{g}}_0\|^2 \leq \epsilon. \tag{4.39}$$

Assume that the angle between $\bar{\boldsymbol{g}}_0$ and $\bar{\boldsymbol{v}}$ is $\bar{\beta}$, and that $\bar{p} = \|\bar{\boldsymbol{v}}\|$. Similar to Lemma 4.4, the optimal $\bar{\boldsymbol{v}}$ lies in a plane spanned by $\hat{\bar{\boldsymbol{g}}}$ and $\hat{\bar{\boldsymbol{g}}}_\perp$, where $\hat{\bar{\boldsymbol{g}}} = \bar{\boldsymbol{g}}_0/\|\bar{\boldsymbol{g}}_0\|$, $\hat{\bar{\boldsymbol{g}}}_\perp = \bar{\boldsymbol{g}}_\perp/\|\bar{\boldsymbol{g}}_\perp\|$, and $\bar{\boldsymbol{g}}_\perp = \bar{\boldsymbol{g}}_s - (\hat{\bar{\boldsymbol{g}}}^H \bar{\boldsymbol{g}}_s)\hat{\bar{\boldsymbol{g}}}$. Thus, if we can determine $\bar{\beta}$ and $\bar{p}$ from (4.39), then the optimal $\bar{\boldsymbol{v}}$ can be identified by

$$\bar{\boldsymbol{v}} = \bar{p}\big(\cos(\bar{\beta})\hat{\bar{\boldsymbol{g}}} + \sin(\bar{\beta})\hat{\bar{\boldsymbol{g}}}_\perp\big). \tag{4.40}$$

Table 4.4: The algorithm for problem $\mathbf{P4}$ in the case where two constraints are satisfied simultaneously.

Algorithm 4
1. Compute $\bar{\beta}$ via (4.44), and compute $\bar{\boldsymbol{v}}$ via (4.40),
2. Based on the relationship between $\bar{\boldsymbol{v}}$ and $\boldsymbol{v}$, compute $\boldsymbol{v}_{\text{opt}}$,
3. $\boldsymbol{S}_{\text{opt}} = \bar{P}\boldsymbol{v}_{\text{opt}}\boldsymbol{v}_{\text{opt}}^H$.

Based on the new variables $\bar{\beta}$ and $\bar{p}$, the constraints (4.39) can be transformed as follows.

$$\bar{p}\left\|\boldsymbol{\Delta}^{1/2}\big(\cos(\bar{\beta})\hat{\bar{\boldsymbol{g}}} + \sin(\bar{\beta})\hat{\bar{\boldsymbol{g}}}_{\perp}\big)\right\| = 1, \tag{4.41}$$

$$\text{and, } \bar{p}\big(\cos(\bar{\beta})\|\bar{\boldsymbol{g}}_0\| + \sqrt{\epsilon}\big) = \sqrt{\frac{\Gamma}{\bar{P}}}. \tag{4.42}$$

According to (4.41), we have

$$\bar{p} = \frac{1}{\left\|\boldsymbol{\Delta}^{1/2}\big(\cos(\bar{\beta})\hat{\bar{\boldsymbol{g}}} + \sin(\bar{\beta})\hat{\bar{\boldsymbol{g}}}_{\perp}\big)\right\|}. \tag{4.43}$$

Substituting (4.43) into (4.42), we have

$$\sqrt{\frac{\Gamma}{\bar{P}}}\left\|\boldsymbol{\Delta}^{1/2}\big(\cos(\bar{\beta})\hat{\bar{\boldsymbol{g}}} + \sin(\bar{\beta})\hat{\bar{\boldsymbol{g}}}_{\perp}\big)\right\| = \cos(\bar{\beta})\|\bar{\boldsymbol{g}}_0\| + \sqrt{\epsilon}. \tag{4.44}$$

Hence, the optimal $\bar{\beta}$ can be obtained by solving (4.44), and $\bar{\boldsymbol{v}}_{\text{opt}}$ can be obtained by substituting $\bar{\beta}$ into (4.40). In summary, the procedure to solve the case in which both constraints are active is listed as Algorithm 4 in Table 4.4. Moreover, we are now ready to present the complete algorithm, namely Algorithm 5, for solving $(\mathbf{P1})$ in Table 4.5.

In Algorithm 5, we obtain the optimal solutions to $\mathbf{SP3}$ and $\mathbf{SP4}$ and the optimal solution to the case where both constraints are active separately. According to Theorem 4.1, the final result obtained in Algorithm 5 is thus the optimal solution of $(\mathbf{P1})$.

Table 4.5: The complete algorithm for ($\mathbf{P1}$).

Algorithm 5
1. Compute the optimal solution $\boldsymbol{S}_3 = \bar{P}\boldsymbol{h}\boldsymbol{h}^H/\|\boldsymbol{h}\|^2$ for $\mathbf{SP3}$,
2. Compute the optimal solution $\boldsymbol{S}_4$ for $\mathbf{SP4}$ via Algorithm 4,
3. If $\boldsymbol{S}_3$ satisfies the interference constraint, then $\boldsymbol{S}_3$ is the optimal solution,
4. Elsif $\boldsymbol{S}_4$ satisfies the transmit power constraint, then $\boldsymbol{S}_4$ is the optimal solution,
5. Otherwise compute the optimal solution through Algorithm 4.

Remark 4.6 *The complexity of the interior point algorithm for the SOCP problem* (4.14) *is* $\mathcal{O}(N^{3.5}\log(\frac{1}{\varepsilon}))$*, where* ε *denotes the error tolerance [53]. For Algorithm 5, a maximum of* $\mathcal{O}(\log(\frac{1}{\varepsilon}))$ *operations is needed to solve* (4.44)*, and the complexity for each operation is* $\mathcal{O}(\log(N^2))$*. Hence, the computation complexity required for Algorithm 5 is* $\mathcal{O}(N^2\log(\frac{1}{\varepsilon}))$*, which is much less than that of the interior point algorithm.*

4.6 Numerical Examples

Numerical examples are provided in this section to evaluate the performance of the proposed algorithms. In the examples, it is assumed that the entries of the channel vectors $\boldsymbol{h}$ and $\boldsymbol{g}_0$ are modeled as independent CSCG RVs with zero mean and unit variance. Moreover, we denote by l_1 the distance between the SU-Tx and the SU-Rx, and by l_2 the distance between the SU-Tx and the PU. It is assumed that the same path loss model is used to describe the transmissions from the SU-Tx to the SU-Rx and to the PU, and the path loss exponent is chosen to be 4. The noise power is chosen to be 1, and the transmit power and interference power are defined in dB relative to the noise power. For all cases, we choose $\Gamma = 0$ dB.

4.6.1 Comparison of the Analytical Solution and the Solution Obtained by the SOCP Algorithm

In this example, we compare the two results obtained by a standard SOCP algorithm (SeDuMi) and Algorithm 3. We consider the system with $N = 3$, $l_2/l_1 = 2$, and $\bar{P}$ ranging from 3 dB to 10 dB. In Fig. 4.4, we can see that the results obtained by different algorithms coincide. This is because both algorithms determine the optimal solution. Compared with the SOCP algorithm solution, Algorithm 3 obtains the solution directly, and thus it has lower complexity. In Fig. 4.5, we compare the two results obtained by SeDuMi and Algorithm 5. We consider the system with $N = 3$, $\bar{P}$ = 5 dB, and l_2/l_1 ranging from 1 to 10. The covariance matrix $\boldsymbol{R}$ is generated by $\boldsymbol{R}_1^H \boldsymbol{R}_1$, where each element of $\boldsymbol{R}_1$ follows Gaussian distribution with zero mean and unit variance. From Fig. 4.5, we can see that the results obtained by the two algorithms coincide again. Moreover, we note that the achievable rate with $\epsilon = 0.2$ is always greater than or equal to the rate with $\epsilon = 0.3$, since a larger ϵ corresponds to the stricter constraints.

4.6.2 Effectiveness of the Interference Constraint

In this example, we apply Algorithm 3 to solve problem $\mathbf{P3}$. In Fig. 4.6, we depict the achievable rate versus the ratio l_2/l_1 under different transmit power constraints. The increase of the ratio l_2/l_1 corresponds the decrease of the interference power constraint. As shown in Fig. 4.6, with an increase of l_2/l_1, the achievable rate increases due to the lower interference constraint. Until the ratio l_2/l_1 reaches a certain value, the achievable rate remains unchanged, since the transmit power constraint dominates the result, and the interference constraint becomes inactive.

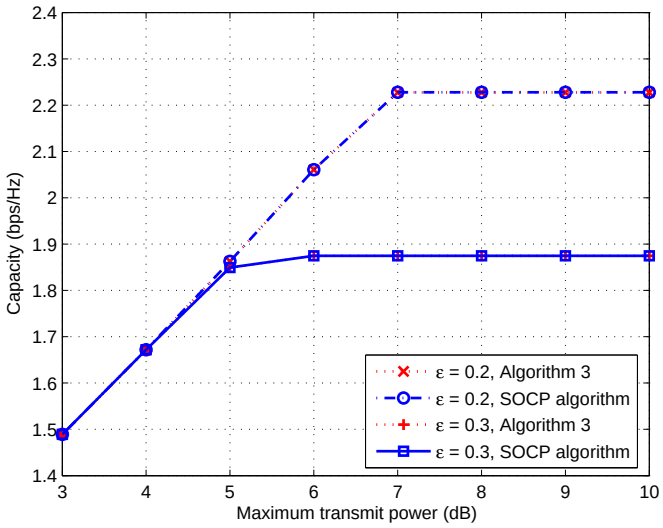

Figure 4.4: Comparison of the results obtained by the SOCP algorithm and Algorithm 3.

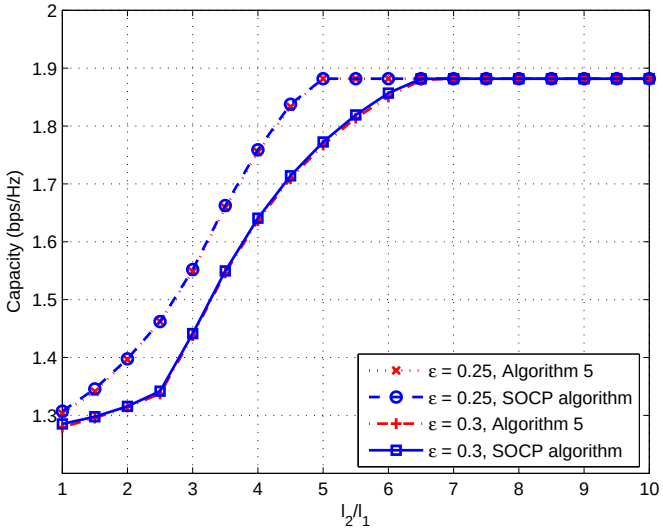

Figure 4.5: Comparison of the results obtained by the SOCP algorithm and Algorithm 5.

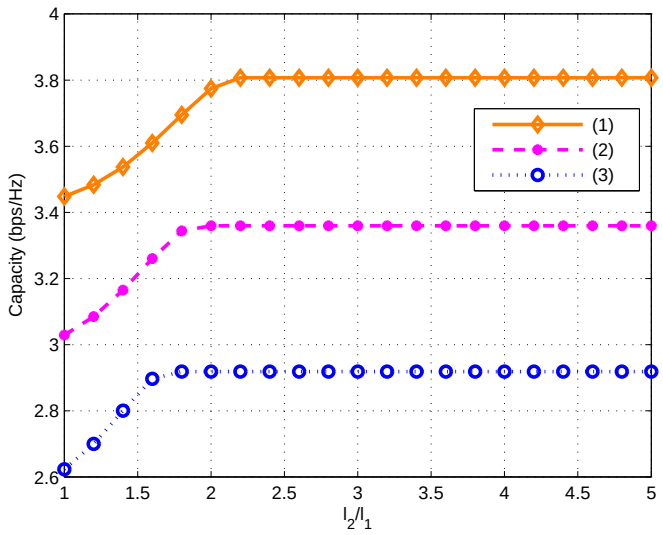

Figure 4.6: Effect of l_2/l_1 on the achievable rate of the CR network ($\epsilon = 1$, $N = 3$). (1) $\bar{P}$ = 10 dB; (2) $\bar{P}$ = 8 dB; (1) $\bar{P}$ = 6 dB.

4.6.3 The Activeness of the Constraints

In this example, we compare the achieved rates of $(\mathbf{P1})$ with a single transmit power constraint, a single interference constraint and both constraints. Here, we choose $N = 3$, $\epsilon = 0.2$, and generate $\boldsymbol{R}$ in the same way as in the first numerical example. Fig. 4.7 plots three achievable rates for different constraints, respectively. It can be observed from Fig. 4.7 that the rate under two constraints is always less than or equal to the rate under a single constraint. Obviously, this is due to the fact that extra constraints reduce the degree of freedom of the transmitter.

4.7 Conclusions

In this chapter, the robust cognitive beamforming design problem has been investigated for CR MISO channel, in which only partial CSI of the link from the SU-Tx to the PU is available at the SU-Tx. The problem can be formulated as an SIP optimization

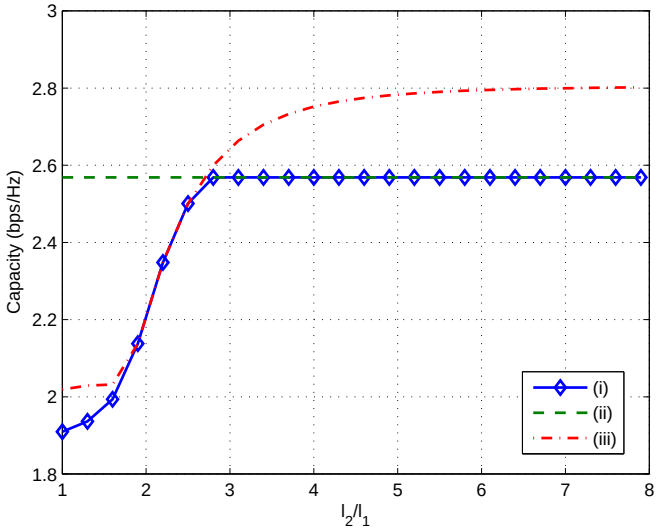

Figure 4.7: Comparison of the rate under different constraints of (**P1**). (i) the maximal rate subject to interference constraint and transmit power constraint simultaneously; (ii) the maximal rate subject to a single transmit power constraint; (iii) the maximal rate subject to a single interference constraint.

problem. Two approaches have been proposed to obtain the optimal solution of the problem: one approach transforms the problem into a SOCP problem, while the other approach solves the problem analytically. Numerical examples have been provided to present a comparison of the two approaches as well as to study the effectiveness and activeness of imposed constraints.

Chapter 5

Applications of the CR Resource Allocation Solution

This chapter applies the solution of the resource allocation problem for CR MIMO channels to solve a capacity computation problem for secrecy MIMO channels. The capacity computation for secrecy MIMO channel can be formulated as a non-convex max-min problem, which cannot be solved efficiently by standard convex optimization techniques. To handle this difficulty, we explore the relationship between the secrecy MIMO channel and the recently developed CR MIMO channel. Based on this relationship, we transform the non-convex secrecy rate maximization problem into a sequence of convex CR spectrum sharing capacity computation problems, under various setups of the secrecy channel. For the case of the MISO secrecy channel with single-antenna eavesdroppers, we propose efficient algorithms to compute the maximum achievable secrecy rate, while for the case with multi-antenna eavesdropper receivers, we obtain various new bounds on the achievable secrecy rate.

5.1 Introduction

As discussed in Chapter 1, in a spectrum sharing CR networks, the SU is allowed to simultaneously transmit with the legal PU over the same spectrum, provided that the SU to PU interference level is regulated subject to a certain interference power constraint. In [36], the resource allocation problem for the CR MIMO channel was formulated as a transmit rate maximization problem while keep the interference power at the PU lower than certain threshold. On the other hand, in a secrecy transmission system, the secrecy transmit is required to send confidential message to its legitimate destinations while guaranteeing that the message cannot be decoded by other eavesdroppers. It is worth noting that the system models of the secrecy MIMO channel and the CR MIMO channel are fairly similar in the sense that the secrecy and SU transmitters need to regulate the resultant signal power level at the eavesdropper and PU, respectively, so as to achieve the goals of confidential transmission and PU protection, respectively.

In this chapter, we study the achievable rates for the MIMO secrecy channel with multiple single-/multi-antenna eavesdroppers. According to [64, 65], by assuming Gaussian input, the achievable secrecy rate can be maximized via optimizing over the transmit covariance matrix of the secrecy user to maximize the minimum difference between the mutual information of the secrecy channel and those of the channels from the secrecy transmitter to different eavesdroppers. It can thus be shown that the resulting secrecy rate maximization problem is a non-convex max-min optimization problem, which is difficult to solve via existing methods. To address this problem, in this chapter we consider an auxiliary CR channel with multiple PUs bearing the same channel responses as those eavesdroppers in the secrecy channel. We then establish a relationship between this auxiliary CR channel and the secrecy channel by proving that the optimal transmit covariance matrix for the secrecy channel is the same as that for the CR channel with properly selected IT constraints for the PUs. Thereby, finding the

optimal complex transmit covariance matrix for the secrecy channel becomes equivalent to searching over a set of real IT constraints in the auxiliary CR channel, thus substantially reducing the computational complexity. Based on this relationship, we transform the non-convex secrecy rate maximization problem into a sequence of convex CR spectrum sharing capacity computation problems, under various setups of the secrecy channel. For the case of MISO or MIMO secrecy channel with single-antenna eavesdroppers, we propose efficient algorithms to compute the maximum achievable secrecy rate, while for the case with multi-antenna eavesdropper receivers, we obtain various new bounds on the achievable secrecy rate.

The rest of this chapter is organized as follows. Section 5.2 presents the system models and problem formulations for the CR transmission and the secrecy transmission. Section 5.3 describes the main theoretical results of this chapter on the relationship between the secrecy achievable rate and the CR spectrum sharing capacity, and develops an efficient algorithm to compute the maximum achievable rate for the MISO secrecy channel with single-antenna eavesdroppers. Section 5.4 and Section 5.5 then extend the results to the cases of multi-antenna secrecy and eavesdropper receivers, respectively. Section 5.6 presents some numerical examples. Finally, Section 5.7 concludes the chapter.

5.2 System Model and Problem Formulation

In this section, we present system models and problem formulations for the CR MIMO channel and the secrecy MIMO channel.

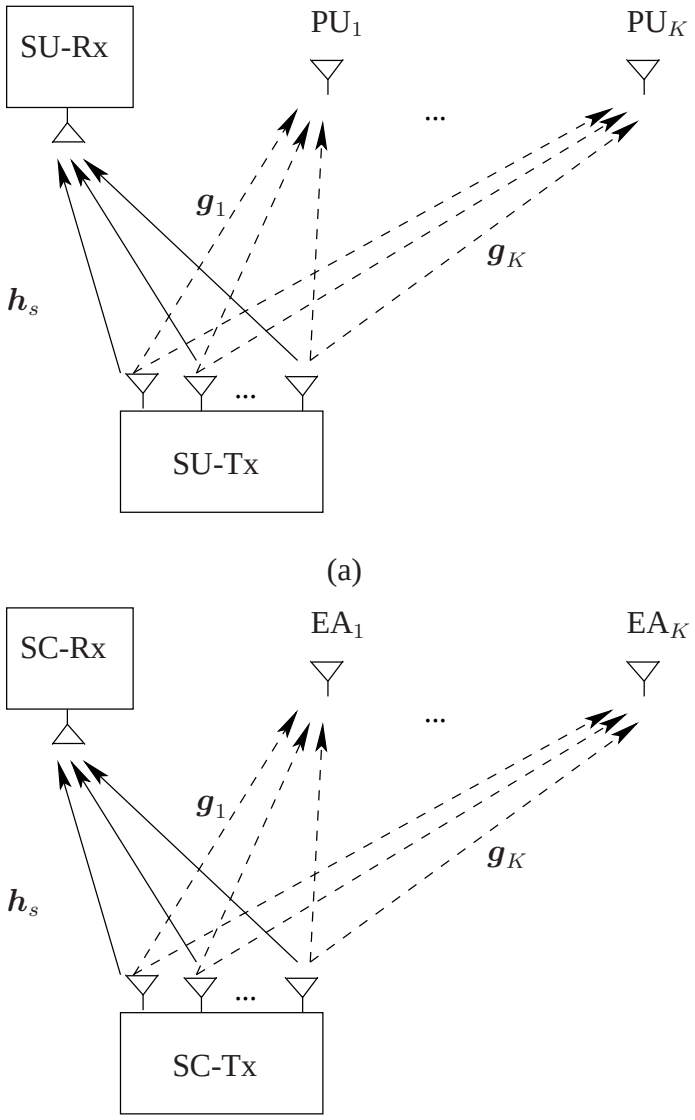

Figure 5.1: The system models: (a) the MISO CR channel with K single-antenna PUs; and (b) the MISO secrecy channel with K single-antenna eavesdroppers.

5.2.1 CR MISO Transmission

As shown in Fig. 5.1(a), we consider a MISO CR channel, where the SU-Tx is equipped with N transmit antennas, and the SU-Rx is equipped with a single receive antennas. The SU-Tx to SU-Rx channel is denoted by a $N \times 1$ matrix $\boldsymbol{h}_s$. Moreover, there are K single-antenna PU receivers denoted by PU$_i$, $i = 1, \cdots, K$, and the channel from SU-Tx to PU$_i$ is denoted by the $N \times 1$ vector $\boldsymbol{g}_i$. The received signal $\boldsymbol{y}$ at SU-Rx is expressed as

$$y = \boldsymbol{h}_s^H \boldsymbol{x} + z \tag{5.1}$$

where $\boldsymbol{x}$ is the transmit signal vector at SU-Tx, and $\boldsymbol{z}$ denotes the noise vector at SU-Rx. The entries of the noise vector are independent CSCG RVs of zero mean and covariance matrix $\boldsymbol{I}$. Since the SU shares the same spectrum with the PUs, there are K interference power constraints imposed to the SU transmission, expressed as $\mathbb{E}[|\boldsymbol{g}_i^H \boldsymbol{x}|^2] \leq \Gamma_i, i = 1, \cdots, K$, where Γ_i denotes the tolerable interference power threshold for PU$_i$.

Consider the CR MIMO transmission problem, in which we determine the optimal transmit covariance matrix for SU-Tx to maximize the data rate subject to the transmit power constraint and the interference power constraints for the K PUs. Mathematically, this problem can be formulated as [36]

$$\begin{aligned} (\mathbf{PA}): \quad & \max_{\boldsymbol{S}} \ \log|\boldsymbol{I} + \boldsymbol{h}_s^H \boldsymbol{S} \boldsymbol{h}_s| \\ & \text{subject to: } \mathrm{tr}(\boldsymbol{S}) \leq \bar{P} \\ & \qquad \boldsymbol{g}_i^H \boldsymbol{S} \boldsymbol{g}_i \leq \Gamma_i, \ i = 1, \cdots, K \end{aligned}$$

where $\boldsymbol{x}$ is CSCG distributed with zero means and a covariance matrix denoted by $\boldsymbol{S} = \mathbb{E}[\boldsymbol{x}\boldsymbol{x}^H]$, and $\bar{P}$ denotes the transmit power constraint. $(\mathbf{PA})$ is termed as spectrum sharing capacity computation problem. Note that $\boldsymbol{S}$ is a positive semi-definite matrix such that $(\mathbf{PA})$ is a convex problem and can be solved efficiently by the standard

interior point method [53].

5.2.2 Secrecy MISO Channel

As shown in Fig. 5.1(b), we consider a MISO secrecy channel, where the secrecy transmitter (SC-Tx) is equipped with N transmit antennas, and the secrecy receiver (SC-Rx) is equipped with M receive antennas. Moreover, there are K single-antenna eavesdroppers. In accordance with the earlier introduced MISO CR channel, the channel response from SC-Tx to SC-Rx is denoted by $\boldsymbol{h}_s$, and the channel response from SC-Tx to the ith eavesdropper (EA$_i$) is denoted by $\boldsymbol{g}_i, i = 1, \cdots, K$. According to the secrecy requirement, the transmitted message W from SC-Tx should not be decoded by any of the eavesdroppers, i.e., $H(W|y_i) \geq r, \forall i$, with y_i denoting the received signal at EA$_i$, and r denoting the secrecy transmit rate. According to the results in [64, 65], the secrecy capacity can be obtained by solving the following optimization problem

$$(\mathbf{PB}): \quad \max_{\boldsymbol{S}} \ \min_{i} \ \log|\boldsymbol{I} + \boldsymbol{h}_s\boldsymbol{S}\boldsymbol{h}_s^H| - \log\left(1 + \frac{\boldsymbol{g}_i^H\boldsymbol{S}\boldsymbol{g}_i}{\sigma_i^2}\right)$$
$$\text{subject to: } \mathrm{tr}(\boldsymbol{S}) \leq \bar{P}$$

where $\boldsymbol{S}$ denotes the transmit covariance matrix of SC-Tx, similar to that of SU-Tx in the CR case, and σ_i^2 denotes the variance of the zero-mean CSCG noise at EA$_i$. $(\mathbf{PB})$ is termed as secrecy capacity computation problem.

We see that $(\mathbf{PB})$ is a non-convex optimization problem since its objective function is the difference between two concave functions of $\boldsymbol{S}$ and thus not necessarily concave. Existing methods in the literature [58, 64, 65, 99] for the MISO secrecy capacity computation is only applicable to the case of a single eavesdropper. However, these methods cannot solve the case with multiple eavesdroppers $(\mathbf{PB})$ even for the case where each eavesdropper has a single antenna.[1]

[1] Problem $(\mathbf{PB})$ in the case of multi-antenna eavesdroppers will be studied later in Section 5.5.

Remark 5.1 *According to Fig. 5.1, it is easy to observe that the system models of the CR transmission and the secrecy transmission bear the similarity that they both need to control the received signal power levels at both PUs and eavesdroppers. However, note that* $(\mathbf{PA})$ *guarantees that the interference power at each PU receiver is below the required threshold without considering the PU noise power, while for* $(\mathbf{PB})$*, through the second term in the objective function, the confidential level at each eavesdropper is not only related to the received signal power from SC-Tx, but also related to the noise power at eavesdroppers. Therefore, one immediate question is whether there exists a relationship between these two systems such that we can solve the non-convex problem* $(\mathbf{PB})$ *by transforming it into some form of* $(\mathbf{PA})$ *that is convex and thus efficiently solvable. With this motivation, we first study the relationship between these two problems, and then propose corresponding algorithms to solve* $(\mathbf{PB})$.

5.3 Relationship Between Secrecy Capacity and Spectrum Sharing Capacity

In this section, we present main theoretical results of the chapter on the relationship between the secrecy capacity computation problem $(\mathbf{PB})$ and the spectrum sharing capacity computation problem $(\mathbf{PA})$. Based on such a relationship, we then propose a new efficient algorithm to compute the MISO secrecy capacity with multiple single-antenna eavesdroppers.

5.3.1 Main Results

Theorem 5.1 *For a given* $(\mathbf{PB})$*, there exists a set of interference power constraint values,* Γ_i*,* $i = 1, \cdots, K$*, such that the resulting* $(\mathbf{PA})$ *has the same solution as that of* $(\mathbf{PB})$.

The proof can be found in Appendix D.1. Theorem 5.1 establishes the relationship between $(\mathbf{PA})$ and $(\mathbf{PB})$. To further investigate this relationship, we define an auxiliary function of Γ_is as

$$\begin{aligned} g(\Gamma_1, \cdots, \Gamma_K) := \max_{\boldsymbol{S}} \ & (\boldsymbol{I} + \boldsymbol{h}_s^H \boldsymbol{S} \boldsymbol{h}_s) \\ \text{subject to: } & \text{tr}(\boldsymbol{S}) \leq \bar{P} \\ & \boldsymbol{g}_i^H \boldsymbol{S} \boldsymbol{g}_i \leq \Gamma_i, i = 1, \cdots, K. \end{aligned} \tag{5.2}$$

Note that the only difference between Problem (5.2) and $(\mathbf{PA})$ lies in their objective functions: The former one does not involve a logarithmic function of matrix determinant while the latter one does. As a result, Problem (5.2) is non-convex since its objective function is not concave in $\boldsymbol{S}$. Also note that Problem (5.2) is equivalent to $(\mathbf{PA})$ since they have the same optimal solution for $\boldsymbol{S}$. Therefore, although Problem (5.2) is non-convex, its optimal solution can be obtained via solving the convex counterpart $(\mathbf{PA})$.

Theorem 5.2 $(\mathbf{PB})$ *is equivalent to the following optimization problem:*

$$\max_{\Gamma_1, \cdots, \Gamma_K} \min_i \ F_i(\Gamma_1, \cdots, \Gamma_K) := \frac{g(\Gamma_1, \cdots, \Gamma_K)}{1 + \Gamma_i / \sigma_i^2}. \tag{5.3}$$

The proof can be found in Appendix D.2. Theorem 5.2 establishes the relationship between $(\mathbf{PB})$ and the auxiliary function $g(\Gamma_1, \cdots, \Gamma_K)$ that is related to $(\mathbf{PA})$. The equivalence between Problem (5.3) and $(\mathbf{PB})$ means that by solving the optimal Γ_is in Problem (5.3), we could solve an optimal $\boldsymbol{S}$ given $g(\Gamma_1, \cdots, \Gamma_K)$ is an embedded optimization problem over $\boldsymbol{S}$ inside Problem (5.3). Such an optimal $\boldsymbol{S}$ is also the solution for $(\mathbf{PB})$, for which the explanation is given in Appendix D.2.

Problem (5.3) can be solved by utilizing an important property of $g(\Gamma_1, \cdots, \Gamma_K)$ described as follows:

Theorem 5.3 *The function $g(\Gamma_1, \cdots, \Gamma_K)$ is a concave function with respect to $\Gamma_1, \cdots, \Gamma_K$, and*

$$\gamma_i(\Gamma_1, \cdots, \Gamma_K) := \frac{\partial g(\Gamma_1, \cdots, \Gamma_K)}{\partial \Gamma_i} = \mu_i^{(1)} |\boldsymbol{I} + \boldsymbol{h}_s^H \boldsymbol{S}^{(1)} \boldsymbol{h}_s|, \ i = 1, \cdots, K \quad (5.4)$$

where $\boldsymbol{S}^{(1)}$ and $\mu_i^{(1)}$ are the optimal solution of $(\mathbf{PA})$ and the corresponding Lagrange multiplier (the dual solution) with respect to the ith interference power constraint, respectively.

The proof can be found in Appendix D.3. Note that from Theorem 5.3, it follows that the gradient of $g(\Gamma_1, \cdots, \Gamma_K)$ in (5.3) can be obtained by solving $(\mathbf{PA})$ via the Lagrange duality method, which completes the equivalence between $(\mathbf{PA})$ and $(\mathbf{PB})$ via the intermediate problem (5.3). At last, we have

Theorem 5.4 *Problem* (5.3) *is a quasi-concave maximization problem.*

The proof can be found in Appendix D.4. Theorem 5.4 suggests that Problem (5.3) can be solved by utilizing convex optimization techniques, for which the details are given in the next section.

5.3.2 Algorithms

In this subsection, we present a new algorithm to compute the MISO secrecy capacity by exploiting the relationship between the secrecy transmission and the CR transmission, which was developed in the previous subsection. According to Theorems 5.2 and 5.4, $(\mathbf{PB})$ is equivalent to the quasi-concave maximization problem (5.3). Thus, we instead study Problem (5.3) since it is easier to handle than $(\mathbf{PB})$.

According to [53], a quasi-concave maximization problem can be reduced to solving a sequence of convex feasibility problems. Thus, Problem (5.3) can be further

transformed as

$$\begin{aligned} &\max_{t,\Gamma_1,\cdots,\Gamma_K} \; t \\ &\text{subject to : } g(\Gamma_1,\cdots,\Gamma_K) \geq t(1+\Gamma_i/\sigma_i^2), i=1,\cdots,K. \end{aligned} \tag{5.5}$$

Let t^* be the optimal solution of Problem (5.5). Clearly, t^* is also the optimal value of Problem (5.3). If the feasibility problem

$$\begin{aligned} &\max_{\Gamma_1,\cdots,\Gamma_K} \; 0 \\ &\text{subject to : } g(\Gamma_1,\cdots,\Gamma_K) \geq t(1+\Gamma_i/\sigma_i^2), i=1,\cdots,K \end{aligned} \tag{5.6}$$

for a given t is feasible, then it follows that $t^* \geq t$. Conversely, if Problem (5.6) is infeasible, then $t^* < t$. Therefore, by assuming an interval $[\,0,\,\bar{t}\,]$ known to contain the optimal t^*, the optimal solution of Problem (5.5) can be found easily via a bisection search. Note that a suitable value for $\bar{t}$ can be chosen as $g(\infty,\cdots,\infty)$ from (5.2).

We next solve the feasibility problem (5.6) by a similar method discussed in [80]. It is worth noting that the feasibility problem (5.6) can be viewed as an optimization problem. The Lagrange function of Problem (5.6) can be written as

$$L_0(\{\nu_i\},\Gamma_1,\cdots,\Gamma_K) = \sum_{i=1}^{K} \nu_i \Big(g(\Gamma_1,\cdots,\Gamma_K) - t(1+\Gamma_i/\sigma_i^2) \Big) \tag{5.7}$$

where ν_i is the non-negative dual variable for the ith constraint, and $\{\nu_i\}$ denotes $\nu_1,\cdots,\nu_K$. The corresponding dual function is then defined as

$$f_0(\{\nu_i\}) = \max_{\Gamma_1,\cdots,\Gamma_K} \; \sum_{i=1}^{K} \nu_i \Big(g(\Gamma_1,\cdots,\Gamma_K) - t(1+\Gamma_i/\sigma_i^2) \Big). \tag{5.8}$$

Due to its convexity, Problem (5.6) can be transformed into its equivalent dual problem as

$$\min_{\{\nu_i\}} \; f_0(\{\nu_i\}) \tag{5.9}$$

and the duality gap between the optimal values of Problem (5.6) and Problem (5.9) is zero if Problem (5.6) is feasible.

Table 5.1: Algorithm for Problem (5.3).

Algorithm 1
1. Initialization: $t^{\min} = 0, t^{\max} = \bar{t}$.
2. repeat
$t \leftarrow \frac{1}{2}(t^{\min} + t^{\max})$.
Solve the feasibility problem (5.6). If Problem (5.6) is feasible, $t^{\min} \leftarrow t$;
otherwise, $t^{\max} \leftarrow t$.
Stop, when $t^{\max} - t^{\min} \leq \epsilon$.
3. The optimal value of Problem (5.3) is taken as $t^{\min}$.

Since it is known from Theorem 5.3 that function $g(\Gamma_1, \cdots, \Gamma_K)$ is concave with respect to $\{\Gamma_1, \cdots, \Gamma_K\}$, Problem (5.8) can be solved via a gradient-based algorithm. According to Theorem 5.3, the gradient of function $g(\Gamma_1, \cdots, \Gamma_K)$ can be obtained by solving $(\mathbf{PA})$. Furthermore, since function $f_0(\{\nu_i\})$ is convex with respect to $\{\nu_i\}$, Problem (5.9) can be solved by a subgradient-based algorithm, such as the ellipsoid method [53]. Similar to Lemma 3.5 in [80], Problem (5.6) is infeasible if and only if there exist $\{\nu_i\}$ such that $f_0(\{\nu_i\}) < 0$. Using this fact along with the subgradient-based search over $\{\nu_i\}$, the feasibility problem (5.6) can be solved. To summarize, the algorithm for Problem (5.3) with a target accuracy parameter ϵ is summarized as Algorithm 1 in Table 5.1.

Since the number of iterations required for the bisection search over t is independent of K, the overall complexity of Algorithm 1 for solving Problem (5.3) bears the same order over K as that for Problem (5.6), which is $\mathcal{O}(K^4)$.

According to Theorem 5.1, we can find a set of parameters Γ_i's such that the corresponding problem $(\mathbf{PA})$ has the same solution as that of $(\mathbf{PB})$. Since the optimal solution of $(\mathbf{PA})$ is known to be a rank-one matrix [68], so is the optimal solution for

$(\mathbf{PB})$. Thus, we obtain the following corollary.

Corollary 5.1 *The optimal solution for Problem* $(\mathbf{PB})$ *is a rank-one matrix.*

It should be pointed out that there in fact exists an alternative method to solve $(\mathbf{PB})$, without resorting to the relationship between the secrecy transmission and the CR transmission. We present this method as follows. Similar to Theorem 5.4, we prove that the function $\hat{F}_i(\boldsymbol{S}) := \frac{1+\boldsymbol{h}_s^H \boldsymbol{S} \boldsymbol{h}_s}{1+(\boldsymbol{g}_i^H \boldsymbol{S} \boldsymbol{g}_i)/\sigma_i^2}$ is quasi-concave with respect to $\boldsymbol{S}$ in the following theorem.

Theorem 5.5 $\hat{F}_i(\boldsymbol{S})$ *is a quasi-concave function for* $i = 1, \ldots, K$.

The proof can be found in Appendix D.5.

Therefore, $(\mathbf{PB})$ can be transformed into the following equivalent problem

$$\begin{aligned} &\max_{\boldsymbol{S},\, t} \ t \\ &\text{subject to: } \mathrm{tr}(\boldsymbol{S}) \le P \\ &\qquad 1 + \boldsymbol{h}_s^H \boldsymbol{S} \boldsymbol{h}_s \ge t\Big(1 + \frac{\boldsymbol{h}_i^H \boldsymbol{S} \boldsymbol{h}_i}{\sigma_i^2}\Big), i = 1, \cdots, K \end{aligned} \tag{5.10}$$

where t is a positive variable. For the fixed t, all the constraints in the above problem are linear matrix inequalities over $\boldsymbol{S}$, and thus the corresponding feasibility problem (similarly defined as Problem (5.6)) can be viewed as a semi-definite programming (SDP) feasibility problem. Correspondingly, the optimal value of t can be obtained by a bisection search. However, without resorting to the secrecy and CR transmission relationship, it would be difficult to prove that the optimal transmit covariance matrix obtained above in (5.10) should be rank-one.

5.4 Multi-Antenna Secrecy Receiver

In this section, we extend our results for the MISO secrecy channel to the case where the secrecy receiver is equipped with M antennas, $M > 1$. In such cases, the MIMO

channel from SC-Tx to SC-Rx can be denoted by a $N \times M$ complex matrix, $\boldsymbol{H}_s$. Without loss of generality, it is assumed that the receiver noise vector at SC-Rx is CSCG distributed with zero means and an identity covariance matrix. Similar to $(\mathbf{PB})$, the secrecy rate computation for the MIMO secrecy channel with multiple single-antenna eavesdroppers can be formulated as the following optimization problem [64–66]

$$(\mathbf{PC}): \max_{\boldsymbol{S}} \min_i \log|\boldsymbol{I}+\boldsymbol{H}_s^H\boldsymbol{S}\boldsymbol{H}_s| - \log\left(1+\frac{\boldsymbol{h}_i^H\boldsymbol{S}\boldsymbol{h}_i}{\sigma_i^2}\right)$$
$$\text{subject to: } \mathrm{tr}(\boldsymbol{S}) \le P.$$

Similar to Theorems 5.1 and 5.2 in the case of MISO secrecy channel, it can be shown (proof is omitted here for brevity) that $(\mathbf{PC})$ is equivalent to the following optimization problem

$$\max_{\Gamma_1,\cdots,\Gamma_K} \min_i \hat{F}_i(\Gamma_1,\cdots,\Gamma_K) := \frac{\hat{g}(\Gamma_1,\cdots,\Gamma_K)}{1+\Gamma_i/\sigma_i^2} \tag{5.11}$$

where $\hat{g}(\Gamma_1,\cdots,\Gamma_K)$ is similarly defined as $g(\Gamma_1,\cdots,\Gamma_K)$ in (5.2), while the objective function for the maximization problem therein is given for the MIMO case as $|\boldsymbol{I}+\boldsymbol{H}_s^H\boldsymbol{S}\boldsymbol{H}_s|$. Note that $\hat{g}(\Gamma_1,\cdots,\Gamma_K)$ for a given set of Γ_i's can be obtained by solving the corresponding CR MIMO channel capacity computation problem, which can be similarly defined as $(\mathbf{PA})$ for the MISO case and efficiently solvable via convex optimization techniques [68]. Therefore, by taking the logarithm of $\min_i \hat{F}_i(\Gamma_1,\cdots,\Gamma_K)$ in (5.11), for a given set of Γ_i's, a corresponding lower bound on the MIMO secrecy channel capacity is obtained. The remaining problem is then to find the set of optimal Γ_i's that attain the secrecy rate, which is the maximum of all the achievable capacity lower bounds. This problem can be easily resolved when the number of eavesdroppers, K, is small, via a simple grid-based search over Γ_i's in $\mathcal{R}_+^K$. Note that when K is small, e.g., $K=1$, the grid-based search over Γ_i's is far more efficient than a direct search over $\boldsymbol{S}$ in $(\mathbf{PC})$. However, the complexity for such a grid-based searching scheme increases exponentially with K.

As for the MISO secrecy channel case, if similar results like Theorems 5.3 and 5.4 can be shown for function $\hat{g}(\Gamma_1, \cdots, \Gamma_K)$ in the MIMO case, Problem (5.11) then becomes a quasi-concave maximization problem and is thus solvable by a similar algorithm like Algorithm 1. As shown in Section 5.3, such an algorithm has only a polynomial complexity over K. However, it is shown via the following example that in general $\hat{g}(\Gamma_1, \cdots, \Gamma_K)$ is not a concave function with respect to Γ_i's. As a result, Theorems 5.3 and 5.4 do not hold in general for the case of secrecy MIMO channel and thus efficient algorithms proposed for the MISO secrecy channel cannot be applied to the MIMO case.

Example 5.1 *Consider a MIMO secrecy channel with $M = N = 2$, $\boldsymbol{H}_s = \boldsymbol{I}$, and two single-antenna eavesdroppers with channels from SC-Tx as $\boldsymbol{h}_1 = [1\ 0]^T$ and $\boldsymbol{h}_2 = [0\ 1]^T$, respectively. Now consider the auxiliary MIMO CR channel for this secrecy channel, for which it can be easily shown that the function $\hat{g}(\Gamma_1, \Gamma_2)$ is equal to $(1 + \Gamma_1)(1 + \Gamma_2)$, with $\Gamma_1 + \Gamma_2 \leq P$. Clearly, $\hat{g}(\Gamma_1, \Gamma_2)$ is neither convex nor concave in this case.*

5.5 Multi-Antenna Eavesdropper Receiver

In this section, we extend our results for the MISO secrecy channel with single-antenna eavesdroppers to the case with multi-antenna eavesdroppers. We assume that each eavesdropper is equipped with N_e receive antennas, and the channel from SC-Tx to the ith eavesdropper receiver is denoted by $\boldsymbol{G}_i$ of size $N_e \times N$. Similar to $(\mathbf{PB})$, the MIMO secrecy capacity in the multi-antenna eavesdropper case can be obtained from the following optimization problem [65]

$$(\mathbf{PE}): \quad \max_{\boldsymbol{S}} \min_{i} \ \log|\boldsymbol{I} + \boldsymbol{h}_s^H \boldsymbol{S} \boldsymbol{h}_s| - \log|\boldsymbol{I} + \boldsymbol{G}_i \boldsymbol{S} \boldsymbol{G}_i^H| \tag{5.12}$$

$$\text{subject to: } \mathrm{tr}(\boldsymbol{S}) \leq \bar{P} \tag{5.13}$$

where without loss of generality, we assume that the noises at the eavesdropper receivers are independent CSCG vectors each with zero means and an identity covariance matrix. Note that unlike the single-antenna eavesdropper case where the IT constraint Γ_i in the auxiliary CR channel uniquely determines the penalty for the secrecy rate due to the ith eavesdropper, there is no such a direct relationship between the IT constraints and the secrecy rate in the case of multi-antenna eavesdroppers. Nevertheless, we could still derive new upper and lower bounds on the MISO secrecy rate in the multi-antenna eavesdropper case based on the relationship between the secrecy transmission and the CR transmission, shown as follows.

5.5.1 Capacity Lower Bound

First, we have the following lemma that relates the constraint on the total receive signal power at the ith eavesdropper, i.e., $\text{tr}(\boldsymbol{G}_i^H \boldsymbol{S} \boldsymbol{G}_i) \leq \Gamma_i$, to an upper bound on the resulting secrecy rate penalty, $\log|\boldsymbol{I} + \boldsymbol{G}_i^H \boldsymbol{S} \boldsymbol{G}_i|$, given as the second term in (5.12).

Lemma 5.1 *If for any $i, i \in \{1, \cdots .K\}$, tr$(\boldsymbol{G}_i \boldsymbol{S} \boldsymbol{G}_i^H) \leq \Gamma_i$, we have $|\boldsymbol{I} + \boldsymbol{G}_i \boldsymbol{S} \boldsymbol{G}_i^H| \leq (1 + \frac{\Gamma_i}{L})^L$, where $L = \min(N_e, N)$.*

The proof can be found in Appendix D.6. Similar to Theorem 5.2, from Lemma 5.1, the following theorem holds:

Theorem 5.6 *The optimal value of $(\mathbf{PE})$ is lower-bounded by that of the following optimization problem*

$$\max_{\Gamma_1, \cdots, \Gamma_K} \ \min_i \ \tilde{F}_i(\Gamma_1, \cdots, \Gamma_K) := \frac{\tilde{g}(\Gamma_1, \cdots, \Gamma_K)}{\left(1 + \frac{\Gamma_i}{L}\right)^L} \tag{5.14}$$

where the function $\tilde{g}(\Gamma_1, \cdots, \Gamma_K)$ *is defined as*

$$\begin{aligned} \tilde{g}(\Gamma_1, \cdots, \Gamma_K) := \max_{\boldsymbol{S}} & |\boldsymbol{I} + \boldsymbol{h}_s^H \boldsymbol{S} \boldsymbol{h}_s| \\ \textit{subject to: } & \textit{tr}(\boldsymbol{S}) \leq \bar{P} \\ & \textit{tr}(\boldsymbol{G}_i \boldsymbol{S} \boldsymbol{G}_i^H) \leq \Gamma_i,\ i = 1, \cdots, K. \end{aligned} \tag{5.15}$$

Problem (5.14) can be solved by the gradient-based method similar to Algorithm 1. Accordingly, the lower bound on the MIMO secrecy capacity is obtained. Note that this capacity lower bound is tight when $N_e = 1$ and thus $L = 1$.

5.5.2 Capacity Upper Bound

In the multi-antenna eavesdropper case, the signals received at different antennas of each eavesdropper are jointly processed to decode the contained secrecy message. Therefore, a straightforward upper bound on the secrecy capacity in this case is obtained by assuming that the signals at different antennas of each eavesdropper are decoded independently. Suppose that $\boldsymbol{g}_{i,j}$ is the jth column of the matrix $\boldsymbol{G}_i, j = 1, \cdots, N_e$, then the upper bound on the secrecy capacity can be obtained as

$$\begin{aligned} \max_{\boldsymbol{S}} \ \min_{\{i,j\}} \ & \log |\boldsymbol{I} + \boldsymbol{h}_s^H \boldsymbol{S} \boldsymbol{h}_s| - \log \left(1 + \frac{\boldsymbol{g}_{i,j}^H \boldsymbol{S} \boldsymbol{g}_{i,j}}{\sigma_{i,j}^2}\right) \\ \text{subject to: } & \text{tr}(\boldsymbol{S}) \leq \bar{P}. \end{aligned} \tag{5.16}$$

The above problem is the same as $(\mathbf{PB})$ with the number of single-antenna eavesdroppers equal to $N_e K$, and thus can be solved by Algorithm 1.

5.6 Numerical Examples

In this section, we provide several numerical examples to illustrate the effectiveness of the proposed algorithms in computing the secrecy channel capacity under different system settings. For the examples on the MISO secrecy channel, it is assumed that

$N = 4$, while for the example of MIMO secrecy channel, it is assumed that $M = N = 4$. The elements in the secrecy channel vectors/matrices as well as those from SC-Tx to eavesdroppers are generated from independent CSCG random variables each with zero mean and unit variance. Moreover, the noise power at each eavesdropper antenna is chosen to be one, and the transmit power of the secrecy transmitter, $\bar{P}$, is defined in dB relative to the noise power.

5.6.1 MISO Secrecy Capacity with Two Single-Antenna Eavesdroppers

In this example, we consider a secrecy MISO channel with $K = 2$ single-antenna eavesdroppers. Fig. 5.2 plots the secrecy capacity of this channel obtained by Algorithm 1, where the transmit power ranges from 0 dB to 10 dB. Moreover, a reference achievable secrecy rate of this channel is obtained by the Projected-Channel SVD (P-SVD) algorithm in [36]. In this algorithm, the channel $\boldsymbol{H}$ is projected into a space, which is orthogonal to $\boldsymbol{g}_1$ and $\boldsymbol{g}_2$, and thus the secrecy signals cannot be received by the eavesdroppers. It is easy to observe from Fig. 5.2 that the secrecy rate obtained by P-SVD is less than the secrecy capacity obtained by Algorithm 1. Moreover, from Theorem 5.4, it is known that the function $F_i(\Gamma_1, \Gamma_2)$ is a quasi-concave function, and thus the function $\min_{i=1,2}\ F_i(\Gamma_1, \Gamma_2)$ is also a quasi-concave function. In Fig. 5.3, we plot the value of this function for $\bar{P} = 5$ dB. It is observed that this function is indeed quasi-concave.

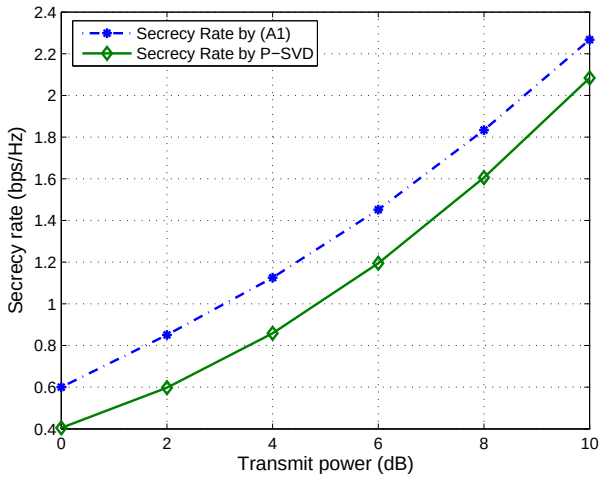

Figure 5.2: Comparison of the secrecy rate by Algorithm 1 (A1) and that by the P-SVD algorithm for the MISO secrecy channel with $N = 4$ and $K = 2$ single-antenna eavesdroppers.

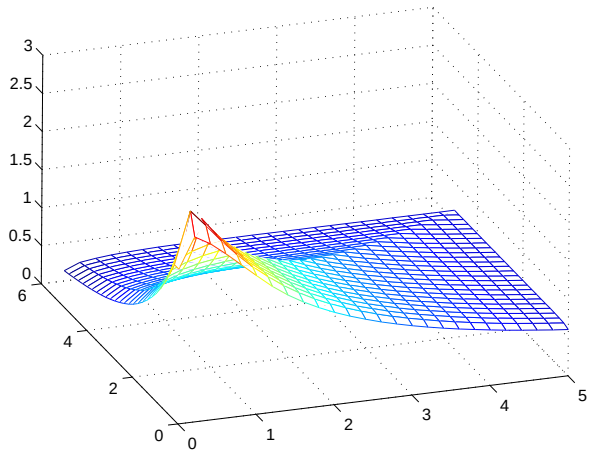

Figure 5.3: Illustration of the function $\min_{i=1,2}\ F_i(\Gamma_1, \Gamma_2)$.

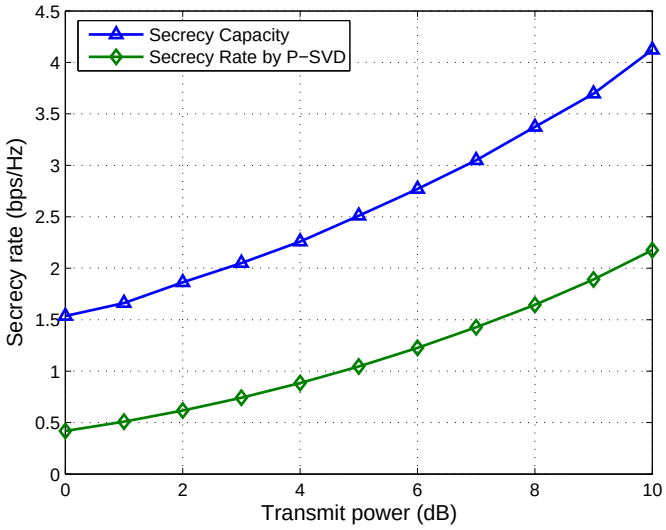

Figure 5.4: Comparison of the secrecy capacity by Algorithm 2 and the secrecy rate by the P-SVD algorithm for $M = N = 4$ and $K = 1$ single-antenna eavesdropper.

5.6.2 MIMO Secrecy Channel with One Single-Antenna Eavesdropper

In this example, we apply Algorithm 2 to compute the secrecy capacity of a MIMO channel with one single-antenna eavesdropper. As shown in Fig. 5.4, the secrecy capacity obtained by Algorithm 2 is larger than the achievable secrecy rate obtained by the P-SVD algorithm.

5.6.3 MISO Secrecy Capacity with One Multi-antenna Eavesdropper

In this example, by applying the methods discussed in Section 5.5, we show in Fig. 5.6 the lower and upper bounds on the MISO secrecy capacity with a single eavesdropper using $N_e = 2$ receive antennas. From the capacity lower bound, we obtain a feasible transmit covariance matrix and thus a corresponding achievable secrecy rate, shown in

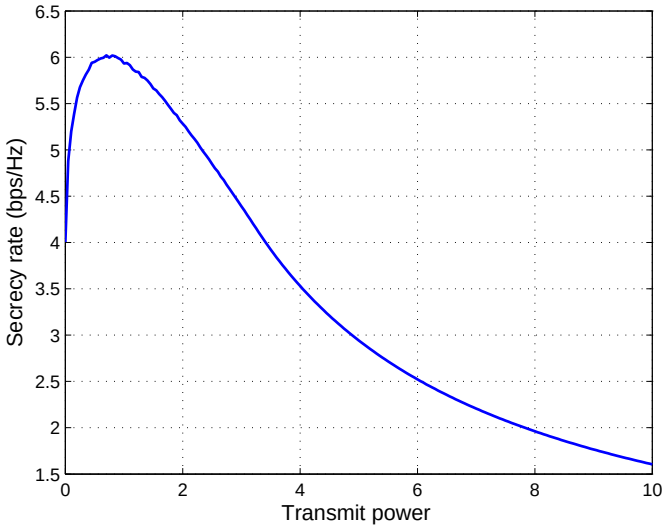

Figure 5.5: The value of the function $F(\Gamma)$ for $M = N = 4$, $K = 1$ single-antenna eavesdropper, and $\bar{P} = 5$ dB.

Fig. 5.6 and named as "Achievable Secrecy Rate". Moreover, the achievable secrecy rate by the P-SVD algorithm is also shown for comparison.

5.7 Conclusions

In this chapter, we have investigated the relationship between the multi-antenna CR transmission problem and the multi-antenna secrecy transmission problem. By exploiting this relationship, we have transformed the non-convex secrecy capacity computation problem into a quasi-convex optimization problem for the MISO case, and developed various algorithms to obtain the maximum achievable secrecy rate or new upper/lower bounds for different cases of the multi-antenna secrecy channel.

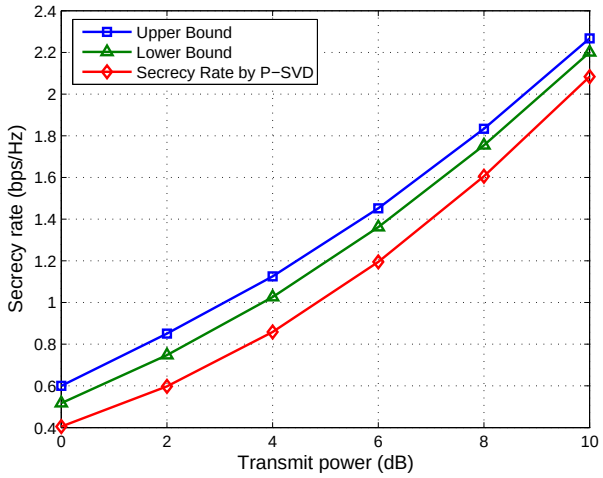

Figure 5.6: Comparison of the lower and upper bounds on the secrecy rate and the secrecy rate by the P-SVD algorithm for the MISO secrecy channel with $N = 4$, and $K = 1$ eavesdropper with $N_e = 2$ receive antennas.

Chapter 6

Conclusions and Future Work

In this chapter, we summarize the main contributions of this thesis, and present some suggestions for future work.

6.1 Conclusions

This thesis has investigated the resource optimization problems for spectrum sharing based CR SIMO-MAC, CR MIMO-BC, and CR MISO channels, and applied the resource allocation solution of CR MIMO channels to solve the capacity computation problem of secrecy MIMO channels.

In particular, for the CR SIMO-MAC, we have considered the sum rate maximization problem and SINR balancing problem. Unlike the conventional SIMO-MAC, the CR SIMO-MAC is not only subject to the transmit power constraints but also the interference power constraints. To exploit the existing algorithms developed for conventional MAC, the multi-constraint problem should be decomposed into several subproblems with a single constraint. We have developed two algorithms to decompose those constraints efficiently. These algorithms could also be extended to solve other multi-constraint optimization problems.

Secondly, we have considered the capacity computation problem for the CR MIMO-BC. Conventionally, the MIMO-BC capacity computation problem is solved by transforming it into an equivalent MIMO-MAC capacity computation problem via the BC-MAC duality. However, this conventional BC-MAC duality can only be applied to the case with a single sum power constraint, and it is not applicable to the CR MIMO BC case with multiple linear constraints. To handle this difficulty, a new BC-MAC duality has been proposed, which generalizes all the existing BC-MAC dualities as its special cases. Moreover, this new duality result can be applied to solve the case with non-linear constraints [85] and the capacity computation problem for the interference channels with degraded message sets [40].

Thirdly, most of the existing CR studies assumed that the CSI is perfectly known by the SU transmitter. However, in practical environment, it would be difficult for the SU to obtain accurate CSI. In Chapter 4, we have considered a scenario where the CSI of the channel from the SU transmitter to the PU is partially known by the SU. The CR performance optimization problem has thus been formulated as a robust design problem where the interference power constraint should be satisfied even for the worst-case channel realization. Similar to the method in [97], the robust design problem can be transformed into a SOCP problem, which can be solved by a standard interior point algorithm. Based on its special geometric structure, the problem has been further solved by a closed-form solution with lower computational complexity.

Finally, we have investigated the relationship between the CR MIMO channel and the secrecy MIMO channel. The two channels are similar in the sense that the secrecy transmitter and SU transmitter need to regulate the resultant signal power level at the eavesdropper and PU, so as to achieve the goals of confidential transmission and PU protection, respectively. The capacity computation problem for the secrecy MIMO channel with multiple eavesdroppers is a non-convex optimization problem, which cannot be solved by the existing algorithms. By exploiting this relationship, we

have transformed the non-convex problem for secrecy MIMO channels into a sequence of transmit optimization problems of the associated CR MIMO channels, which are convex and easy to be solved.

6.2 Future Work

The following problems can be studied as future work.

6.2.1 Resource Allocation in Fading CR Channels

In Chapter 2 and Chapter 3, we considered the resource allocation problems for CR SIMO-MAC and CR MIMO-BC with deterministic channel responses. In wireless environments, it could be more practical to consider the fading channel models. Thus, one future direction is to study the resource allocation strategies for corresponding CR channels under fading scenarios, where ergodic or outage sum rate maximization problems would be of interest.

6.2.2 Optimization for CR Beamforming with Completely Imperfect CSI

In Chapter 4, we considered the scenario, where the CSI of the channel from the SU transmitter to PU is partially known, but the CSI of the SU link is assumed to be perfectly known by the SU transmitter. In practice, it would be more reasonable to assume that both the CSI of the SU link and the CSI of the channel from the SU transmitter to the PU are partially known. Under this set-up, a new robust optimization problem could be formulated.

6.2.3 Upper Layer Issues for CR Networks

In addition to the aforementioned CR research, which mainly focuses on the problems related with physical layer, the studies for upper layer protocols are also important for the realization of CR networks. Compared with the conventional wireless systems, it would be a challenging issue in designing the protocols, such as medium access control, for CR networks with the requirements of protecting the PU transmission as well as the performance optimization for the SU networks. Although some research work has been done in this area, there are still quite many open research topics that have not been addressed before. Further research efforts on this research area are needed.

Appendix A

Appendices to Chapter 2

A.1 Proof of Lemma 2.1

In the following proof, F_1 and F_2 denote the feasible regions of SP1 and SP2 respectively. Moreover, $R^{(1)}$ represents the optimal sum rate corresponding to the power vector $\boldsymbol{p}^{(1)}$, and $R^{(2)}$ represents the optimal sum rate corresponding to the power vector $\boldsymbol{p}^{(2)}$. Note that (2.6) is a convex optimization problem, and $\boldsymbol{p}^{(1)}$ is the optimal power vector for SP1. It means that $R^{(1)} > R(\tilde{\boldsymbol{p}})$, where $R(\tilde{\boldsymbol{p}})$ denotes the sum rate under the power vector $\tilde{\boldsymbol{p}}$, $\tilde{\boldsymbol{p}} \in F_1$, and $\tilde{\boldsymbol{p}} \neq \boldsymbol{p}^{(1)}$. If $\sum_{i=1}^{K} g_{1,i} p_i^{(2)} < \Gamma_1$, then $\boldsymbol{p}^{(2)} \in F_1$. Therefore, $R^{(1)} > R^{(2)}$. On the other hand, $\boldsymbol{p}^{(2)}$ is the optimal power vector for SP2. It means that $R^{(2)} > R(\tilde{\boldsymbol{p}})$, where $R(\tilde{\boldsymbol{p}})$ denotes the sum rate corresponding to $\tilde{\boldsymbol{p}}$, and $\tilde{\boldsymbol{p}} \in F_2$, and $\tilde{\boldsymbol{p}} \neq \boldsymbol{p}^{(2)}$. If $\sum_{i=1}^{K} g_{2,i} p_i^{(1)} < \Gamma_2$, then $\boldsymbol{p}^{(1)} \in F_2$. Therefore, $R^{(2)} > R^{(1)}$. It is a contradiction. Therefore, it is impossible that both $\sum_{i=1}^{K} g_{2,i} p_i^{(1)} < \Gamma_2$ and $\sum_{i=1}^{K} g_{1,i} p_i^{(2)} < \Gamma_1$ can be satisfied simultaneously.

A.2 Proof of Lemma 2.2

The Lagrange function of the optimization problem (2.15) can be written as

$$L(\boldsymbol{p}, \lambda, \nu_1, \cdots, \nu_K) = \sum_{i=1}^{K} \log\left(1 + \frac{p_i d_i}{\sigma_i^2}\right) + \sum_{j=1}^{2} \lambda_j \Big(\Gamma_j - \sum_{i=1}^{K} g_{j,i} p_i\Big) + \sum_{k=1}^{K} \nu_k (\bar{P}_k - p_k), \tag{A.1}$$

where λ_j is the Lagrange multiplier for the jth PU's interference constraint, and ν_k is the Lagrange multiplier for the kth transmit power constraint. Since the optimal point must locate on the boundary, i.e., it satisfies at least one interference constraint with equality. If we assume that the optimal point $\boldsymbol{p}^{(o)}$ satisfies $\sum_{i=1}^{K} g_{1,i} p_i^{(o)} = \Gamma_1$ and $\sum_{i=1}^{K} g_{2,i} p_i^{(o)} < \Gamma_2$, then, according to the complementary slackness condition $\lambda_2 = 0$, (A.1) reduces to

$$L(\lambda, \mu) = \sum_{i=1}^{K} \log\left(1 + \frac{d_i p_i}{\sigma_i^2}\right) + \lambda_1 \big(\Gamma_1 - \sum_{i=1}^{K} g_{1,i} p_i\big) + \sum_{k=1}^{K} \nu_k (\bar{P}_k - p_k),$$

which corresponds to the Lagrange function of SP1, and thus its optimal power allocation is $\boldsymbol{p}^{(1)}$. According to Lemma 2.1, it is impossible $\sum_{i=1}^{K} g_{1,i} p_i^{(2)} < \Gamma_1$. Therefore, our assumption does not hold.

On the other hand, if $\sum_{i=1}^{K} g_{2,i} \boldsymbol{p}^{(o)} = \Gamma_2$, then, $R^{(2)} \geq R(\tilde{\boldsymbol{p}})$, where $R(\tilde{\boldsymbol{p}})$ denotes the sum rate under the power vector $\tilde{\boldsymbol{p}}$, and $\tilde{\boldsymbol{p}} \in F_2$. Because $\boldsymbol{p}^{(2)}$ is optimal in F_2 and $\boldsymbol{p}^{(o)} \in F_2$, it is impossible that $\boldsymbol{p}^{(o)} \neq \boldsymbol{p}^{(2)}$.

Similarly, the second part of the lemma can be proved.

A.3 Proof of Lemma 2.3

It is obvious that the optimal power vector is on the boundary of the feasible region, i.e., at least one interference constraint is satisfied with equality. If we assume that the optimal solution $\boldsymbol{p}^{(o)}$ satisfies $\sum_{i=1}^{K} g_{2,i} p_i^{(o)} = \Gamma_2$ and $\sum_{i=1}^{K} g_{1,i} p_i^{(o)} < \Gamma_1$, then by the

complementary slackness condition, $\lambda_1 = 0$, the Lagrange function (A.1) reduces to

$$L(\lambda, \mu) = \sum_{i=1}^{K} \log\left(1 + \frac{d_i p_i}{\sigma_i^2}\right) + \lambda_2\left(P_{th}^{(2)} - \sum_{i=1}^{K} g_{2,i} p_i\right) + \sum_{k=1}^{K} \nu_k(\bar{P}_k - p_k),$$

which is the Lagrange function of SP2, and its optimal power vector $\boldsymbol{p}^{(2)}$ does not satisfy $\sum_{i=1}^{K} g_{1,i} p_i^{(2)} < \Gamma_1$. Similarly, we can prove that $\boldsymbol{p}^{(o)}$ does not satisfy $\sum_{i=1}^{K} g_{2,i} p_i^{(o)} < \Gamma_2$ and $\sum_{i=1}^{K} g_{1,i} p_i^{(o)} = \Gamma_1$ simultaneously. Due to the fact that $\boldsymbol{p}^{(o)}$ must locate on the boundary, it must satisfy the two interference equalities simultaneously.

A.4 Lemma A.1 and Its Proof

Lemma A.1 *If $\boldsymbol{A}$ is a positive matrix*[1]*, and $\epsilon_{\max}$ is its maximum eigenvalue, there is no vector $\boldsymbol{v}$ such that $\boldsymbol{A}\boldsymbol{v} > \epsilon_{\max}\boldsymbol{v}$.*

$Proof:$ We prove it by contradiction. Suppose that there exists a vector $\boldsymbol{v}$ satisfying the inequality

$$\boldsymbol{A}\boldsymbol{v} > \epsilon_{\max}\boldsymbol{v}. \tag{A.2}$$

The maximal eigenvalue of the positive matrix $\boldsymbol{A}$ can be expressed as [100]

$$\epsilon_{\max} = \min_{\boldsymbol{x}>\boldsymbol{0}} \max_{\boldsymbol{y}>\boldsymbol{0}} \frac{\boldsymbol{x}^T \boldsymbol{A} \boldsymbol{y}}{\boldsymbol{x}^T \boldsymbol{y}}. \tag{A.3}$$

Therefore,

$$\epsilon_{\max} \geq \min_{\boldsymbol{x}>\boldsymbol{0}} \frac{\boldsymbol{x}^T \boldsymbol{A} \boldsymbol{v}}{\boldsymbol{x}^T \boldsymbol{v}} = \frac{\boldsymbol{a}^T \boldsymbol{A} \boldsymbol{v}}{\boldsymbol{a}^T \boldsymbol{v}}, \tag{A.4}$$

where $\boldsymbol{a}$ is the value of $\boldsymbol{x}$ such that the equality holds. On the other hand, multiplying both sides of (A.2) with $\frac{\boldsymbol{a}^T}{\boldsymbol{a}^T \boldsymbol{v}}$, we can derive

$$\frac{\boldsymbol{a}^T \boldsymbol{A} \boldsymbol{v}}{\boldsymbol{a}^T \boldsymbol{v}} > \epsilon_{\max}. \tag{A.5}$$

Combining (A.4) and (A.5), we reach a contradiction $\epsilon_{\max} > \epsilon_{\max}$. Therefore, the assumption is wrong and the Lemma holds. ■

[1] A positive matrix is a matrix whose entries are all positive.

A.5 Proof of Lemma 2.4

We prove it by contradiction. Suppose that $\sum_{i=1}^{K} g_{2,i}p_i^{(1)} > \Gamma_2$ and $\sum_{i=1}^{K} g_{1,i}p_i^{(2)} > \Gamma_1$ can hold simultaneously, i.e., $\boldsymbol{g}_2^T\boldsymbol{p}^{(1)} > \Gamma_2$ and $\boldsymbol{g}_1^T\boldsymbol{p}^{(2)} > \Gamma_1$. Under the PU_1's interference power constraint, since $\tilde{\boldsymbol{p}}^{(1)} = [(\boldsymbol{p}^{(1)})^T, 1]^T$ is the eigenvector corresponding to the maximum eigenvalue, $\epsilon_{\max}^{(1)}$, of $\boldsymbol{\Phi}_1(\boldsymbol{U}, \Gamma_1)$, we have

$$\epsilon_{\max}^{(1)} \begin{bmatrix} \boldsymbol{p}^{(1)} \\ 1 \end{bmatrix} = \boldsymbol{\Phi}_1(\boldsymbol{U}, \Gamma_1) \begin{bmatrix} \boldsymbol{p}^{(1)} \\ 1 \end{bmatrix}. \tag{A.6}$$

Similarly, for the sub-problem with the PU_2's interference power constraint, we define

$$\boldsymbol{\Phi}_2(\boldsymbol{U}, \Gamma_2) = \begin{bmatrix} \boldsymbol{D}\boldsymbol{\Psi}^T(\boldsymbol{U}) & \boldsymbol{D}\boldsymbol{q} \\ \frac{1}{\Gamma_2}\boldsymbol{g}_2^T\boldsymbol{D}\boldsymbol{\Psi}^T(\boldsymbol{U}) & \frac{1}{\Gamma_2}\boldsymbol{g}_2^T\boldsymbol{D}\boldsymbol{q} \end{bmatrix}, \tag{A.7}$$

$\boldsymbol{g}_2 = [g_{1,2}, ..., g_{K,2}]^T$, and $\tilde{\boldsymbol{p}}^{(2)} = [(\boldsymbol{p}^{(2)})^T, 1]^T$, which is the eigenvector corresponding to the maximum eigenvalue, $\epsilon_{\max}^{(2)}$, of $\boldsymbol{\Phi}_2(\boldsymbol{U}, \Gamma_2)$:

$$\epsilon_{\max}^{(2)} \begin{bmatrix} \boldsymbol{p}^{(2)} \\ 1 \end{bmatrix} = \boldsymbol{\Phi}_2(\boldsymbol{U}, \Gamma_2) \begin{bmatrix} \boldsymbol{p}^{(2)} \\ 1 \end{bmatrix}. \tag{A.8}$$

Without loss of generality, we assume $\epsilon_{\max}^{(2)} \geq \epsilon_{\max}^{(1)}$. One observation from (A.6) and (A.8) is that the first K rows in $\boldsymbol{\Phi}_1(\boldsymbol{U}, \Gamma_1)$ and $\boldsymbol{\Phi}_2(\boldsymbol{U}, \Gamma_2)$ are the same. From the first K rows of (A.8), $\boldsymbol{p}^{(2)}$ can be represented as

$$\boldsymbol{p}^{(2)} = \frac{\boldsymbol{D}\boldsymbol{\Psi}^T(\boldsymbol{U})\boldsymbol{p}^{(2)} + \boldsymbol{D}\boldsymbol{q}}{\epsilon_{\max}^{(2)}}.$$

Using assumption $\boldsymbol{g}_1^T\boldsymbol{p}^{(2)} > \Gamma_1$, we have

$$\boldsymbol{g}_1^T\boldsymbol{p}^{(2)} = \frac{\boldsymbol{g}_1^T\boldsymbol{D}\boldsymbol{\Psi}^T(\boldsymbol{U})\boldsymbol{p}^{(2)} + \boldsymbol{g}_1^T\boldsymbol{D}\boldsymbol{q}}{\epsilon_{\max}^{(2)}} > \Gamma_1. \tag{A.9}$$

Therefore, replacing $\boldsymbol{p}^{(1)}$ in (A.6) with $\boldsymbol{p}^{(2)}$ yields

$$\begin{bmatrix} \boldsymbol{D}\boldsymbol{\Psi}^T(\boldsymbol{U}) & \boldsymbol{D}\boldsymbol{q} \\ \frac{1}{\Gamma_1}\boldsymbol{g}_1^T\boldsymbol{D}\boldsymbol{\Psi}^T(\boldsymbol{U}) & \frac{1}{\Gamma_1}\boldsymbol{g}_1^T\boldsymbol{D}\boldsymbol{q} \end{bmatrix} \begin{bmatrix} \boldsymbol{p}^{(2)} \\ 1 \end{bmatrix} \overset{(a)}{>} \begin{bmatrix} \epsilon_{\max}^{(2)}\boldsymbol{p}^{(2)} \\ \epsilon_{\max}^{(2)} \end{bmatrix} \overset{(b)}{\geq} \epsilon_{\max}^{(1)} \begin{bmatrix} \boldsymbol{p}^{(2)} \\ 1 \end{bmatrix}, \tag{A.10}$$

where (a) is due to (A.9), and (b) is due to the assumption that $\epsilon_{\max}^{(2)} \geq \epsilon_{\max}^{(1)}$. Since $\epsilon_{\max}^{(1)}$ is the maximal eigenvalue of $\Phi_1(\boldsymbol{U}, \Gamma_1)$, (A.10) contradicts to Lemma A.1. So the assumption does not hold.

A.6 Proof of Lemma 2.5

Let $\epsilon_{\max}^{(1)}$ and $\epsilon_{\max}^{(2)}$ be the maximum eigenvalues of $\boldsymbol{\Phi}_1(\boldsymbol{U}, \Gamma_1)$ and $\boldsymbol{\Phi}_2(\boldsymbol{U}, \Gamma_2)$, respectively. According to [51], we have

$$\epsilon_{\max}^{(1)} = \frac{1}{C_1(\boldsymbol{U}, \Gamma_1)}, \text{ and } \epsilon_{\max}^{(2)} = \frac{1}{C_2(\boldsymbol{U}, \Gamma_2)}. \tag{A.11}$$

Now, for the first part of the lemma, if we assume $C_1(\boldsymbol{U}, \Gamma_1) \leq C_2(\boldsymbol{U}, \Gamma_2)$, then from (A.11) we have $\epsilon_{\max}^{(1)} \geq \epsilon_{\max}^{(2)}$. Replacing $\boldsymbol{p}^{(2)}$ in (A.8) with $\boldsymbol{p}^{(1)}$, we can derive

$$\begin{bmatrix} \boldsymbol{D}\boldsymbol{\Psi}^T(\boldsymbol{U}) & \boldsymbol{D}\boldsymbol{q} \\ \frac{1}{\Gamma_2}\mathbf{g}_2^T\boldsymbol{D}\boldsymbol{\Psi}^T(\boldsymbol{U}) & \frac{1}{\Gamma_2}\mathbf{g}_2^T\boldsymbol{D}\boldsymbol{q} \end{bmatrix} \begin{bmatrix} \boldsymbol{p}^{(1)} \\ 1 \end{bmatrix} > \begin{bmatrix} \epsilon_{\max}^{(1)}\boldsymbol{p}^{(1)} \\ \epsilon_{\max}^{(1)} \end{bmatrix} \geq \epsilon_{\max}^{(2)} \begin{bmatrix} \boldsymbol{p}^{(1)} \\ 1 \end{bmatrix}. \tag{A.12}$$

On the other hand, $\epsilon_{\max}^{(2)}$ is the maximum eigenvalue of $\boldsymbol{\Phi}_2(\boldsymbol{U}, \Gamma_2)$. Thus, (A.12) is contradictory to Lemma A.1. Similarly, the second part of the lemma can be proved.

A.7 Proof of Lemma 2.6

In [51] and [72], it has been shown that for a fixed $\boldsymbol{U}$ there is a unique power allocation vector and a unique balanced level which are optimal. Therefore, if $\boldsymbol{p}^{(2)}$ satisfies the condition $\sum_{i=1}^{K} g_{1,i}p_i^{(2)} < \Gamma_1$, then $\boldsymbol{p}^{(2)}$ is in the feasible region of SP3', and thus $C_2(\boldsymbol{U}, \Gamma_2) < C_1(\boldsymbol{U}, \Gamma_1)$. On the other hand, if $\boldsymbol{p}^{(1)}$ satisfies the condition $\sum_{i=1}^{K} g_{2,i}p_i^{(1)} < \Gamma_2$, then $\boldsymbol{p}^{(1)}$ is in the feasible region of SP4', and thus $C_1(\boldsymbol{U}, \Gamma_1) < C_2(\boldsymbol{U}, \Gamma_2)$. Thus the two inequalities are contradictory to each other, and they cannot be satisfied simultaneously.

A.8 Proof of Lemma 2.7

Let $C_1(\boldsymbol{U}_o^{(2)}, \Gamma_1)$ be the optimal balanced SINR level and $\bar{\boldsymbol{p}}^{(1)}$ be the optimal power vector for the fixed beamforming matrix $\boldsymbol{U}_o^{(2)}$ of SP3', respectively. According to Lemma 2.5, we have

$$C_1(\boldsymbol{U}_o^{(2)}, \Gamma_1) > C_o^{(2)}(\Gamma_2). \tag{A.13}$$

Since there is only one optimal balanced SINR level $C_o^{(1)}(\Gamma_1)$ achieved by $\boldsymbol{p}_o^{(1)}$ for SP3, $\bar{\boldsymbol{p}}^{(1)}$ is not necessary to be the optimal power allocation for SP3, and thus we have

$$C_1(\boldsymbol{U}_o^{(2)}, \Gamma_1) \leq C_o^{(1)}(\Gamma_1). \tag{A.14}$$

Combining (A.13) and (A.14), we have

$$C_o^{(2)}(\Gamma_2) < C_o^{(1)}(\Gamma_1). \tag{A.15}$$

Similarly, let $C_2(\boldsymbol{U}_o^{(1)}, \Gamma_2)$ be the optimal balanced SINR level and $\bar{\boldsymbol{p}}^{(2)}$ be the optimal power vector for the fixed beamforming matrix $\boldsymbol{U}_o^{(1)}$ of SP4', respectively. According to Lemma 2.5, we have

$$C_2(\boldsymbol{U}_o^{(1)}, \Gamma_2) > C_o^{(1)}(\Gamma_1). \tag{A.16}$$

Since there is only one optimal balanced SINR level $C_o^{(2)}(\Gamma_2)$ achieved by $\boldsymbol{p}_o^{(2)}$ for SP4, $\bar{\boldsymbol{p}}^{(2)}$ is not necessary to be the globally optimal power vector for SP4, and thus we have

$$C_2(\boldsymbol{U}_o^{(1)}, \Gamma_2) \leq C_o^{(2)}(\Gamma_2). \tag{A.17}$$

Combining (A.16) and (A.17), we have $C_o^{(1)}(\Gamma_1) < C_o^{(2)}(\Gamma_2)$, which contradicts to (A.15).

Appendix B

Appendices to Chapter 3

B.1 Proof of Lemma 3.1

According to previous discussions, the signal from each SU is divided into several data streams. We now show that the optimal encoding order of these data streams are arbitrary. It is well known that the optimal objective value of the MAC equally weighted sum rate problem can be achieved by adopting any ordering [47] [77] [78]; that is, when all the users have the same weights, the optimal solution of the weighted sum rate maximization problem is independent of the decoding order. Analogously, the data streams within a SU share the same weight. Thus, an arbitrary encoding order of those data streams within a SU can achieve the optimal solution. ■

B.2 Proof of Lemma 3.2

Let s be the subgradient of $g(\tilde{\lambda})$. For a given $\tilde{\lambda} \geq 0$, the subgradient s of $g(\tilde{\lambda})$ satisfies $g(\check{\lambda}) \geq g(\tilde{\lambda}) + s(\check{\lambda} - \tilde{\lambda})$, where $\check{\lambda}$ is any feasible value. Let $\check{\boldsymbol{S}}_i^{\mathrm{m}},\ i = 1, \ldots, K$, be the optimal covariance matrices in (3.27) for $\lambda = \check{\lambda}$, and $\tilde{\boldsymbol{S}}_i^{\mathrm{m}},\ i = 1, \ldots, K$, be the optimal

covariance matrices in (3.27) for $\lambda = \tilde{\lambda}$. We express $g(\check{\lambda})$ as

$$
\begin{aligned}
g(\check{\lambda}) &= \max_{\boldsymbol{S}_1^{\mathrm{m}},\cdots,\boldsymbol{S}_K^{\mathrm{m}}} \Big(f(\boldsymbol{S}_1^{\mathrm{m}},\cdots,\boldsymbol{S}_K^{\mathrm{m}}) - \check{\lambda}(\sum_{i=1}^{K} \mathrm{tr}(\boldsymbol{S}_i^{\mathrm{m}}) - P) \Big) \\
&= f(\check{\boldsymbol{S}}_1^{\mathrm{m}},\cdots,\check{\boldsymbol{S}}_K^{\mathrm{m}}) - \check{\lambda}\Big(\sum_{i=1}^{K} \mathrm{tr}(\check{\boldsymbol{S}}_i^{\mathrm{m}}) - \bar{P} \Big) \\
&\geq f(\tilde{\boldsymbol{S}}_1^{\mathrm{m}},\cdots,\tilde{\boldsymbol{S}}_K^{\mathrm{m}}) - \check{\lambda}\Big(\sum_{i=1}^{K} \mathrm{tr}(\tilde{\boldsymbol{S}}_i^{\mathrm{m}}) - \bar{P} \Big) \\
&= f(\tilde{\boldsymbol{S}}_1^{\mathrm{m}},\cdots,\tilde{\boldsymbol{S}}_K^{\mathrm{m}}) - \tilde{\lambda}\Big(\sum_{i=1}^{K} \mathrm{tr}(\tilde{\boldsymbol{S}}_i^{\mathrm{m}}) - \bar{P} \Big) + \tilde{\lambda}\Big(\sum_{i=1}^{K} \mathrm{tr}(\tilde{\boldsymbol{S}}_i^{\mathrm{m}}) - \bar{P} \Big) - \check{\lambda}\Big(\sum_{i=1}^{K} \mathrm{tr}(\tilde{\boldsymbol{S}}_i^{\mathrm{m}}) - \bar{P} \Big) \\
&= g(\tilde{\lambda}) + \Big(\bar{P} - \sum_{i=1}^{K} \mathrm{tr}(\tilde{\boldsymbol{S}}_i^{\mathrm{m}}) \Big)(\check{\lambda} - \tilde{\lambda}),
\end{aligned}
$$

where $s := P - \sum_{i=1}^{K} \mathrm{tr}(\tilde{\boldsymbol{S}}_i^{\mathrm{m}})$ is the subgradient of $g(\tilde{\lambda})$. This concludes the proof. ■

Appendix C

Appendices to Chapter 4

C.1 Proof of Lemma 4.1

($\mathbf{P1}$) involves infinitely many constraints. Denote the set of active constraints by $\mathcal{C}$, the cardinality of the set $\mathcal{C}$ by K, and the channel response related to the kth element of the set $\mathcal{C}$ by $\boldsymbol{g}_k$. According to the Karush-Kuhn-Tucker (KKT) conditions for $\mathbf{P1}$, we have:

$$\boldsymbol{h}(1+\boldsymbol{h}^H\boldsymbol{S}\boldsymbol{h})^{-1}\boldsymbol{h}^H+\boldsymbol{\Phi}=\lambda\boldsymbol{I}+\sum_{i=1}^{K}\mu_i\boldsymbol{g}_i\boldsymbol{g}_i^H, \tag{C.1}$$

$$\text{tr}(\boldsymbol{\Phi}\boldsymbol{S})=0, \tag{C.2}$$

where $\boldsymbol{\Phi}$ is the dual variable associated with the constraint $\boldsymbol{S}\geq 0$, and λ and μ_i are the dual variables associated with the transmit power constraint and the interference constraint, respectively. First, we assume that $\lambda\neq 0$, and thus the rank of the right hand side of (C.1) is N. Since the first term on the left hand side of (C.1) has rank one, we have

$$\text{Rank}(\boldsymbol{\Phi})\geq N-1. \tag{C.3}$$

Moreover, since $\boldsymbol{S}\geq 0$ and $\boldsymbol{\Phi}\geq 0$, from (C.2) we have $\text{tr}(\boldsymbol{\Phi}\boldsymbol{S})=\text{tr}(\boldsymbol{V}^H\boldsymbol{\Lambda}\boldsymbol{V}\boldsymbol{S})=\text{tr}(\boldsymbol{\Lambda}\boldsymbol{V}\boldsymbol{S}\boldsymbol{V}^H)=\text{tr}(\boldsymbol{\Lambda}\tilde{\boldsymbol{S}})=0$, where $\boldsymbol{V}^H\boldsymbol{\Lambda}\boldsymbol{V}$ is the eigenvalue decomposition of ma-

trix $\boldsymbol{\Phi}$, and $\tilde{\boldsymbol{S}} := \boldsymbol{V}\boldsymbol{S}\boldsymbol{V}^H$. By applying eigenvalue decomposition to $\tilde{\boldsymbol{S}}$, we have $\tilde{\boldsymbol{S}} = \sum_i \tau_i \boldsymbol{s}_i \boldsymbol{s}_i^H$, where τ_i is the ith eigenvalue and $\boldsymbol{s}_i$ is the corresponding eigenvector. We next show $\text{Rank}(\boldsymbol{S}) + \text{Rank}(\boldsymbol{\Phi}) \leq N$ by contradiction. Suppose that $\text{Rank}(\boldsymbol{S}) + \text{Rank}(\boldsymbol{\Phi}) > N$. Then, there exists an index j such that the jth element of $\boldsymbol{s}_i$ and the jth diagonal element of $\boldsymbol{\Lambda}$ are non-zero simultaneously. Thus, it is impossible that the equation $\text{tr}(\boldsymbol{\Lambda}\tilde{\boldsymbol{S}}) = 0$ holds. It follows that $\text{Rank}(\boldsymbol{S}) + \text{Rank}(\boldsymbol{\Phi}) \leq N$. Combining this with (C.3), we have $\text{Rank}(\boldsymbol{S}) \leq 1$.

Second, we assume that $\lambda = 0$ in (C.1). In this case, $\boldsymbol{S}$ must lie in the space spanned by $\boldsymbol{g}_i$, $i = 1, \cdots, K$. Let the dimensionality of the space be M, where $M \leq N$ even if K is an infinite large value. Therefore, $\boldsymbol{\Phi}$ and $\boldsymbol{S}$ are confined in a M-dimension space. Thus, the reminder of the proof is the same as that of the case $\lambda \neq 0$, and the proof is complete. ■

C.2 Proof of Lemma 4.2

The objective function $p\boldsymbol{g}^H\boldsymbol{v}\boldsymbol{v}^H\boldsymbol{g}$ is a convex function. The duality gap for a convex maximization problem is zero. The Lagrange function is

$$L(\boldsymbol{g}, \lambda) = p\boldsymbol{g}^H\boldsymbol{v}\boldsymbol{v}^H\boldsymbol{g} - \lambda\Big((\boldsymbol{g} - \boldsymbol{g}_0)^H\boldsymbol{R}^{-1}(\boldsymbol{g} - \boldsymbol{g}_0) - \epsilon\Big), \tag{C.4}$$

where λ is the Lagrange multiplier. According to the KKT condition, we have $\frac{\partial L}{\partial \boldsymbol{g}} = 2p\boldsymbol{v}\boldsymbol{v}^H\boldsymbol{g} - 2\lambda\boldsymbol{R}^{-1}(\boldsymbol{g} - \boldsymbol{g}_0) = 0$. Thus,

$$p(\boldsymbol{v}^H\boldsymbol{g})\boldsymbol{v} = \lambda\boldsymbol{R}^{-1}(\boldsymbol{g} - \boldsymbol{g}_0). \tag{C.5}$$

We have $\boldsymbol{g}_{\max} = \boldsymbol{g}_0 + b\alpha\boldsymbol{R}\boldsymbol{v}$, where $b \in \mathbb{R}$, $\alpha \in \mathbb{C}$, and $|\alpha| = 1$. Since $(\boldsymbol{g} - \boldsymbol{g}_0)^H\boldsymbol{R}^{-1}(\boldsymbol{g} - \boldsymbol{g}_0) = \epsilon$, we have $b = \sqrt{\epsilon}/\sqrt{\boldsymbol{v}^H\boldsymbol{R}^H\boldsymbol{v}}$. Moreover, by observing (C.5), we have $\alpha = t\boldsymbol{v}^H\boldsymbol{g} = t\boldsymbol{v}^H(\boldsymbol{g}_0 + b\alpha\boldsymbol{R}\boldsymbol{v}) = t\boldsymbol{v}^H\boldsymbol{g}_0 + tb\alpha\boldsymbol{v}^H\boldsymbol{R}\boldsymbol{v}$, where t is a real scalar such that $|t\boldsymbol{v}^H\boldsymbol{g}| = 1$. Thus, we have $\boldsymbol{v}^H\boldsymbol{g}_0/|\boldsymbol{v}^H\boldsymbol{g}_0| = \alpha$. The proof follows immediately. ■

C.3 Proof of Lemma 4.3

First, we consider the sufficiency part of this lemma. We assume that there exists a covariance matrix $\boldsymbol{S}_{\text{opt}}$ and an $\boldsymbol{g}_{\text{opt}}$ that satisfy the conditions (4.5) and (4.6) simultaneously. Since $\boldsymbol{S}_{\text{opt}}$ satisfies both the transmit power constraint and the interference constraint, $\boldsymbol{S}_{\text{opt}}$ is a feasible solution for $(\mathbf{P1})$. Moreover, if we assume that there exists another solution $\boldsymbol{S}_s$, which results in a larger achievable rate for the SU link, then a contradiction will be derived. Without loss of generality, we assume that the constraint set, which consists of all the active interference constraints for $\boldsymbol{S}_s$, is denoted by $\mathcal{T}$. We divide the set $\mathcal{T}$ into two types: one type is $\boldsymbol{g}_{\text{opt}} \in \mathcal{T}$, and the other type is $\boldsymbol{g}_{\text{opt}} \notin \mathcal{T}$.

Assume that C_s and C_{opt} are the achievable rates for the covariance matrices $\boldsymbol{S}_s$ and $\boldsymbol{S}_{\text{opt}}$, respectively. In the case of $\boldsymbol{g}_{\text{opt}} \in \mathcal{T}$, we have $C_s \leq C_{\text{opt}}$, since C_{opt} is obtained with fewer constraints. Since $(\mathbf{P1})$ is a convex optimization problem that has a unique optimal solution, $\boldsymbol{S}_{\text{opt}}$ is indeed the optimal solution. In the case of $\boldsymbol{g}_{\text{opt}} \notin \mathcal{T}$, we can observe that $\boldsymbol{S}_{\text{opt}}$ satisfies the constraints in $\mathcal{T}$, and $\boldsymbol{S}_s$ satisfies the constraint $\boldsymbol{g}_{\text{opt}}$. According to the lemma in [68], this case does not exist.

We next proceed to prove the necessity part. Suppose that $\boldsymbol{S}_{\text{opt}}$ is the optimal solution of $(\mathbf{P1})$. According to Lemma 4.1, we have $\boldsymbol{S}_{\text{opt}} = p_{\text{opt}}\boldsymbol{v}_{\text{opt}}\boldsymbol{v}_{\text{opt}}^H$. Thus, $(\mathbf{P1})$ is equivalent to

$$\begin{aligned} &\max_{\boldsymbol{S}\geq 0} \ \log(1+\boldsymbol{h}^H\boldsymbol{S}\boldsymbol{h}) \\ \text{subject to}: \ &\text{tr}(\boldsymbol{S}) \leq p_{\text{opt}}, \ \boldsymbol{g}^H\boldsymbol{S}\boldsymbol{g} \leq \Gamma, \ \text{for} \ (\boldsymbol{g}-\boldsymbol{g}_0)^H\boldsymbol{R}^{-1}(\boldsymbol{g}-\boldsymbol{g}_0) \leq \epsilon. \end{aligned} \tag{C.6}$$

According to Lemma 4.2, there is a unique

$$\boldsymbol{g}_{\text{opt}} = \boldsymbol{g}_0 + \sqrt{\frac{\epsilon}{\boldsymbol{v}_{\text{opt}}^H\boldsymbol{R}\boldsymbol{v}_{\text{opt}}}}\alpha\boldsymbol{R}\boldsymbol{v}_{\text{opt}}, \tag{C.7}$$

which is the optimal solution of $\max\limits_{\boldsymbol{h}\in\mathcal{H}(\epsilon)} \boldsymbol{g}^H\boldsymbol{S}\boldsymbol{g} \leq \Gamma$. Thus, for problem (C.6), only $\text{tr}(\boldsymbol{S}) \leq p_{\text{opt}}$ and $\boldsymbol{g}_{\text{opt}}^H\boldsymbol{S}\boldsymbol{g}_{\text{opt}} \leq \Gamma$ are active constraints. Thus, it is obvious that problem

(C.6) and problem (4.5) have the same optimal solution. Hence, the proof is complete.

■

C.4 Proof of Lemma 4.4

The proof of Lemma 4.4 is divided into two parts. The first part is to prove that $\boldsymbol{v}_{\text{opt}}$ is in the form of $\alpha_v \hat{\boldsymbol{g}}_{//} + \beta_v \hat{\boldsymbol{g}}_{\perp}$, where $\alpha_v \in \mathbb{C}$ and $\beta_v \in \mathbb{C}$. The second part is to prove $\alpha_v \in \mathbb{R}$ and $\beta_v \in \mathbb{R}$. In the following proof, we assume that $\alpha_k \in \mathbb{C}$ are some proper complex scalars.

According to Lemma 4.3, and Theorem 2 in [36], we have

$$\boldsymbol{v}_{\text{opt}} = \alpha_1 \boldsymbol{g}_{\text{opt}} + \alpha_2 \boldsymbol{h}. \tag{C.8}$$

According to Lemma 4.2, we have

$$\boldsymbol{g}_{\text{opt}} = \boldsymbol{g}_0 + \alpha_3 \boldsymbol{v}_{\text{opt}} = \boldsymbol{g}_0 + \alpha_3\big(\alpha_1 \boldsymbol{g}_{\text{opt}} + \alpha_2 \boldsymbol{h}\big) = \boldsymbol{g}_0 + \alpha_1\alpha_3 \boldsymbol{g}_{\text{opt}} + \alpha_2\alpha_3 \boldsymbol{h}. \tag{C.9}$$

According to (C.9), it can be observed that $\boldsymbol{g}_{\text{opt}}$ can be expressed by the linear combination of $\boldsymbol{g}_0$ and $\boldsymbol{h}$, where the coefficients are complex. Combining this with (C.8), we have $\boldsymbol{v}_{\text{opt}} = \alpha_4 \boldsymbol{g}_0 + \alpha_5 \boldsymbol{h}$, where $\alpha_4 \in \mathbb{C}$ and $\alpha_5 \in \mathbb{C}$. Moreover, since both $\boldsymbol{g}_0$ and $\boldsymbol{h}$ can be expressed as a linear combination of $\hat{\boldsymbol{g}}_{//}$ and $\hat{\boldsymbol{g}}_{\perp}$, we have $\boldsymbol{v}_{\text{opt}} = \alpha_v \hat{\boldsymbol{g}}_{//} + \beta_v \hat{\boldsymbol{g}}_{\perp}$. Since rotating $\boldsymbol{v}_{\text{opt}}$ does not affect the final result, we can assume $\alpha_v \in \mathbb{R}$.

We next prove that $\beta_v \in \mathbb{R}$ by contradiction. At first, we assume that $\beta_v = a + jb \notin \mathbb{R}$. Then we can find an equivalent $\hat{\beta}_v = \sqrt{a^2 + b^2} \in \mathbb{R}$ which is a better solution of **(P1)** than β_v. Assume that $\hat{\boldsymbol{v}}_{\text{opt}} = \alpha_v \hat{\boldsymbol{g}}_{//} + \hat{\beta}_v \hat{\boldsymbol{g}}_{\perp}$. It is clear that $\|\hat{\boldsymbol{v}}_{\text{opt}}\| = \|\boldsymbol{v}_{\text{opt}}\|$, and the interference caused by $\hat{\boldsymbol{v}}_{\text{opt}}$ is

$$p\boldsymbol{g}_{\text{opt}}^H \hat{\boldsymbol{v}}_{\text{opt}} \hat{\boldsymbol{v}}_{\text{opt}}^H \boldsymbol{g}_{\text{opt}} = p(\boldsymbol{g}_0 + \sqrt{\frac{\epsilon}{\hat{\boldsymbol{v}}_{\text{opt}}^H \boldsymbol{R} \hat{\boldsymbol{v}}_{\text{opt}}}} \alpha \boldsymbol{R} \hat{\boldsymbol{v}}_{\text{opt}})^H \hat{\boldsymbol{v}}_{\text{opt}} \hat{\boldsymbol{v}}_{\text{opt}}^H (\boldsymbol{g}_0 + \sqrt{\frac{\epsilon}{\hat{\boldsymbol{v}}_{\text{opt}}^H \boldsymbol{R} \hat{\boldsymbol{v}}_{\text{opt}}}} \alpha \boldsymbol{R} \hat{\boldsymbol{v}}_{\text{opt}}) \tag{C.10}$$

$$= p\big(\alpha_v \|\boldsymbol{g}_0\| + \sqrt{\frac{\epsilon}{\hat{\boldsymbol{v}}_{\text{opt}}^H \boldsymbol{R} \hat{\boldsymbol{v}}_{\text{opt}}}} \alpha^H \hat{\boldsymbol{v}}_{\text{opt}}^H \boldsymbol{R} \hat{\boldsymbol{v}}_{\text{opt}}\big)^2, \tag{C.11}$$

which is equal to that of $\boldsymbol{v}_{\text{opt}}$. However, the corresponding objective function with $\hat{\boldsymbol{v}}_{\text{opt}}$ is

$$\begin{aligned}
&\log(1+p\boldsymbol{h}^H\hat{\boldsymbol{v}}_{\text{opt}}\hat{\boldsymbol{v}}_{\text{opt}}^H\boldsymbol{h})\\
&=\log(1+p(a_{h_s}\hat{\boldsymbol{g}}_{//}+b_{h_s}\hat{\boldsymbol{g}}_{\perp})^H(\alpha_v\hat{\boldsymbol{g}}_{//}+\hat{\beta}_v\hat{\boldsymbol{g}}_{\perp})(\alpha_v\hat{\boldsymbol{g}}_{//}+\hat{\beta}_v\hat{\boldsymbol{g}}_{\perp})^H(a_{h_s}\hat{\boldsymbol{g}}_{//}+b_{h_s}\hat{\boldsymbol{g}}_{\perp}))\\
&=\log(1+p(a_{h_s}\alpha_v+b_{h_s}\hat{\beta}_v)(a_{h_s}\alpha_v+b_{h_s}\hat{\beta}_v^H)),
\end{aligned}\tag{C.12}$$

and the objective value with $\boldsymbol{v}_{\text{opt}}$ is

$$\begin{aligned}
&\log(1+p\boldsymbol{h}^H\boldsymbol{v}_{\text{opt}}\boldsymbol{v}_{\text{opt}}^H\boldsymbol{h})\\
&=\log(1+p(a_{h_s}\hat{\boldsymbol{g}}_{//}+b_{h_s}\hat{\boldsymbol{g}}_{\perp})^H(\alpha_v\hat{\boldsymbol{g}}_{//}+\beta_v\hat{\boldsymbol{g}}_{\perp})(\alpha_v\hat{\boldsymbol{g}}_{//}+\beta_v\hat{\boldsymbol{g}}_{\perp})^H(a_{h_s}\hat{\boldsymbol{g}}_{//}+b_{h_s}\hat{\boldsymbol{g}}_{\perp}))\\
&=\log(1+p(a_{h_s}\alpha_v+b_{h_s}\beta_v)(a_{h_s}\alpha_v+b_{h_s}\beta_v^H)).
\end{aligned}\tag{C.13}$$

According to (C.12) and (C.13), we can conclude that $\hat{\boldsymbol{v}}_{\text{opt}}$ is a better solution. The proof follows. ■

C.5 Proof of Lemma 4.5

Similar to the proof of Lemma 4.3, we can show that the problem

$$\boldsymbol{S}_{\text{opt}}=\arg\max_{\boldsymbol{S},p}\log(1+\boldsymbol{h}^H\boldsymbol{S}\boldsymbol{h})\text{ subject to : }\boldsymbol{g}_{\text{opt}}^H\boldsymbol{S}\boldsymbol{g}_{\text{opt}}\leq\Gamma,\tag{C.14}$$

where $\boldsymbol{g}_{\text{opt}}=\arg\max_{\boldsymbol{h}}\boldsymbol{g}^H\boldsymbol{S}_{\text{opt}}\boldsymbol{g},\ \text{for }(\boldsymbol{g}-\boldsymbol{g}_0)^H\boldsymbol{R}^{-1}(\boldsymbol{g}-\boldsymbol{g}_0)\leq\epsilon$, is equivalent to **SP2**.

Since $\boldsymbol{S}_{\text{opt}}$ is a rank-1 matrix, according to Lemma 4.2, we have $\boldsymbol{g}_{\text{opt}}=\boldsymbol{g}_0+\sqrt{\epsilon}\sigma\boldsymbol{v}$. Combining this with (C.14), we have $\boldsymbol{S}_{\text{opt}}=\arg\max_{\boldsymbol{S},p}\log(1+\boldsymbol{h}^H\boldsymbol{S}\boldsymbol{h})$ s.t. : $(\boldsymbol{g}_0+\sqrt{\epsilon}\sigma\boldsymbol{v})^H\boldsymbol{S}(\boldsymbol{g}_0+\sqrt{\epsilon}\sigma\boldsymbol{v})\leq\Gamma$, which is equivalent to (4.20). The proof is complete. ■.

C.6 Proof of Theorem 4.1

Assume that $\boldsymbol{S}_{\text{opt}}$ is the optimal solution for problem $\mathbf{P3}$. If $\boldsymbol{S}_1$ satisfies the interference constraint, then $\boldsymbol{S}_1$ is a feasible solution for problem $\mathbf{P3}$. The optimal rate achieved by $\boldsymbol{S}_{\text{opt}}$ cannot be larger than that of $\boldsymbol{S}_1$, since the constraint of $\mathbf{SP1}$ is a subset of problem $\mathbf{P3}$. Similarly, we can prove the second part of the Lemma. We now focus on the third part of this lemma. For problem $\mathbf{P3}$, at least one of $\text{tr}(\boldsymbol{S}) \leq \bar{P}$ and $\boldsymbol{g}_{\text{opt}}^H \boldsymbol{S} \boldsymbol{g}_{\text{opt}} \leq \Gamma$ is an active constraint, since if neither of them is active, we can always find an ϵ such that $\boldsymbol{S}_{\text{opt}} + \epsilon \boldsymbol{I}$ is a feasible and better solution. Moreover, if only $\text{tr}(\boldsymbol{S}) \leq \bar{P}$ is active, then $\boldsymbol{S}_1$ is the optimal solution, which contradicts with $\boldsymbol{g}_{\text{opt}}^H \boldsymbol{S}_1 \boldsymbol{g}_{\text{opt}} \geq \Gamma$. Similarly, it is impossible that only $\boldsymbol{g}_{\text{opt}}^H \boldsymbol{S} \boldsymbol{g}_{\text{opt}} \leq \Gamma$ is active. Therefore, both constraints are active constraints. ■

Appendix D

Appendices to Chapter 5

D.1 Proof of Theorem 5.1

Theorem 5.1 can be proved by contradiction. For the fixed σ_is, suppose that the optimal solution of $(\mathbf{PB})$ is $\boldsymbol{S}_o$. Define $\bar{\Gamma}_i = \boldsymbol{g}_i^H \boldsymbol{S}_o \boldsymbol{g}_i, i = 1, \ldots, K$. If the optimal solution of $(\mathbf{PA})$ with $\Gamma_i = \bar{\Gamma}_i, \forall i$, denoted by $\bar{\boldsymbol{S}}_o$, satisfies $\log|\boldsymbol{I}+\boldsymbol{h}_s^H \bar{\boldsymbol{S}}_o \boldsymbol{h}_s| > \log|\boldsymbol{I}+\boldsymbol{h}_s^H \boldsymbol{S}_o \boldsymbol{h}_s|$, then $\bar{\boldsymbol{S}}_o$ is a better solution for $(\mathbf{PB})$ than $\boldsymbol{S}_o$, which contradicts the preassumption that $\boldsymbol{S}_o$ is the optimal solution of $(\mathbf{PB})$. Then there must be $\log(\boldsymbol{I} + \boldsymbol{h}_s^H \bar{\boldsymbol{S}}_o \boldsymbol{h}_s^H) \leq \log(\boldsymbol{I} + \boldsymbol{h}_s^H \boldsymbol{S}_o \boldsymbol{h}_s)$, which means that $\boldsymbol{S}_o$ is also the optimal solution of $(\mathbf{PA})$, with $\Gamma_i = \boldsymbol{g}_i^H \boldsymbol{S}_o \boldsymbol{g}_i, i = 1, \ldots, K$. Theorem 5.1 thus follows.

D.2 Proof of Theorem 5.2

It is easy to observe that $(\mathbf{PB})$ can be re-expressed as

$$\begin{aligned} &\max_{\boldsymbol{S}} \ \min_{i} \ \frac{(\boldsymbol{I} + \boldsymbol{h}_s^H \boldsymbol{S} \boldsymbol{h}_s)}{1 + \boldsymbol{g}_i^H \boldsymbol{S} \boldsymbol{g}_i / \sigma_i^2} \\ &\text{subject to: } \mathrm{tr}(\boldsymbol{S}) \leq \bar{P}. \end{aligned} \tag{D.1}$$

Suppose that $\boldsymbol{S}_o$ is the optimal solution of Problem (D.1) and $(\mathbf{PB})$. Define $T_o := \boldsymbol{I} + \boldsymbol{h}_s^H \boldsymbol{S}_o \boldsymbol{h}_s$ and $\bar{\Gamma}_i := \boldsymbol{g}_i^H \boldsymbol{S}_o \boldsymbol{g}_i, i = 1, \cdots, K$, then the optimal objective value of Problem (D.1) is $\bar{F} = \min\Big(T_o/(1+\bar{\Gamma}_1), \cdots, T_o/(1+\bar{\Gamma}_K)\Big)$.

Suppose that the optimal solution $\bar{\boldsymbol{S}}_o$ of Problem (5.2) with $\Gamma_i = \bar{\Gamma}_i, \forall i$, satisfies $(\boldsymbol{I} + \boldsymbol{h}_s^H \bar{\boldsymbol{S}}_o \boldsymbol{h}_s) > T_o$, then $\bar{\boldsymbol{S}}_o$ is a better solution for Problem (D.1) than $\boldsymbol{S}_o$, which contradicts the preassumption that $\boldsymbol{S}_o$ is the optimal solution of Problem (D.1). On the other hand, suppose that $1 + \boldsymbol{h}_s^H \bar{\boldsymbol{S}}_o \boldsymbol{h}_s < T_o$. In this case, $\boldsymbol{S}_o$ is a better solution than $\bar{\boldsymbol{S}}_o$ for Problem (5.2), which contradicts the presumption that $\bar{\boldsymbol{S}}_o$ is the optimal solution of Problem (5.2). Therefore, we have $T_o = g(\bar{\Gamma}_1, \cdots, \bar{\Gamma}_K)$. Thus, $\bar{F}$ is achievable for Problem (5.3) with the particular choice of $\Gamma_i = \bar{\Gamma}_i, \forall i$.

Furthermore, suppose that $\tilde{\Gamma}_i$s are the optimal solutions of Problem (5.3), and the corresponding optimal objective value is $\tilde{F}$. For Problem (5.2) with $\Gamma_i = \tilde{\Gamma}_i$, suppose that the optimal solution is $\tilde{\boldsymbol{S}}$. We can prove that $\tilde{F} \leq \bar{F}$ by contradiction: If $\tilde{F} > \bar{F}$, $\tilde{\boldsymbol{S}}$ is a better solution for Problem (D.1) than $\boldsymbol{S}_o$, which contradicts the preassumption that $\boldsymbol{S}_o$ is the optimal solution of Problem (D.1). As such, we see that $\bar{F}$ is not only achievable for Problem (5.3), but also the optimal value of Problem (5.3) with the optimal solutions given as $\tilde{\boldsymbol{S}} = \boldsymbol{S}_o$ and $\tilde{\Gamma}_i = \boldsymbol{g}_i^H \boldsymbol{S}_o \boldsymbol{g}_i, \forall i$ (Note that $\boldsymbol{S}$ is a hidden design variable for Problem (5.3).).

Theorem 5.2 thus follows.

D.3 Proof of Theorem 5.3

We first study several important properties of Problem (5.2) that is known to be an equivalent problem of $(\mathbf{PA})$. Considering $(\mathbf{PA})$ first, its Lagrangian function can be written as

$$L_1(\boldsymbol{S}, \lambda, \{\mu_i\}) = \log|\boldsymbol{I} + \boldsymbol{h}_s^H \boldsymbol{S} \boldsymbol{h}_s| - \lambda(\text{tr}(\boldsymbol{S}) - P) - \sum_{i=1}^{K} \mu_i (\boldsymbol{g}_i^H \boldsymbol{S} \boldsymbol{g}_i - \Gamma_i) \quad \text{(D.2)}$$

where λ and μ_i are the non-negative Lagrange multipliers/dual variables with respect to the transmit power constraint and the interference power constraint at PU$_i$, respectively. Since $(\mathbf{PA})$ is a convex optimization problem, the Karush-Kuhn-Tucker (KKT) conditions [53] are both sufficient and necessary for a solution to be optimal, and solving $(\mathbf{PA})$ is equivalent to solving its dual problem

$$\min_{\lambda,\{\mu_i\}} \max_{\boldsymbol{S}} L_1(\boldsymbol{S}, \lambda, \{\mu_i\}). \tag{D.3}$$

On the other hand, the auxiliary problem (5.2) is non-convex due to the fact that its objective function is not concave. In general, the KKT conditions may not be sufficient for a feasible solution to be optimal when we have a non-convex optimization problem. However, we prove in the following lemma that this is not the case for Problem (5.2).

Lemma D.1 *With Problem* (5.2)*, the KKT conditions are both sufficient and necessary for a solution to be optimal.*

$Proof$: The necessary part of Lemma D.1 is obvious even for a non-convex optimization problem [53]. The sufficient part of Lemma D.1 can be proved via contradiction as follows. The Lagrangian of Problem (5.2) can be written as

$$L_2(\boldsymbol{S}, \delta, \{\gamma_i\}) = |\boldsymbol{I} + \boldsymbol{h}_s^H \boldsymbol{S} \boldsymbol{h}_s| - \delta(\text{tr}(\boldsymbol{S}) - P) - \sum_{i=1}^{K} \gamma_i (\boldsymbol{g}_i^H \boldsymbol{S} \boldsymbol{g}_i - \Gamma_i) \tag{D.4}$$

where δ and γ_i are the non-negative dual variables with respect to the transmit power constraint and the interference power constraint at PU$_i$, respectively. We first list the KKT conditions of Problem (5.2) as follows:

$$\boldsymbol{h}_s \boldsymbol{h}_s^H = \delta \boldsymbol{I} + \sum_{i=1}^{K} \gamma_i \boldsymbol{g}_i \boldsymbol{g}_i^H \tag{D.5}$$

$$\delta(\text{tr}(\boldsymbol{S}) - P) = 0 \tag{D.6}$$

$$\gamma_i (\boldsymbol{g}_i^H \boldsymbol{S} \boldsymbol{g}_i - \Gamma_i) = 0, \ i = 1, \cdots, K. \tag{D.7}$$

Suppose that $\boldsymbol{S}^{(0)}$, $\delta^{(0)}$, and $\gamma_i^{(0)}$ are a set of primal and dual variables that satisfy the above KKT conditions, and the corresponding optimal value of Problem (5.2) is $C^{(0)}$.

The KKT conditions of $(\mathbf{PA})$ are expressed as

$$(\boldsymbol{I} + \boldsymbol{h}_s^H \boldsymbol{S} \boldsymbol{h}_s)^{-1} \boldsymbol{h}_s \boldsymbol{h}_s^H = \lambda \boldsymbol{I} + \sum_{i=1}^{K} \mu_i \boldsymbol{g}_i \boldsymbol{g}_i^H \tag{D.8}$$

$$\lambda(\text{tr}(\boldsymbol{S}) - P) = 0 \tag{D.9}$$

$$\mu_i(\boldsymbol{g}_i^H \boldsymbol{S} \boldsymbol{g}_i - \Gamma_i) = 0,\ i = 1, \cdots, K. \tag{D.10}$$

Suppose that $\boldsymbol{S}^{(1)}$, $\lambda^{(1)}$, and $\mu_i^{(1)}$ are the optimal primal and dual variables that satisfy the above KKT conditions, and the corresponding optimal value of $(\mathbf{PA})$ is $C^{(1)}$. Note that since $(\mathbf{PA})$ is convex, the KKT conditions are both necessary and sufficient.

If (D.5)-(D.7) are not sufficient such that $\log(C^{(0)}) \neq C^{(1)}$, i.e., $\boldsymbol{S}^{(0)} \neq \boldsymbol{S}^{(1)}$, we could choose

$$\boldsymbol{S} = \boldsymbol{S}^{(0)} \tag{D.11}$$

$$\lambda = \delta^{(0)} / |\boldsymbol{I} + \boldsymbol{h}_s^H \boldsymbol{S}^{(0)} \boldsymbol{h}_s| \tag{D.12}$$

$$\mu_i = \gamma_i^{(0)} / |\boldsymbol{I} + \boldsymbol{h}_s^H \boldsymbol{S}^{(0)} \boldsymbol{h}_s|,\ i = 1, \cdots, K \tag{D.13}$$

for $(\mathbf{PA})$, which clearly also satisfy the KKT conditions of $(\mathbf{PA})$. Given the sufficiency of the KKT conditions for $(\mathbf{PA})$, $\boldsymbol{S}^{(0)}$ is also optimal for $(\mathbf{PA})$ based on (D.11) such that $\log(C^{(0)}) = C^{(1)}$, which contradicts our assumption that $\log(C^{(0)}) \neq C^{(1)}$. Lemma D.1 thus follows. ■

Essentially, it is due to the equivalence between the non-convex Problem (5.2) and the convex $(\mathbf{PA})$ that Lemma D.1 holds. From Lemma D.1, it follows that the duality gap between Problem (5.2) and its dual problem, defined as

$$D = \min_{\delta, \{\gamma_i\}} \max_{\boldsymbol{S}}\ L_2(\boldsymbol{S}, \delta, \{\gamma_i\}), \tag{D.14}$$

is zero, i.e., $g(\Gamma_1, \cdots, \Gamma_K) = \min_{\delta, \{\gamma_i\}} \max_{\boldsymbol{S}}\ L_2(\boldsymbol{S}, \delta, \{\gamma_i\})$. As such, from (D.4) we

have

$$\frac{\partial g(\Gamma_1, \cdots, \Gamma_K)}{\partial \Gamma_i} = \frac{\partial D}{\partial \Gamma_i} = \gamma_i^{(0)}, i = 1, \cdots, K. \tag{D.15}$$

Combining (D.13) and (D.15), the latter part of Theorem 5.3 thus follows.

Now we prove the concavity of $g(\Gamma_1, \cdots, \Gamma_K)$. For the function $g(\boldsymbol{q})$, where $\boldsymbol{q} := [\Gamma_1, \cdots, \Gamma_K]^T \in \mathcal{R}_+^K$, its concavity can be verified by considering an arbitrary line given by $\boldsymbol{q} = \boldsymbol{x} + t\boldsymbol{v}$, where $\boldsymbol{x} \in \mathcal{R}_+^K$, $\boldsymbol{v} \in \mathcal{R}^K$, $t \in \mathcal{R}_+$, and $\boldsymbol{x} + t\boldsymbol{v} \in \mathcal{R}_+^K$ [53]. In the sequel, we just need to prove that the function $g(\boldsymbol{x} + t\boldsymbol{v})$ is concave with respect to t. Moreover, if the ith IT constraint is not active for Problem (5.2), we have $\gamma_i = 0$ from the KKT condition such that the concavity holds. To exclude the above trivial case, we assume that all K IT constraints are active for Problem (5.2) in the following.

Define

$$f_2(\delta, \gamma_1, \cdots, \gamma_K) := \max_{\boldsymbol{S}} L_2(\boldsymbol{S}, \delta, \gamma_1, \cdots, \gamma_K) \tag{D.16}$$

as the dual function of Problem (5.2). Let $\boldsymbol{s}$ be the subgradient of $f_2(\delta, \gamma_1, \cdots, \gamma_K)$. According to the definition of subgradient, the subgradient at the point $[\tilde{\delta}, \tilde{\gamma}_1, \cdots, \tilde{\gamma}_K]$ satisfies

$$f_2(\bar{\delta}, \bar{\gamma}_1, \cdots, \bar{\gamma}_K) \geq f_2(\tilde{\delta}, \tilde{\gamma}_1, \cdots, \tilde{\gamma}_K) + ([\bar{\delta}, \bar{\gamma}_1, \cdots, \bar{\gamma}_K] - [\tilde{\delta}, \tilde{\gamma}_1, \cdots, \tilde{\gamma}_K]) \cdot \boldsymbol{s}, \tag{D.17}$$

where $[\bar{\delta}, \bar{\gamma}_1, \cdots, \bar{\gamma}_K]$ is another arbitrary feasible point.

Lemma D.2 *The subgradient $\boldsymbol{s}$ of function $f_2(\delta, \gamma_1, \cdots, \gamma_K)$ at point $[\tilde{\delta}, \tilde{\gamma}_1, \cdots, \tilde{\gamma}_K]$ is $[P - tr(\tilde{\boldsymbol{S}}), \Gamma_1 - \boldsymbol{g}_1^H \tilde{\boldsymbol{S}} \boldsymbol{g}_1, \cdots, \Gamma_K - \boldsymbol{g}_K^H \tilde{\boldsymbol{S}} \boldsymbol{g}_K]$, where $\tilde{\boldsymbol{S}}$ is the optimal solution of Problem* (D.16) *at this point.*

$Proof$: Let $\bar{\boldsymbol{S}}$ be the optimal solution of Problem (D.16) with $\delta = \bar{\delta}$ and

$\gamma_i = \bar{\gamma}_i, i = 1, \cdots, K$. Thus, we have

$$\begin{aligned} f_2(\bar{\delta}, \bar{\gamma}_1, \cdots, \bar{\gamma}_K) &= \bar{r} - \bar{\delta}(\text{tr}(\bar{\boldsymbol{S}}) - P) - \sum_{i=1}^{K} \bar{\gamma}_i(\boldsymbol{g}_i^H \bar{\boldsymbol{S}} \boldsymbol{g}_i - \Gamma_i) \\ &\geq \tilde{r} - \bar{\delta}(\text{tr}(\tilde{\boldsymbol{S}}) - P) - \sum_{i=1}^{K} \bar{\gamma}_i(\boldsymbol{g}_i^H \tilde{\boldsymbol{S}} \boldsymbol{g}_i - \Gamma_i) \\ &= \tilde{r} - \tilde{\delta}(\text{tr}(\tilde{\boldsymbol{S}}) - P) - \sum_{i=1}^{K} \tilde{\gamma}_i(\boldsymbol{g}_i^H \tilde{\boldsymbol{S}} \boldsymbol{g}_i - \Gamma_i) + \tilde{\delta}(\text{tr}(\tilde{\boldsymbol{S}}) - P) \\ &\quad + \sum_{i=1}^{K} \tilde{\gamma}_i(\boldsymbol{g}_i^H \tilde{\boldsymbol{S}} \boldsymbol{g}_i - \Gamma_i) - \bar{\delta}(\text{tr}(\tilde{\boldsymbol{S}}) - P) - \sum_{i=1}^{K} \bar{\gamma}_i(\boldsymbol{g}_i^H \tilde{\boldsymbol{S}} \boldsymbol{g}_i - \Gamma_i) \\ &= f_2(\tilde{\delta}, \bar{\gamma}_1, \cdots, \bar{\gamma}_K) + (\text{tr}(\tilde{\boldsymbol{S}}) - P)(\tilde{\delta} - \bar{\delta}) \\ &\quad + \sum_{i=1}^{K} (\boldsymbol{g}_i^H \tilde{\boldsymbol{S}} \boldsymbol{g}_i - \Gamma_i)(\tilde{\gamma}_i - \bar{\gamma}_i) \end{aligned} \tag{D.18}$$

where $\bar{r} = |\boldsymbol{I} + \boldsymbol{h}_s^H \bar{\boldsymbol{S}} \boldsymbol{h}_s|$ and $\tilde{r} = |\boldsymbol{I} + \boldsymbol{h}_s^H \tilde{\boldsymbol{S}} \boldsymbol{h}_s|$. According to (D.18), we have Lemma D.2. ■

According to Lemma D.1, Problem (5.2) is equivalent to its dual problem

$$\min_{\delta, \gamma_1, \cdots, \gamma_K} \; f_2(\delta, \gamma_1, \cdots, \gamma_K) \tag{D.19}$$

where $f_2(\delta, \gamma_1, \cdots, \gamma_K)$ is convex. We next consider Problem (5.2) with parameters $P, \Gamma_1, \cdots, \Gamma_K$, denoted as Problem I. Assume that $\boldsymbol{S}^{(1)}$, $\delta^{(1)}, \gamma_1^{(1)}, \cdots, \gamma_K^{(1)}$ are its primal and dual optimal solutions. Moreover, we have another form of Problem (5.2) with parameters $P, \Gamma_1 + tv_1, \cdots, \Gamma_K + tv_K$, denoted as Problem II, where t is a positive constant and v_i is a real constant. Assume that $\boldsymbol{S}^{(2)}$, $\delta^{(2)}, \gamma_1^{(2)}, \cdots, \gamma_K^{(2)}$ are the primal and dual optimal solutions of Problem II. According to (D.16), we can write the dual function of Problem II as

$$f_2^{\text{II}}(\delta, \gamma_1, \cdots, \gamma_K) := \max_{\boldsymbol{S}} \; |\boldsymbol{I} + \boldsymbol{h}_s^H \boldsymbol{S} \boldsymbol{h}_s| - \delta\big(\text{tr}(\boldsymbol{S}) - P\big) - \sum_{i=1}^{K} \gamma_i(\boldsymbol{g}_i^H \boldsymbol{S} \boldsymbol{g}_i - \Gamma_i - tv_i) \tag{D.20}$$

To solve Problem II, we apply the subgradient-based algorithm to search the minimum of its dual function $f_2^{\text{II}}(\delta, \gamma_1, \cdots, \gamma_K)$ along the subgradient direction. Suppose

that we start from the point $[\delta^{(1)}, \gamma_1^{(1)}, \cdots,$

$\gamma_K^{(1)}]$. Based on Lemma D.2, one valid subgradient of $f_2(\delta, \gamma_1, \cdots, \gamma_K)$ at this point is

$$\begin{aligned}&[0, \Gamma_1 + tv_1 - \boldsymbol{g}_1^H \boldsymbol{S}^{(1)} \boldsymbol{g}_1, \cdots, \Gamma_K + tv_K - \boldsymbol{g}_K^H \boldsymbol{S}^{(1)} \boldsymbol{g}_K] \\ =&[0, tv_1, \cdots, tv_K], \end{aligned} \tag{D.21}$$

where (D.21) is due to the KKT condition of Problem I: $\Gamma_i^{(1)} - \boldsymbol{g}_i^H \boldsymbol{S}^{(1)} \boldsymbol{g}_i = 0$ given $\gamma_i^{(1)} > 0, \forall i$. Moreover, according to (D.17), we have

$$f_2^{\mathrm{II}}(\delta^{(2)}, \gamma_1^{(2)}, \cdots, \gamma_K^{(2)}) \tag{D.22}$$

$$\geq f_2^{\mathrm{II}}(\delta^{(1)}, \gamma_1^{(1)}, \cdots, \gamma_K^{(1)}) + ([\delta^{(2)}, \gamma_1^{(2)}, \cdots, \gamma_K^{(2)}] - [\delta^{(1)}, \gamma_1^{(1)}, \cdots, \gamma_K^{(1)}]) \cdot \boldsymbol{s}^{(1)}, \tag{D.23}$$

where $\boldsymbol{s}^{(1)}$ is the subgradient at the point $[\delta^{(1)}, \gamma_1^{(1)}, \cdots, \gamma_K^{(1)}]$. Since $\delta^{(2)}, \gamma_1^{(2)}, \cdots, \gamma_K^{(2)}$ are the dual optimal solutions of Problem II, we have $f_2^{\mathrm{II}}(\delta^{(2)}, \gamma_1^{(2)}, \cdots, \gamma_K^{(2)}) \leq f_2^{\mathrm{II}}(\delta^{(1)},$ $\gamma_1^{(1)}, \cdots, \gamma_K^{(1)})$. Combining this with (D.21) and (D.22), we have

$$\sum_{i=1}^{K} \gamma_i^{(2)} t v_i \leq \sum_{i=1}^{K} \gamma_i^{(1)} t v_i. \tag{D.24}$$

Thus,

$$\sum_{i=1}^{K} \gamma_i^{(2)} v_i \leq \sum_{i=1}^{K} \gamma_i^{(1)} v_i, \text{ given } t > 0. \tag{D.25}$$

Moreover, according to Lemma D.1 and (D.4), we have

$$\frac{\partial g(\boldsymbol{x} + t\boldsymbol{v})}{\partial t} = \sum_{i=1}^{K} \gamma_i v_i. \tag{D.26}$$

Note that γ_i is the Lagrange multiplier of Problem (5.2) with respect to the ith IT constraint. With different IT threshold, i.e., different value of t, γ_is are not necessarily the same, and thus γ_is can be viewed as implicit functions of t. Combining (D.25) with (D.26), it is easy to observe $\frac{\partial g(\boldsymbol{x}+t\boldsymbol{v})}{\partial t}$ decreases with the increase of t since the derivative change over t is given as $\sum_{i=1}^{K} \gamma_i^{(2)} v_i - \sum_{i=1}^{K} \gamma_i^{(1)} v_i \leq 0$, i.e., the second order derivative of function $g(\boldsymbol{x} + t\boldsymbol{v})$ over t is negative on an arbitrary line $\boldsymbol{x} + t\boldsymbol{v}$ in the feasible region. Therefore, $g(\boldsymbol{q})$ is concave. Theorem 5.3 thus follows.

D.4 Proof of Theorem 5.4

The quasi-concavity is defined as follows [53]:

Definition D.1 *A function $f : \mathcal{R}^K \to \mathcal{R}$ is called* quasi-concave *if all its sublevel sets*

$$S_\alpha = \{\boldsymbol{x} \in \boldsymbol{dom} f | f(\boldsymbol{x}) \geq \alpha\} \tag{D.27}$$

for $\alpha \in \mathcal{R}$, are convex sets.

According to Theorem 5.3, $g(\Gamma_1, \cdots, \Gamma_K)$ is a concave function of Γ_is. Therefore, the α-sublevel set of $F_i(\Gamma_1, \cdots, \Gamma_K)$

$$S_\alpha = \{\boldsymbol{q} | \frac{g(\Gamma_1, \cdots, \Gamma_K)}{1 + \Gamma_i/\sigma_i^2} \geq \alpha\} \tag{D.28}$$

$$= \{\boldsymbol{q} | g(\Gamma_1, \cdots, \Gamma_K) \geq \alpha(1 + \Gamma_i/\sigma_i^2)\} \tag{D.29}$$

is a convex set for any α, and thus the function $F_i(\Gamma_1, \cdots, \Gamma_K)$ is a quasi-concave function. Since the objective function of Problem (5.3) is the minimum of K quasi-concave functions, $F_i(\Gamma_1, \cdots, \Gamma_K)$, $i = 1, \cdots, K$, it is still quasi-concave [53]. Theorem 5.4 thus follows.

D.5 Proof of Theorem 5.5

Similar to the proof given in Appendix D.4, the α-sublevel set of $\hat{F}_i(\boldsymbol{S})$

$$S_\alpha = \{\boldsymbol{S} | \frac{1 + \boldsymbol{h}_s^H \boldsymbol{S} \boldsymbol{h}_s}{1 + (\boldsymbol{g}_i^H \boldsymbol{S} \boldsymbol{g}_i)/\sigma_i^2} \geq \alpha\} \tag{D.30}$$

$$= \{\boldsymbol{S} | 1 + \boldsymbol{h}_s^H \boldsymbol{S} \boldsymbol{h}_s \geq \alpha(1 + (\boldsymbol{g}_i^H \boldsymbol{S} \boldsymbol{g}_i)/\sigma_i^2)\}. \tag{D.31}$$

is a convex set. Thus, $\hat{F}_i(\boldsymbol{S})$ is a quasi-concave function.

D.6 Proof of Lemma 5.1

We have

$$|\boldsymbol{I} + \boldsymbol{G}_i \boldsymbol{S} \boldsymbol{G}_i^H| = |\boldsymbol{I} + \boldsymbol{U}_i^H \boldsymbol{\Lambda}_i \boldsymbol{U}_i| = |\boldsymbol{I} + \boldsymbol{\Lambda}_i| \tag{D.32}$$

where $\boldsymbol{G}_i \boldsymbol{S} \boldsymbol{G}_i^H := \boldsymbol{U}_i^H \boldsymbol{\Lambda}_i \boldsymbol{U}_i$ is the eigenvalue decomposition. Since $\text{tr}(\boldsymbol{G}_i \boldsymbol{S} \boldsymbol{G}_i^H) = \text{tr}(\boldsymbol{\Lambda}_i)$, from $\text{tr}(\boldsymbol{G}_i \boldsymbol{S} \boldsymbol{G}_i^H) \leq \Gamma_i$ it follows that

$$\text{tr}(\boldsymbol{\Lambda}_i) \leq \Gamma_i. \tag{D.33}$$

Combining (D.32) and (D.33) and denoting $L = \min(N_e, N)$, we have

$$|\boldsymbol{I} + \boldsymbol{G}_i \boldsymbol{S} \boldsymbol{G}_i^H| \leq |\boldsymbol{I} + \frac{\Gamma_i}{L} \boldsymbol{I}| = (1 + \frac{\Gamma_i}{L})^L \tag{D.34}$$

where the inequality is obtained by solving the following problem: $\max_{\text{tr}(\boldsymbol{\Lambda}_i) \leq \Gamma_i} |\boldsymbol{I} + \boldsymbol{\Lambda}_i|$. Lemma 5.1 thus follows.

Bibliography

[1] Federal Communications Commission, "Spectrum policy task force," *Rep. ET Docket*, pp. 1–135, Nov. 2002.

[2] M. Islam, C. Koh, S. Oh, X. Qing, Y. Lai, C. Wang, Y.-C. Liang, B. Toh, F. Chin, G. Tan, and W. Toh, "Spectrum survey in singapore: Occupancy measurements and analyses," in *Proc. the Second Int. Conf. on Cognitive Radio Oriented Wireless Networks and Comm. (CrownCom)*, Singapore, May 2008.

[3] J. Mitola and G. Q. Maguire, "Cognitive radios: Making software radios more personal," *IEEE Personal Commun.*, vol. 6, no. 4, pp. 13–18, Aug. 1999.

[4] S. Haykin, "Cognitive radio: Brain-empowered wireless communications," *IEEE J. Select. Areas Commun.*, vol. 23, no. 2, pp. 201–202, Feb. 2005.

[5] D. Cabric, S. M. Mishra, and R. W. Brodersen, "Implementation issues in spectrum sensing for cognitive radios," in *Proc. Asilomar Conference on Signals, Systems and Computers*, Berkeley, CA, USA, Nov. 2004.

[6] H. Tang, "Some physical layer issues of wide-band cognitive radio systems," in *Proc. Int. Symp. on Dynamic Spec. Access Networks (DySPAN)*, Baltimore Harbor, Maryland, USA, Nov. 2005.

[7] A. Sahai and D. Cabric, "Spectrum sensing: fundamental limits and practical challenges," in *Proc. Int. Symp. on Dynamic Spec. Access Networks (DySPAN)*, Baltimore Harbor, Maryland, USA, Nov. 2005.

[8] D. Cabric, A. Tkachenko, and R. W. Brodersen, "Spectrum sensing measurements of pilot, energy, and collaborative detection," in *Proc. Military Comm. Conf. (MILCOM)*, Washington, D.C., USA, Oct. 2006.

[9] H.-S. Chen, W. Gao, and D. G. Daut, "Signature based spectrum sensing algorithms for IEEE 802.22 WRAN," in *IEEE Intern. Conf. Comm. (ICC)*, Glasgow, Scotland, 19-23, June, 2007.

[10] S. Shankar, C. Cordeiro, and K. Challapali, "Spectrum agile radios: Utilization and sensing architectures," in *Proc. Int. Symp. on Dynamic Spec. Access Networks (DySPAN)*, Baltimore Harbor, Maryland, USA, Nov. 2005.

[11] A. Fehske, J. D. Gaeddert, and J. H. Reed, "A new approach to signal classification using spectral correlation and neural networks," in *Proc. Int. Symp. on Dynamic Spec. Access Networks (DySPAN)*, Baltimore Harbor, Maryland, USA, Nov. 2005.

[12] Y. Zeng and Y.-C. Liang, "Maximum-minimum eigenvalue detection for cognitive radio," in *Proc. of IEEE Personal, Indoor and Mobile Radio Commun. (PIMRC)*, Athens, Greece, Sept. 2007.

[13] ——, "Eigenvalue based spectrum sensing algorithms for cognitive radio," *IEEE Trans. Commun.*, accepted for publication, 2008.

[14] ——, "Covariance based signal detections for cognitive radio," in *Proc. Int. Symp. on Dynamic Spec. Access Networks (DySPAN)*, Dublin, Ireland, Apr. 2007.

[15] ——, "Spectrum sensing algorithms for cognitive radio based on statistical covariances," *IEEE Trans. Veh. Technol.*, accepted for publication, 2008.

[16] J. Unnikrishnan and V. V. Veeravalli, "Cooperative sensing for primary detection in cognitive radio," *IEEE J. Select. Topics in Signal Processing*, vol. 2, no. 1, pp. 18–27, Feb. 2008.

[17] G. Ganesan and Y. Li, "Cooperative spectrum sensing in cognitive radio networks," in *Proc. Int. Symp. on Dynamic Spec. Access Networks (DySPAN)*, Baltimore Harbor, Maryland, USA, Nov. 2005.

[18] J. Zhao, H. Zheng, and G.-H. Yang, "Distributed coordination in dynamic spectrum allocation networks," in *Proc. Int. Symp. on Dynamic Spec. Access Networks (DySPAN)*, Baltimore Harbor, Maryland, USA, Nov. 2005.

[19] H. Kim and K. G. Shin, "Efficient discovery of spectrum opportunities with MAC-layer sensing in cognitive radio networks," *IEEE Trans. Mobile Comput.*, vol. 7, no. 5, pp. 533–545, May 2008.

[20] Z. Quan, S. Cui, and A. Sayed, "Optimal linear cooperation for spectrum sensing in cognitive radio networks," *IEEE J. Select. Topics in Signal Processing*, vol. 2, no. 1, pp. 28–40, Feb. 2008.

[21] Y.-C. Liang, Y. Zeng, E. Peh, and A. Hoang, "Sensing-throughput tradeoff for cognitive radio networks," *IEEE Trans. Wireless Commun.*, vol. 7, no. 4, pp. 1326–1337, Apr. 2008.

[22] M. Gastpar, "On capacity under receive and spatial spectrum-sharing constraints," *IEEE Trans. Inform. Theory*, vol. 53, no. 2, pp. 471–487, Feb. 2007.

[23] Y. Xing, C. Mathur, M. Haleem, R. Chandramouli, and K. Subbalakshmi, "Dynamic spectrum access with QoS and interference temperature constraints," *IEEE Trans. Mobile Comput.*, vol. 6, no. 4, pp. 423–433, Apr. 2007.

[24] G. Scutari, D. Palomar, and S. Barbarossa, "Cognitive MIMO radio," *IEEE Signal Processing Mag.*, vol. 25, no. 6, pp. 46–59, Nov. 2008.

[25] W. Wang and X. Liu, "List-coloring based channel allocation for open-spectrum wireless networks," in *Proc. of IEEE VTC-2005 Fall*, Dallas, Texas, Sept. 2005, pp. 690–694.

[26] H. Zheng and C. Peng, "Collaboration and fairness in opportunistic spectrum access," in *Proc. IEEE of ICC-2005*, Seoul, Korea, May 2005, pp. 3132–3136.

[27] A. T. Hoang and Y.-C. Liang, "Maximizing spectrum utilization of cognitive radio networks using channel allocation and power control," in *Proc. IEEE VTC-2006 Fall*, Montreal, Quebec, Canada, Sept. 2006, pp. 1–5.

[28] F. Wang, M. Krunz, and S. Cui, "Price-based spectrum management in cognitive radio networks," *IEEE J. Select. Topics in Signal Processing*, vol. 2, no. 1, pp. 74–87, Feb. 2008.

[29] A. Ghasemi and E. S. Sousa, "Fundamental limits of spectrum-sharing in fading environments," *IEEE Trans. Wireless Commun.*, vol. 6, no. 2, pp. 649–658, Feb. 2007.

[30] X. Kang, Y.-C. Liang, A. Nallanathan, H. K. Garg, and R. Zhang, "Optimal power allocation for fading channels in cognitive radio networks: Ergodic capacity and outage capacity," *IEEE Trans. Wireless Commun.*, accepted for publication, July 2008.

[31] Y. Chen, G. Yu, Z. Zhang, H. H. Chen, and P. Qiu, "On cognitive radio networks with opportunistic power control strategies in fading channels," *IEEE Trans. Wireless Commun.*, vol. 7, no. 7, pp. 2752–2761, July 2008.

[32] R. Zhang, "On peak versus average interference power constraints for protecting primary users in cognitive radio networks," 2008. [Online]. Available: http://arxiv.org/abs/cs/0806.0676v2.

[33] P. Rashid-Farrokhi, K. J. R. Liu, and L. Tassiulas, "Transmit beamforming and power control for cellular wireless systems," *IEEE J. Select. Areas Commun.*, vol. 16, no. 8, pp. 1437–1449, Oct. 1998.

[34] I. E. Telatar, "Capacity of multi-antenna Gaussian channels," *European Trans. on Telecomm.*, vol. 10, no. 6, pp. 585–595, Oct. 1999.

[35] V. Tarokh, N. Seshadri, and A. R. Calderbank, "Space-time codes for high data rate wireless communication: performance criterion and code construction," *IEEE Trans. Inform. Theory*, vol. 44, no. 2, pp. 744–765, Mar. 1998.

[36] R. Zhang and Y.-C. Liang, "Exploiting multi-antennas for opportunistic spectrum sharing in cognitive radio networks," *IEEE J. Select. Topics in Signal Processing*, vol. 2, no. 1, pp. 88–102, Feb. 2008.

[37] N. Devroye, P. Mitranand, and V. Tarokh, "Achievable rates in cognitive radio channels," *IEEE Trans. Inform. Theory*, vol. 52, no. 5, pp. 1813–1827, May 2006.

[38] I. Marić, A. Goldsmith, G. Kramer, and S. Shamai(Shitz), "On the capacity of interference channels with one cooperating transmitter," 2008. [Online]. Available: arXiv:0710.3375.

[39] J. Jiang and Y. Xin, "On the achievable rate regions for interference channels with degraded message sets," *IEEE Trans. Inform. Theory*, vol. 54, no. 10, pp. 4707–4712, Oct. 2008.

[40] W. Wu, S. Vishwanath, and A. Arapostathis, "Capacity of a class of cognitive radio channels: Interference channels with degraded message sets," *IEEE Trans. Inform. Theory*, vol. 53, no. 11, pp. 4391–4399, Nov. 2007.

[41] A. Jovicic and P. Viswanath, "Cognitive radio: An information-theoretic perspective," 2006. [Online]. Available: http://arxiv.org/abs/cs/0604107.

[42] I. Maric, R. Yates, and G. Kramer, "The strong interference channel with unidirectional cooperation," in *Proc. UCSD Workshop on Information Theory and its Applications*, San Diego, CA, USA, Feb. 2006.

[43] S. H. Seyedmehdi, Y. Xin, and Y. Lian, "An achievable rate region for the causal cognitive radio," in *Proc. of Allerton Conf. on Comm., Control, and Comp.*, Monticello, IL, USA, 2007.

[44] S. Sridharan and S. Vishwanath, "On the capacity of a class of MIMO cognitive radios," *IEEE J. Select. Topics in Signal Processing*, vol. 2, no. 1, pp. 103–117, Feb. 2008.

[45] N. Devroye, M. Vu, and V. Tarokh, "Cognitive radio networks: Information theory limits, models and design," *IEEE Signal Processing Mag.*, vol. 25, no. 6, pp. 12–23, Nov. 2008.

[46] Z.-Q. Luo and W. Yu, "An introduction to convex optimization for communications and signal processing," *IEEE J. Select. Areas Commun.*, vol. 24, no. 8, pp. 1426–1438, Aug. 2006.

[47] W. Yu, W. Rhee, S. Boyd, and J. M. Cioffi, "Iterative water-filling for Gaussian vector multiple-access channels," *IEEE Trans. Inform. Theory*, vol. 50, no. 1, pp. 145–152, Jan. 2004.

[48] S. Vishwanath, N. Jindal, and A. Goldsmith, "Duality, achievable rates, and sum-rate capacity of Gaussian MIMO broadcast channels," *IEEE Trans. Inform. Theory*, vol. 49, no. 10, pp. 2658–2668, Oct. 2003.

[49] E. Visotsky and U. Madhow, "Space-time transmit precoding with imperfect feedback," *IEEE Trans. Inform. Theory*, vol. 47, no. 6, pp. 2632–2639, Sept. 2001.

[50] A. Wiesel, Y. C. Eldar, and S. Shamai, "Linear precoding via conic optimization for fixed MIMO receivers," *IEEE Trans. Signal Processing*, vol. 54, no. 1, pp. 161–176, Jan. 2006.

[51] W. Yang and G. Xu, "Optimal downlink power assignment for smart antenna systems," in *Proc. IEEE Int. Conf. Acoust. Speech and Signal Proc. (ICASSP)*, Seattle, Washington, USA, May 1998.

[52] F. Rashid-Farrokhi, L. Tassiulas, and K. J. R. Liu, "Joint optimal power control and beamforming in wireless networks using antenna arrays," *IEEE Trans. Commun.*, vol. 46, no. 10, pp. 1313–1324, Oct. 1998.

[53] S. Boyd and L. Vandenberghe, *Convex Optimization*. Cambridge, UK: Cambridge University Press, 2004.

[54] A. Wyner, "The wire-tap chnnel," *Bell. Syst. Tech. J.*, vol. 54, no. 8, pp. 1355–1387, Jan. 1975.

[55] I. Csiszar and J. Korner, "Broadcast channels with confidential messages," *IEEE Trans. Inform. Theory*, vol. 24, no. 5, pp. 339–348, May 1978.

[56] Y. Liang, H. V. Poor, and S. Shamai(Shitz), "Secrecy capacity region of fading broadcast channels," in *Proc. of IEEE Int. Symp. Inf. Theory (ISIT)*, Nice, France, June 2007.

[57] R. Liu, I. Marić, P. Spasojević, and R. D. Yates, "Discrete memoryless interference and broadcast channels with confidential messages: secrecy rate regions," *IEEE Trans. Inform. Theory*, vol. 54, no. 6, pp. 2493 – 2507, June 2008.

[58] R. Liu and H. V. Poor, "Secrecy capacity region of a multi-antenna gaussian boradcast channel with confidential messages," 2008. [Online]. Available: arXiv:0804.4195v1.

[59] Y. Liang and H. V. Poor, "Multiple access channels with confidential messages," *IEEE Trans. Inform. Theory*, vol. 54, no. 3, pp. 976–1002, Mar. 2008.

[60] ——, "Generalized multiple access channels with confidential messages," in *Proc. IEEE Int. Symp. Inf. Theory (ISIT)*, Seattle, Washington, July 2006.

[61] E. Tekin and A. Yener, "Achievable rates for the general gaussian multiple access wiretap channel with collective secrecy," in *Proc. 44th Annual Allerton Conf. Comm., Control, and Comp.*, Monticello, IL, Sept. 2006.

[62] R. Liu, I. Marić, P. Spasojević, and R. D. Yates, "Discrete memoryless interference and broadcast channels with confidential messages: secrecy rate regions," *IEEE Trans. Inform. Theory*, vol. 54, no. 6, pp. 2493–2507, June 2008.

[63] Y. Liang, A. Somekh-Baruch, H. V. Poor, S. Shamai(Shitz), and S. Verdu, "Cognitive interference channels with confidential messages," in *Proc. of Allerton Conf. on Comm., Control, and Comp. (Allerton)*, Monticello, IL, 2007.

[64] A. Khisti and G. W. Wornell, "Secure transmission with multiple antennas: The misome wiretap channel," 2007. [Online]. Available: arXiv:0708.4219v1

[65] F. Oggier and B. Hassibi, "The secrecy capacity of the mimo wiretap channel," 2007. [Online]. Available: arXiv:0710.1920v1

[66] T. Liu and S. Shamai, "A note on the secrecy capacity of the multi-antenna wiretap channel," 2007. [Online]. Available: arXiv:0710.4105

[67] H. Weingarten, Y. Steinberg, and S. Shamai, "The capacity region of the Gaussian multiple-input multiple-output broadcast channel," *IEEE Trans. Inform. Theory*, vol. 52, no. 9, pp. 3936–64, Sept. 2006.

[68] L. Zhang, Y.-C. Liang, and Y. Xin, "Joint beamforming and power allocation for multiple access channels in cognitive radio networks," *IEEE J. Select. Areas Commun.*, vol. 26, no. 1, pp. 38–51, Jan. 2008.

[69] D. Gerlach and A. Paulraj, "Adaptive transmitting antenna arrays with feedback," *IEEE Signal Processing Letters*, vol. 1, no. 10, pp. 150–152, Oct. 1994.

[70] M. K. Varanasi and T. Guess, "Optimal decision feedback multiuser equalization with successive decoding achieves the total capacity of the Gaussian multiple access channel," in *Proc. Asilomar Conf. Signals, Syst., Comput.*, Monterey, CA, Nov. 1997, pp. 1405–1409.

[71] G. Caire and S. Shamai, "On the achievable throughput of a multiantenna Gaussian broadcast channel," *IEEE Trans. Inform. Theory*, vol. 49, pp. 1691–1706, July 2003.

[72] M. Schubert and H. Boche, "Solution of the multiuser downlink beamforming problem with individual sinr constraints," *IEEE Transactions on Vehicular Technology*, vol. 53, pp. 18–28, Jan. 2004.

[73] Y.-C. Liang, F. Chin, and K. J. R. Liu, "Downlink beamforming for ds-cdma mobile radio with multimedia services," *IEEE Trans. Commun.*, vol. 49, no. 7, pp. 1288–1298, July 2001.

[74] M. Schubert and H. Boche, "Iterative multiuser uplink and downlink beamforming under SINR constraints," *IEEE Trans. Signal Processing*, vol. 53, no. 7, pp. 2324–2334, July 2005.

[75] T. M. Cover and J. A. Thomas, *Elements of Information Theory*. New York: John Wiley & Sons, 1994.

[76] L. Zhang, Y.-C. Liang, and Y. Xin, "Optimal SINR balancing for multiple access channels in cognitive radio networks," in *Proc. Military Comm. Conf. (MILCOM)*, Orlando, Florida, Oct. 2006, pp. 2575–2579.

[77] N. Jindal, W. Rhee, S. Vishwanath, S. A. Jafar, and A. Goldsmith, "Sum power iterative water-filling for multi-antenna Gaussian broadcast channels," *IEEE Trans. Inform. Theory*, vol. 51, no. 4, pp. 1570–1580, Apr. 2005.

[78] W. Yu, "Sum-capacity computation for the Gaussian vector broadcast channel via dual decomposition," *IEEE Trans. Inform. Theory*, vol. 52, no. 2, pp. 754–759, Feb. 2006.

[79] W. Yu and T. Lan, "Transmitter optimization for the multi-antenna downlink with per-antenna power constraints," *IEEE Trans. Signal Processing*, vol. 55, no. 6, pp. 2646–2660, June 2007.

[80] M. Mohseni, R. Zhang, and J. M. Cioffi, "Optimized transmission for fading multiple-access and broadcast channels with multiple antennas," *IEEE J. Select. Areas Commun.*, vol. 24, no. 8, pp. 1627–1639, Aug. 2006.

[81] D. Tse and P. Viswanath, "Downlink-uplink duality and effective bandwidths," in *Proc. IEEE Int. Symp. Inf. Theory (ISIT)*, Lausanne, Switzerland, July 2002.

[82] P. Viswanath and D. N. C. Tse, "Sum capacity of the vector Gaussian broadcast channel and uplink-downlink duality," *IEEE Trans. Inform. Theory*, vol. 49, no. 8, pp. 1912–1921, Aug. 2003.

[83] W. Yu, "Uplink-downlink duality via minimax duality," *IEEE Trans. Inform. Theory*, vol. 52, no. 2, pp. 361–374, Feb. 2006.

[84] D. Tse and S. Hanly, "Multiaccess fading channels-part I: Polymatriod structure, optimal resource allocation and throughtput capacities," *IEEE Trans. Inform. Theory*, vol. 44, no. 7, pp. 2796–2815, Nov. 1998.

[85] L. Zhang, R. Zhang, Y.-C. Liang, Y. Xin, and H. V. Poor, "On Gaussian MIMO BC-MAC duality with multiple transmit covariance constraints," 2008. [Online]. Available: arxiv.org/abs/0809.4101v1

[86] M. H. M. Costa, "Writing on dirty paper," *IEEE Trans. Inform. Theory*, vol. 29, no. 3, pp. 439–441, May 1983.

[87] D. G. Luenberger, *Optimization by Vector Space Methods*. New York: John Wiley, 1969.

[88] S. Boyd, L. Xiao, and A. Mutapcic, "Subgradient methods," 2003. [Online]. Available: http://mit.edu/6.976/www/notes/subgrad_method.pdf.

[89] S. Zhou and G. B. Giannakis, "Optimal transmitter eigen-beamforming and space-time block coding based on channel mean feedback," *IEEE Trans. Signal Processing*, vol. 50, no. 10, pp. 2599–2613, Oct. 2002.

[90] S. A. Jafar and A. J. Goldsmith, "Transmitter optimization and optimality of beamforming for multiple antenna systems with imperfect feedback," *IEEE Trans. Wireless Commun.*, vol. 3, no. 4, pp. 1165–1175, July 2004.

[91] K. K. Mukkavilli, A. Sabharwal, E. Erkip, and B. Aazhang, "On beamforming with finite rate feedback in multiple antenna systems," *IEEE Trans. Inform. Theory*, vol. 49, no. 10, pp. 2562–2579, Oct. 2003.

[92] Y.-C. Liang and F. P. S. Chin, "Downlink channel covariance matrix (DCCM) estimation and its applications in wireless DS-CDMA systems," *IEEE J. Select. Areas Commun.*, vol. 19, no. 2, pp. 222–232, Feb. 2001.

[93] S. Srinivasa and S. A. Jafar, "The optimality of transmit beamforming: a unified view," *IEEE Trans. Inform. Theory*, vol. 53, no. 4, pp. 1558–1564, Apr. 2007.

[94] E. Jorswieck and H. Boche, "Optimal transmission with imperfect channel state information at the transmit antenna array," *Wireless Pers. Commun.*, vol. 27, no. 1, pp. 33–56, Jan. 2003.

[95] A. Ben-Tal and A. Nemirovski, "Selected topics in robust convex optimization," *Mathematical Programming*, vol. 1, no. 1, pp. 125–158, July 2007.

[96] R. Reemtsen and J.-J. Ruckmann, *Semi-Infinite Programming*. Boston: Kluwer Academic Publishers, 1998.

[97] S. Vorobyov, A. Gershman, and Z.-Q. Luo, "Robust adaptive beamforming using worst-case performance optimization: A solution to the signal mismatch problem," *IEEE Trans. Signal Processing*, vol. 51, no. 2, pp. 313–323, Feb. 2003.

[98] J. F. Sturm, "Using sedumi 1.02, a MATLAB toolbox for optimization over symmetric cones," *Optim. Meth. Softw.*, vol. 11, pp. 625–653, 1999.

[99] S. Shafiee and S. Ulukus, "Achievable rates in gaussian MISO channels with secrecy constraints," in *Proc. IEEE Int. Symp. Inf. Theory (ISIT)*, Nice, France, June 2007.

[100] E. Seneta, *Non-Negative Matrices and Markov Chains*. Berlin, Germany: Springer-Verlag, 1981.

List of Publications

Journal Papers

1. Lan Zhang, Ying-Chang Liang, and Yan Xin,"Joint beamforming and power allocation for multiple access channels in cognitive radio networks," *IEEE J. of Select. Areas in Commun.*, vol. 26, no. 1, pp. 38-51, Jan. 2008.

2. Lan Zhang, Yan Xin, Ying-Chang Liang, and H. Vincent Poor, "Cognitive multiple access channels: optimal power allocation for weighted sum rate maximization," *IEEE Trans. Commun.*, accepted to publish, Oct. 2008.

3. Lan Zhang, Yan Xin, and Ying-Chang Liang,"Weighted sum rate optimization for cognitive radio MIMO broadcast channels," *IEEE Trans. Wireless Commun.*, accepted to publish, Feb. 2009.

4. Lan Zhang, Ying-Chang Liang, Yan Xin, and H. Vincent Poor, "Robust design for MIMO based cognitive radio network with partial channel state information," *submitted to IEEE Trans. Wireless Commun.*, 2008.

5. Lan Zhang, Rui Zhang, Ying-Chang Liang, Yan Xin, and H. Vincent Poor, "On the Gaussian MIMO BC-MAC duality with multiple transmit covariance constraints," *submitted to IEEE Trans. Inform. Theory*, 2008.

6. Lan Zhang, Rui Zhang, Ying-Chang Liang, Yan Xin, and Shuguang Cui, "On the

relationship between the multi-antenna secrecy communications and cognitive radio communications," *submitted to IEEE Trans. Commun.*, 2009.

Conference Papers

1. Lan Zhang, Yan Xin, and Ying-Chang Liang, "Power allocation for multi-antenna multiple access channels in cognitive radio networks", in *Proc. of 41th Annual Conf. on Inform. Sciences and Systems (CISS)*, Glasgow, Princeton University, N.J., Mar. 2007.

2. Lan Zhang, Ying-Chang Liang, and Yan Xin, "Joint admission control and power allocation for cognitive radio networks", in *Proc. IEEE Int. Conf. Acoust. Speech and Signal Proc. (ICASSP)*, Honolulu, Hawaii, Apr. 2007.

3. Lan Zhang, Ying-Chang Liang, and Yan Xin, "Optimal SINR balancing for multiple access channels in cognitive radio networks", in *Proc. Military Comm. Conf. (MILCOM)*, Orlando, FL., Oct. 2007.

4. Lan Zhang, Ying-Chang Liang, and Yan Xin, "Robust cognitive beamforming with partial channel state information", in *Proc. of 42th Annual Conf. on Inform. Sciences and Systems (CISS)*, Glasgow, N.J., Mar. 2008.

5. Lan Zhang, Yan Xin, and Ying-Chang Liang, "Optimal power allocation for multiple access channels in cognitive radio networks", in *Proc. of Veh. Tech. Conf. (VTC)*, Singapore, May 2008.

6. Lan Zhang, Ying-Chang Liang, and Yan Xin, "Optimal transmission covariance matrix for cognitive radio system with partial channel state information", in *Proc. of The third Int. Conf. on Cognitive Radio Oriented Wireless Networks and Commun. (CrownCom)*, Singapore, May 2008.

7. Lan Zhang, Yan Xin, and Ying-Chang Liang, "Weighted sum rate optimization for cognitive radio MIMO broadcast channels", in *Proc. of IEEE Intern. Conf. Commun. (ICC)*, Beijing, China, May 2008.

8. Lan Zhang, Yan Xin, and Ying-Chang Liang, "Robust design for MISO based cognitive radio networks with partial channel state information", in *Proc. of IEEE Global Commun. Conf. (Globecom)*, New Orleans, LA, USA, Nov. 2008.

9. Lan Zhang, Yan Xin, Ying-Chang Liang, and Xiaodong Wang "On the achievable rate regions for multi-antenna Gaussian cognitive radio channel with confidential messages", accepted to *Proc. of 43th Annual Conf. on Inform. Sciences and Systems (CISS)*, Baltimore, MD, Mar. 2009.

10. Lan Zhang, Rui Zhang, Ying-Chang Liang, Yan Xin, and H. Vincent Poor, "On Gaussian MIMO BC-MAC duality with multiple transmit covariance Constraints," submitted to publish in *IEEE Int. Symp. on Inform. Theory (ISIT)*, Seoul, Korea, June 2009.

11. Lan Zhang, Rui Zhang, Ying-Chang Liang, Yan Xin, and Shuguang Cui, "On the relationship between the multi-antenna secrecy communications and cognitive radio communications," submitted to *IEEE Int. Symp. on Inform. Theory (ISIT)*, Seoul, Korea, June 2009.